Ruprecht-Karls-Universität Heidelberg
Fakultät für Biowissenschaften

Analysis of annexin-mediated antigen-specific immunosuppression

M. Sc. Corinna Link
born in Mannheim, Germany

Dissertation
submitted to the Combined Faculty of Natural Sciences and Mathematics of the Ruperto Carola University Heidelberg, Germany
for the degree of Doctor of Natural Sciences

20th September 2018

Dissertation
submitted to the
Combined Faculty of Natural Sciences and Mathematics
of the Ruperto Carola University Heidelberg, Germany
for the degree of
Doctor of Natural Sciences

Presented by
M.Sc. Corinna Link
born in Mannheim

Oral examination: 21.11.2018

Analysis of annexin-mediated antigen-specific immunosuppression

Referees: Prof. Dr. Martin Müller

Prof. Dr. Peter H. Krammer

“ *Daß ich nicht mehr in kaltem Schweiß, zu sagen brauche, was ich nicht weiß;*
Daß ich erkenne was den Mensch, im Innersten zusammenhält. ”

---

nach Johann Wolfgang von Goethe,
Faust: Der Tragödie Erster Teil

Contents

Zusammenfassung

Apoptotische Zellen induzieren einen tolerogenen Phänotyp in dentritischen Zellen (DC) und tragen damit zur Entwicklung und Erhaltung von peripherer Toleranz bei. Unsere Gruppe erforscht den Einfluss von apoptotischen Zellen auf DC und entdeckte, dass die evolutionär konservierte Annexin-Kerndomäne (Anx) auf der Oberfläche von apoptotischen Zellen präsent ist und als immunsuppressiver Mediator der Aktivierung von Toll-like Rezeptor (TLR) signalling entgegenwirkt.
Diese Studie analysierte, ob die tolerogenen Eigenschaften von Anx darüber hinaus Antigen-spezifische Immunreaktionen gegen das Modellantigen Ovalbumin (Ova) regulieren kann. Sowohl die Vorbehandlung von bone marrow-derived dendritic cells (BMDC) mit löslichem Anx als auch die Behandlung von BMDC mit Beads, an die Anx und Ova gebunden wurde, führte zu einer reduzierten Ova-spezifischen T-Zell-Antwort. Die Ova-spezifischen OT-II T-Zellen zeigten vermindertes Wachstum und verminderte Zytokinsekretion und somit einen Anergie-ähnlichen Phänotyp nach der Ko-Kultivierung mit behandelten BMDC.
Die anti-inflammatorische Aktivität von Anx wird über die DC vermittelt. Allerdings sind die dafür verantwortlichen Mechanismen noch unklar. Im Gegensatz zu apoptotischen Zellen, induzierte Anx keinen tolerogenen Phänotyp in BMDC. Es konnte sogar gezeigt werden, dass die zuvor in der Literatur beschriebene Zytokinsuppression keinen Einfluss auf die Inhibition von T-Zellen hat. In dieser Studie konnte jedoch eine erhöhte Produktion von reaktive Sauerstoffspezies (ROS) als ein neuer Anx-induzierte Effektor in BMDC identifiziert werden. Diese ROS könnten sowohl die DC selbst als auch die DC-T-Zell-Interaktion beeinflussen.
Obwohl die Mechanismen hinter der Anx-vermittelten Suppression nicht aufgeklärt werden konnten, demonstriert diese Studie, dass Anx genutzt werden kann, um ein Partikel-basiertes System mit Antigen-spezifischen, immunsuppressiven Eigenschaften zu entwickeln. Anx-Partikel dieser Art könnten als neue Therapieoption in Autoimmunerkrankungen genutzt werden und könnten somit eine Alternative zu der aktuellen Behandlung mit allgemeinen Immunsuppresiva darstellen.

Abstract

Apoptotic cells mediate the development of tolerogenic dendritic cells (DC) and thus facilitate the induction and maintenance of peripheral tolerance. Our group investigated the influence of apoptotic cells on DC and identified the cell surface exposure of the evolutionary conserved annexin core domain (Anx) as a specific signal which antagonises Toll-like receptor (TLR) signalling.

This study examined whether the tolerogenic capacity of Anx can be exploited to down-regulate antigen-specific immune responses to the model antigen ovalbumin (Ova). The treatment of bone marrow-derived dendritic cells (BMDC) with soluble Anx prior to Ova administration or the treatment with beads harbouring Anx as well as Ova attenuated the response of Ova-specific OT-II T cells. The co-culture of treated DC and T cells resulted in an anergy-like phenotype characterised by reduced proliferation and cytokine secretion. The anti-inflammatory effects of Anx are mediated through DC by yet unknown mechanisms. Anx did not lead to the tolerogenic DC phenotype described to be induced by apoptotic cells and also the previously reported suppression of anti-inflammatory cytokines by Anx was dispensable for the effect on T cells. However, this study revealed enhanced production od reactive oxygen species (ROS) in BMDC in response to Anx which might affect the DC/T cell interactions.

Although the underlying mechanisms remain to be elucidated, this study demonstrates that Anx can be used as a tool to generate a particle-based antigen delivery system that promotes antigen-specific immunosuppression. Such Anx-particles may be a new therapeutic approach for the treatment of autoimmune disease.

1 Introduction

1.1 The immune system

1.1.1 Innate immunity

The immune system is vital to protect the organism from invading pathogens, toxins and other dangers. The innate immune response is evolutionary well conserved and can be found, at least partially, in all living organisms. It represents a first line of defence and can be sufficient to eliminate an infection. Innate immunity relies on the recognition of common pathogen structures called pathogen-associated molecular patterns (PAMP) which in turn are sensed by a defined set of pattern recognition receptors (PRR). Granulocytes, NK cells, macrophages (Mϕ) and dendritic cells (DC) are cells of the innate immune system and have three major tasks: phagocytose pathogens and infected cells, lyse them and activate the adaptive immune system. [1]

Mϕ, as their name implies (greek: big eaters), are the main phagocytes of the immune system. In addition to engulfing pathogens and infected cells they are also responsible for clearance of apoptotic cells and their debris. They are also capable of shaping immune responses by the secretion of inflammatory mediators including cytokines. [2] However, their direct interaction with cells of the adaptive immune system is rather limited [3].

The main inducers of adaptive immune responses are DC [2]. They continuously sample their environment *via* phagocytosis, receptor-mediated endocytosis and macropinocytosis to present antigens to the adaptive immune system. DC are the most efficient antigen presenting cells (APC) since they are capable of presenting even picomolar concentrations of antigen [3,4]. Antigens must be presented in a specific form, hence the antigens are processed and loaded onto major histocompatibility complexes (MHC). Depending on the mechanism of uptake and compartment localisation, the antigen is presented on MHC class I or II and thus presented to $CD8^+$ or $CD4^+$ T cells, respectively. Exogenous antigens but also cytosolic proteins that are processed in endolysosomes can be loaded onto MHC II. Endogenous proteins are rather processed by the proteasome in the cytosol and then transported into the endoplasmatic reticulum (ER) where they are loaded onto MHC I molecules. Under certain conditions, exogenous proteins can escape into the cytosol where they are subject to proteasomal degradation and hence get loaded onto MHC I. Presentation of exogenous antigens within MHC I is also called cross-presentation. [5,6]

1.1.2 Adaptive immunity

The adaptive immune system comprises B and T lymphocytes and, in contrast to the innate immune system, elicits antigen specific immune responses. A lymphocyte can only respond to a single antigen defined by the specificity of the T cell and B cell receptor (TCR and BCR, respectively) which are generated *via* somatic recombination. [7,8]

T cells can only be activated upon interaction with APC and the resulting T cell response is shaped by three signals. The first signal is the binding of the TCR to antigen-loaded MHC on the DC which assures antigen specificity. $CD8^+$ T cells can only recognise MHC I while $CD4^+$ T cells recognise MHC II. The second signal is co-stimulation, referring to an interaction of CD28 on the T cell with B7 molecules on the APC. The third signal are cytokines which are necessary for differentiation of naive T cells into effector T cells. [7,9] Signal 2 and 3 are decisive for the type of T cell response, which can be immunogenic or tolerogenic. Immunogenic responses on the one side can be triggered by engagement of CD28 with CD80 or CD86 in conjugation with pro-inflammatory cytokines like interleukin-6 (IL-6) or IL-12 and is also supported by CD40/CD40L interaction. The latter acts as a positive feedback loop for the DC [9,10]. On the other side, a tolerogenic outcome is favoured by interactions of inhibitory co-receptors and supported by anti-inflammatory cytokines like IL-10 or transforming growth factor β (TGF-β). [9,11]

Co-inhibition is essential to regulate and limit T cell responses (fig. 1). The most critical co-receptor on the T cell surface in this respect seems to be cytotoxic T-lymphocyte-associated protein 4 (CTLA-4) since the loss of only this receptor leads to severe and fatal autoimmune disease [12,13]. Furthermore, the blockade of CTLA-4 is associated with severe autoimmune-like toxicities [14,15]. CTLA-4 is expressed upon T cell activation and, as a homologue of CD28, it also binds CD80 and CD86, but with an opposing, inhibitory outcome. [16] CTLA-4 has a higher binding affinity to CD80/CD86 than CD28 and can limit the interaction of CD80/CD86 with CD28. [17] Besides being a competitor for CD28, CTLA-4 interferes with TCR signalling and hence acts as an intrinsic T cell regulator. [16]
The second most important co-inhibitor seems to be programmed cell death protein 1 (PD-1). Albeit, deficiency or blockade of PD-1 provokes autoimmunity, the etiology and symptoms are milder than those observed in the context of CTLA-4. [15,18,19] Similar to CTLA-4, PD-1 is expressed upon T cell activation and binds to PD-L1 and PD-L2 on the APC surface. PD-L1 is constitutively expressed whereas PD-L2 expression depends on the maturation status of the APC. [20] Upon ligation with one of its ligands, PD-1 antagonises T cell activation by initiating dephosphorylation of TCR and CD28 signalling molecules. [21]
PD-1 seems to be co-expressed and to have synergistic functions with other co-receptors,

e.g. lymphocyte activation gene-3 (Lag-3) and T cell immunoglobulin-3 (Tim-3). [22] Lag-3 is structurally similar to CD4 and binds to MHC II. Lag-3 interaction with the TCR complex counteracts Ca^{2+} induction and hence inhibits T cell proliferation and cytokine production. [23]

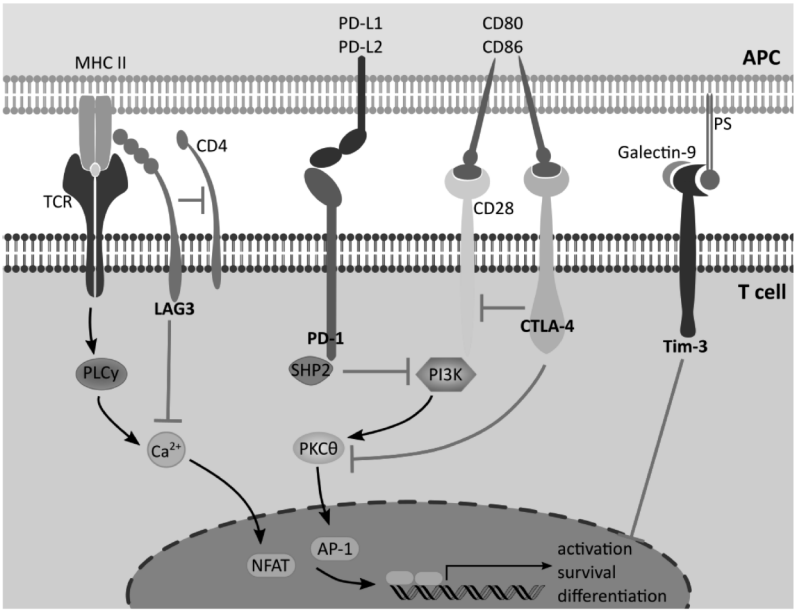

Figure 1: T cell co-stimulation and co-inhibition T cell activation requires signalling via TCR and CD28 to induce transcription via NFAT and AP-1. Lag-3 inhibits TCR signalling as a competitor of CD4 as well as by inhibiting Ca^{2+} flux. CTLA-4 and PD-1 inhibit the co-stimulatory signalling *via* CD28. CTLA-4 is a direct competitor of CD28 with higher affinity to the ligands CD80/CD86. Moreover, CTLA-4 inhibits signalling events downstream of PI3K. PD-1 inhibits CD28 signalling *via* recruitment of SHP2. Tim-3 supports unresponsiveness and counteracts T cell activation. However, the signalling following ligation of Tim-3 is not yet clarified.

Tim-3 is known to restrict TCR signalling and support tolerance which is also exploited by cancer cells and viruses. [24–28] Although Tim-3 was suggested to interact with several components of the TCR signalling complex, the distinct mechanisms by which Tim-3 regulates T cell signalling remain elusive. This might be partly attributed to the fact that Tim-3 has diverse ligands, including galectin-9 [29], phosphatidyl serine (PS) [30] and cecam-1 [31], which might also trigger different signalling pathways. [22]

A variety of co-receptors exist (only a selection of them is described here) and most of them are clearly characterised as stimulatory or inhibitory. The inducible T-cell co-stimulator (ICOS) can however not be categorised as easily. ICOS is another homologue of CD28 and is indicated to substitute CD28 in secondary T cell responses. This alternative co-stimulation can occur in the absence of CD80/CD86 *via* ICOS-ligand (ICOSL) and seems to promote T_H2 responses (see next paragraph) in this setting. [16] However, ICOS can also induce IL-10 secretion and in contrast to CD28, shows only a minor induction of IL-2. [32,33] The latter phenotype is associated with tolerance [34,35] (see 1.2.2.3), indicating that ICOS has a role in co-stimulation as well as in co-inhibition.

The above described activation process leads to the differentiation of naive T cells into different subtypes of effector T cells. A primary distinction has to be made for $CD8^+$ T cells and $CD4^+$ T cells. Upon activation, $CD8^+$ T cells become cytotoxic T lymphocytes (CTL) which can directly attack and lyse other cells. $CD4^+$ T cell can differentiate into several

subtypes of T helper (T_H) cells. T_H1 responses are characterised by IL-2 and IFN-γ secretion which can counteract e.g. intracellular pathogens and tumours. T_H2 cells secrete IL-4, IL-5 and IL-13 to support B cell responses against exogenous pathogens or allergens. And T_H17 cells, which mainly produce IL-17, are implicated in maintaining mucosal barriers. [7] Tolerogenic T cell differentiation will be addressed in 1.2.2.3.

1.2 Immunotolerance

Somatic recombination generates a diverse TCR repertoire which is essential to ensure a response against a huge variety of pathogenic antigens. However, this random gene rearrangement also leads to TCRs recognising structures of the own tissue called self-antigens. Self-reactive T cells can cause autoimmune disease and hence must be eliminated or tightly controlled.

1.2.1 Central tolerance

Central tolerance is a two step process that controls T cell reactivity during T cell development in the thymus. First, thymocytes, which are precursors of T cells, are positively selected for a functional TCR, which can recognise MHC molecules. Upon TCR rearrangement and upregulation of CD4 and CD8 co-receptors, the thymocytes are tested for binding to peptide-MHC complex (pMHC) in the thymic cortex. Thymocytes without a functional TCR die while thymocytes with baseline binding to pMHC migrate to the thymic medulla where they encounter medullary thymic epithelial cells (mTEC) and thymic DC presenting self-antigens. Recognitions of self-antigens by the TCR leads to negative selection and hence elimination of thymocytes with strong self-reactivity. Thymocytes with a TCR that binds weakly to self-antigens can survive negative selection and are programmed to become regulatory T cells (Treg) by the upregulation of the transcription factor Foxp3. [36]

1.2.2 Peripheral tolerance

Although many self-reactive T cell clones undergo apoptosis during central tolerance, this system is imperfect and self-reactive T cells escape into the periphery where they must be controlled by peripheral tolerance mechanisms.

1.2.2.1 Tolerogenic dendritic cells

DC are in the centre of immunity and thus control pro- and anti-inflammatory T cell responses. Deletion of DC in mice results in severe autoimmunity emphasising the role of DC in maintaining tolerance [37]. However, DC can also contribute to autoimmunity. Dysregulated or aberrant DC activation can break tolerance and drive autoimmunity which is illustrated in various mouse models where transfer of such DC promote autoimmune

disease in healthy recipients [38–40]. Moreover, human patients show high numbers of DC in autoimmune lesions [41].

DC with the capacity to maintain tolerance are commonly referred to as tolerogenic DC (tolDC) but whether location, subtype or maturation state characterise tolDC is still a matter of debate. The subtype of CD8α^+ DC, for example, is often mentioned in this context despite the fact that this subset is the only subset inducing tolerance [42,43].
The location or environment can have great influence on the function of DC. Organs like the spleen, where CD8α^+ DC are mainly located, or the liver are described to favour tolerance e.g. by the presence of anti-inflammatory factors such as retinoic acid or vitamin D3. [44,45]
Another major hypothesis puts the maturation state rather than a specific subset or location of DC into the focus. These concepts do not necessarily exclude each other and some propose that the immature state is the common factor after all. An anti-inflammatory environment can promote an immature DC state. Moreover, it was also described that DC in peripheral organs like the spleen are generally immature. [46]
Activation or maturation of DC lead to a number of phenotypical changes including upregulation of MHC moleculres, co-stimulatory molecules, migratory factors like CCR7 and the secretion of cytokines and chemokines. These alterations are important to mount a protective inflammatory T cell response [47]. Immature DC retain low expression of co-stimulatory molecules resulting in insufficient T cell activation which in turn can lead to tolerance. This classical view is however challenged by observations that DC with increased expression of co-stimulatory molecules and CCR7 can be anti-inflammatory leading to the term semi-mature DC [45,48–50]. This indicates that insufficient T cell activation represents only one mechanism used by DC to induce tolerance.

DC modulate T cell responses *via* soluble mediators and *via* direct cell contact. The most prominent anti-inflammatory cytokines secreted by DC are IL-10 [51,52] and TGF-β [53]. But there are additional cytokines supporting tolerance, e.g. IFN-α is described to synergise with IL-10 to downregulate T cell cytokines like IL-2 or IL-4 [54] and IL-27 was found to antagonise IL-2 transcription and to promote IL-10 secretion from different T cell subsets [55]. Furthermore, DC use soluble mediators influencing the metabolism of T cells. Such metabolites include retinoic acid, a vitamin A derivate, [56] or indoleamine-pyrrole 2,3-dioxygenase (IDO), which is a rate-limiting enzyme in the metabolism of tryptophane [57].
DC also regulate T cell activity in a contact-dependent manner. The B7 molecules PD-L1 and PD-L2 serve as co-inhibititory ligands [45]. PD-L1, which was found to be upregulated on tolDC [46], seems to play a more important role in this context. Blockade of PD-1/PD-L1 interactions leading to a re-activation of the anti-tumour response revolutionised cancer immunotherapy [58] and highlights the strong regulatory capacity of PD-L1.

PD-1/PD-L1 or PD-L2 interaction are just one example of promoting tolerance *via* co-inhibitory receptors on T cells. The co-stimulatory ligands CD80 and CD86 on DC can also transfer inhibitory signals when interacting with CTLA-4. Furthermore, the family of immunoglobulin-like transcript (ILT) receptors expressed on DC is implicated to promote T cell tolerance. As most of the other described co-inhibitory molecules, ILTs have a dual function on both DC and T cells. In the case of ILT3, the tolerogenic phenotype of the DC is stabilised by NF-κB inhibition while T cell proliferation can be suppressed independently. [59,60] Although the molecular mechanism on T cells is not yet understood, the suppressive function of ILT3 was clearly illustrated, e.g. by using soluble ILT3-Fc (in the absence of DC) [61] or by the detection of increased serum concentrations of ILT3 in patients with cancer or chronic infections [62,63].

1.2.2.2 Apoptotic cell-mediated tolerance

Around one million cells of the human body die every second due to physiological tissue turnover and are rapidly cleared by phagocytes, e.g. Mϕ and DC. [64] Apoptotic cells are intrinsically immunosuppressive and hence their engulfment promotes a tolerogenic phenotype and supports the presentation of self-antigens in a tolerogenic context. [65–67] The importance of apoptotic cells for peripheral tolerance was highlighted by the fact that all mouse models harbouring defects in the clearance or processing of apoptotic cells developed autoimmune disease [68–70].

Effects of apoptotic cells on Mϕ were already described in 1997 by Voll *et al.* in co-culture experiments. Pre-incubation of monocytes with apoptotic cells followed by LPS stimulation resulted in reduced secretion of pro-inflammatory cytokines like IL-12 and TNF-α when compared to monocytes only stimulated with LPS. Additionally, secretion of the anti-inflammatory cytokine IL-10 was increased in pre-treated monocytes. Using cells from different species rendered apoptotic by different stimuli further suggested a conserved anti-inflammatory function of apoptotic cells. [71] The capacity of apoptotic cells to suppress inflammatory cytokine secretion from monocytes as well as from Mϕ was demonstrated in several other studies and some gave also further insight into the underlying mechanisms [72–76]. It was shown that apoptotic cell mediated suppression is an immediate-early event which is independent of *de novo* protein synthesis [73] potentially including enhanced transcription of suppressor of cytokine signaling (SOCS)1 and SOCS3 [76].

Similarly, inflammatory cytokine secretion from DC and upregulation of costimulatory molecules and MHC II on the DC is impaired following pre-treatment with apoptotic cells. [77–81] However, the secretion of IL-10 in response to apoptotic cells is controversial for DC. [77,81,82] Regardless of IL-10, apoptotic cell treated DC show a rather tolerogenic phenotype and a diminished ability to stimulate T cells. [77–79]

1.2.2.3 T cell tolerance

Tolerogenic DC, as described above, are key regulators of peripheral tolerance, but the ultimate outcome of peripheral tolerance must be silencing of the adaptive immune system against self. Autoreactive T cells in the periphery are controlled by three mechanisms: deletion, anergy and Treg.

T cells undergo CD95- and Bim-mediated apoptosis following repeated TCR engagement with pMHC. This process is important to limit T cell responses against pathogens but also results in the elimination of autoreactive T cells since they encounter their antigen frequently due to the expression within the own tissue. [83]

Anergy is a state of T cell unresponsiveness that was first described by Rammensee and colleagues in 1989 [84]. Anergic cells are long-lived and show no or only diminished proliferation and cytokine secretion. Importantly, not only the typically assessed T_H1 cytokines IL-2 and IFN-γ are reduced but there is no production of anti-inflammatory cytokines such as IL-10 or TGF-β, either. [85–87] This phenotype is generally insusceptible to restimulation but can be reversed by large amounts of exogenous IL-2 *in vitro*. The phenotype seems to be more stable *in vivo* and resists IL-2 exposure but persistent presence of the antigen is required to sustain unresponsiveness. [88,89]

Anergic T cells are believed to develop upon suboptimal activation which mainly refers to TCR stimulation in the absence of co-stimulation. [91,92] Additionally, immunomodulators like IL-10 were described to be involved in anergy induction in some cases. [93] Lack of co-stimulation can be directly associated with inhibited IL-2 production. Full T cell activation combines nuclear translocation of nuclear factor of activated T-cells (NFAT) following TCR signalling induced calcium flux and nuclear translocation of activator protein 1 (AP-1) resulting from CD28 dependent protein kinase C (PKC)-θ (fig. 2). Translocation of both NFAT and AP-1 leads to IL-2 transcription, whereas signalling through the TCR alone triggers only NFAT translocation and thereby transcription of a different, rather inhibitory gene set. [90] The molecular mechanisms behind T cell anergy are not completely understood, yet it is generally accepted that the transcription factor early growth response protein 2 (Egr2) and post-transcriptional modifications *via* ubiquitinylation are essential. [87,94] Egr2 is an immediate target of NFAT and is found to be upregulated in anergic T cells *in vitro* and *in vivo*. [95,96] Egr2 in concert with NFAT triggers an alternative gene programme including Cblb, gene related to anergy in lymphocytes (GRAIL), cyclin dependent kinase inhibitors and enhanced SOCS1 and SOCS3 activity. [29,97,98] Thus, Egr2 is an initiator of anergy.

Cblb is a E3 ubiquitin ligase that counteracts association of CD28 and PI3K by ubiquitinylation of the latter (fig. 2). As such, Cblb serves as a negative regulator that needs to

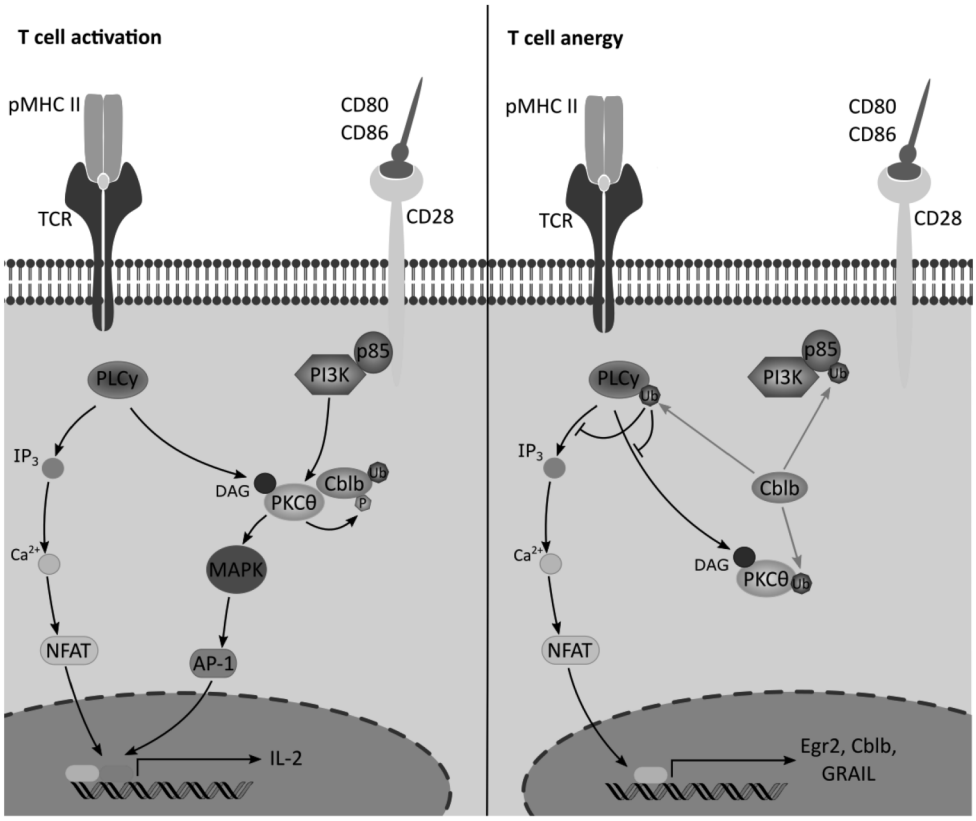

Figure 2: T cell activation. T cell anergy is associated with activation without co-stimulation. The right panel shows the TCR dependent signalling leading to calcium dependent translocation of NFAT to the nucleus. NFAT supports transcription of regulatory proteins such as Cblb, GRAIL and Itch. The left panel illustrates full T cell activation including costimulatory signalling *via* CD28. CD28 engagement recruits p85 and PI3K which in turn activates PKC-θ, MAPK and finally triggers translocation of AP-1 and NF-κB. DNA binding of NFAT and AP-1 induces IL-2 transcription. Figure adapted from Schmitz *et al.* [90]

be inactivated or degraded to allow effective T cell activation. Without the threshold set by Cblb, T cells show a hyperproliferative phenotype and Cblb$^{-/-}$ mice spontaneously develop autoimmunity. [99–101]

Another E3 ubiquitin ligase regulating T cell signalling is GRAIL which is also upregulated rapidly after anergy induction. GRAIL restricts proliferation and IL-2 production by modulation the actin cytoskeleton and the expression of co-stimulatory molecules like CD40L. [102–104]

Anergy silences autoreactive T cells but it does not seem to have active suppressive functions. However, it was reported that Treg can evolve from anergic T cells. [105,106]

Treg, as anergic T cells, are poorly proliferative but additionally exert active suppression on surrounding cells. [107,108] Two major subsets of Treg can be distinguished: natural and induced Treg. Natural Treg are CD4$^+$CD25$^+$FoxP3$^+$ cells that are generated during thymic selection whereas induced Treg develop independent of FoxP3 from CD4$^+$CD25$^-$ cells in the periphery and can be further subdivided into type 1 regulatory (Tr1) and T_H3

cells. [109] Tr1 and T_H3 cells are assumed to result from repetitive stimulation by tolDC in the presence of IL-10 and TGF-β, respectively. [110,111]
Despite the antigen-specific activation *via* the TCR, all Treg subsets suppress in antigen-unspecific manner once they are activated. [107,108] $CD25^+FoxP3^+$ Treg exert their function mainly *via* cell-cell contact but the details remain elusive. Aside from effects mediated through Treg/effector T cell contact, $CD25^+FoxP3^+$ Treg modulate T cell responses indirectly by interacting with DC. Treg might limit the contact of effector T cells to DC due to increased expression of adhesion molecules and hence stronger binding to DC [112]. Another example for this indirect functions is the downregulation of costimulatory molecules (e.g. CD80) on DC *via* CTLA-4 on the Treg [113]. The suppressive function of induced Treg on the other side, relies mainly on contact-independent cytokine secretion. Despite some studies linking Lag-3 expression to Tr1 cells, Tr1 cells are mainly defined by the production of large amounts of IL-10 while T_H3 primarily produce TGF-β. [110,111,114]

Although T cell tolerance includes quite different mechanisms, namely deletion, anergy and Treg, the criteria leading to their induction are very similar and even overlapping. Antigen presentation in absence of inflammation or co-stimulation is described for both Treg and anergic T cells [91,92,115,116]. Moreover, tolDC are fundamental for all types of tolerance and it seems that the distinct outcome of tolDC/T cell interaction is difficult to predict. Hawiger and colleagues described that tolDC induced initial proliferation followed mainly by deletion but also unresponsiveness of the remaining T cells after challenge [117]. Furthermore, two similar models of tolerance using adoptively transferred T cells resulted in different modes of tolerance. Kurts *et al.* observed T cell deletion of Ovalbumin (Ova)-specific T cells transferred into transgenic mice expressing Ova in pancreatic cells [118], whereas Adler *et al.* observed anergy in influenza hemagglutinin (HA)-specific T cells transferred into mice expressing HA on parenchymal cells [119]. These studies clearly indicate that there are further unknown factors that regulate the induction of different modes of T cell tolerance and emphasise the complexity of peripheral tolerance.

1.3 Autoimmunity and tolerogenic therapy

About 1 in 15 individuals in developed countries is affected by autoimmune disease. In these individuals misdirected immune responses attack healthy tissue leading to chronic and sometimes even fatal pathologies. Autoimmune disease can be systemic like rheumathoid arthritis and systemic lupus erythematosus or organ-specific as in the case of type 1 diabetes (T1D), or multiple sclerosis (MS). But in either case there is no cure and patients need life-long treatment to control the disease. [120]
Current therapies are based on general immunosuppression using corticosteroids or biologics. The latter target different parts of the immune system like the inflammatory cy-

tokines IL-6 (Tocilizumab) and TNF-α (Etanercept) or the complete B- and T-lymphocyte compartment (Rituximab and Teplizumab, respectively).[120–122] These treatments are rather unspecific and hence associated with numerous side effects. New therapeutic options that only inhibit the misguided immune response while sparing protective immunity are urgently needed. Different approaches to achieve antigen-specific modulation of the immune system are currently under investigation and described in the following sections.

1.3.1 Peptide therapy

Antigen presentation in the absence of inflammatory signals is generally thought to result in tolerance. Thus, it seems straightforward to use soluble antigen for therapy.
Although administration of full protein was tested, current development is more focused on using MHC trimmed epitopes. These include natural antigen peptides but also altered peptide ligands, which are the predicted epitopes harbouring modifications of single amino acids leading to an altered affinity to MHC or TCR. High doses of protein or peptide were capable of inducing tolerance in different mouse models.[123–125] However, the outcome of this type of therapy showed quite some variance and was even reported to induce anaphylactic responses.[123,126] Furthermore, attempts to translate peptide therapy into the clinic failed due to a lack of efficiency or adverse affects. Peptides or full-length insulin could so far not be proven to be an effective therapy in diabetes.[127,128] Altered peptide ligands designed for MS were already quite advanced but could not pass phase 3 clinical trials after all and even worsened the condition of some patients.[129–131]
A different approach to deliver antigen is to trigger antigen expression in healthy organs *via* DNA vaccination. While the risk of anaphylaxia can be reduced, reliable immunosuppression is also an critical issue of this approach.[123,132,133]

1.3.2 Cell-based therapy

DC and Treg are important regulators of tolerance induction and maintenance. Using or targeting these cells is therefore a promising concept for the treatment of autoimmune disease. Transfer of *ex vivo* expanded Treg populations had beneficial effects in several mouse models of autoimmunity.[134–136] Clinical translation is however hampered by phenotypic instability of *ex vivo* generated or expanded Treg observed after reinfusion.[137,138] Nonetheless, Marek-Trzonkowska and colleagues recently reported encouraging results from a phase I clinical trial suggesting a protective effect of Treg transfer in T1D patients.[139] The positive outcome of this trial may have benefited from the fact that the treated patients had just been diagnosed and hence it can be assumed that the transferred Treg faced a less inflammatory environment as compared to established disease. This may have also been a reason for the reduced efficacy of a second Treg infusion after the protective effects of the first infusion had faded[139].

Shifting the focus from Treg transfer to DC therapy might circumvent the mentioned instability problems since DC could induce and also maintain Treg populations directly *in vivo*. tolDC can be exploited for treatment by generating tolDC populations loaded with the desired antigen *ex vivo*. Antigen-pulsed DC can be rendered tolerogenic with a variety of methods but immunosuppressive molecules (e.g. IL-10 or vitamin D3) or drugs (e.g. rapamycin or dexamethasone) are most commonly used and ameliorated autoimmunity in different mouse models. [41] The promising results from these animal studies encouraged a number of clinical studies. The first proof of safety of tolDC in humans was reported in 2011. In this trial, autologous monocyte-derived DC were tolerised with antisense oligonucleotides against CD40, CD80 and CD86 and showed no adverse effects in diabetes patients. [140] This study is now continued with a phase II study (NCT02354911). Furthermore, several phase I trials are ongoing in Crohn's disease [141], rheumatoid arthritis [142,143] and MS using peptide-pulsed DC modulated with dexamethasone or vitamin D3 [144].

Another approach to exploit tolDC-mediated immunosuppression is the use of apoptotic cells which can serve as antigen delivery system and immunomodulator at the same time. This idea was realised in the lab of Stephen Miller by coupling antigens to splenocytes *via* 1-ethyl-3-(3-dimethylaminopropyl) carbodiimide (ECDI). The use of ECDI results in apoptosis of the splenocytes and supports their localisation to the spleen where they are ingested by marginal zone Mϕ. The antigen-loaded apoptotic splenocytes (Ag-SP) induced prolonged tolerance that seems to rely on both anergy and Treg. [145,146] Ag-SP treatment was able to control aberrant immune responses in mouse models of islet grafts, allergy, MS and T1D. [145–148] Analogous to the generation of Ag-SP , autologous peripheral blood mononuclear cells (PBMC) were coupled with seven different myelin peptides and tested in a clinical phase I trial in MS patients. The study demonstrated a favourable safety profile and even gave preliminary evidence for efficacy measured by reduced antigen-specific T cell responses. [149]

Erythrocytes are an interesting alternative vehicle. Billions of erythrocytes die every day by eryptosis, which is comparable to apoptosis, as a consequence of natural turnover [150]. Thus, antigens attached to this cell population can be expected to be engulfed tolerogenically in the context of eryptotic debris. Pishesha *et al.* coupled antigenic peptides to erythrocytes *ex vivo* using sortase A. Transfusion of the engineered erythrocytes could reduce disease burden in diabetic mice and experimental autoimmune encephalomyelitis (EAE), a mouse model of MS. [151] Erythrocyte physiology was further exploited even without the need of cell transfer. The lab of Jeffrey Hubbell modified antigens to bind to glycophorin A, which allows their binding to erythrocytes *in situ*. This targeting approach triggered antigen-specific tolerance in an Ova and T1D model. [152,153]

1.3.3 Nanoparticle-based therapy

Cell therapies are individualised and show promising results, but their translation to the clinic and to large patient cohorts is challenging. Mimicking apoptotic cells with synthetic particles is a cell-free alternative that is easier to handle in a clinical setting. Nanoparticles (NP) can be generated from different materials and their properties can be adapted to a variety of applications and needs. This allows to incorporate multiple signals to deliver complex messages to the immune system. NP are efficiently taken up which is attributed to the fact that APC evolved to readily phagocytose and process particulate structures of nano- and micrometer size like bacteria and viruses. Furthermore, association of antigens with NP may circumvent the risk of anaphylaxia described for soluble peptide therapy by limiting the concentration of free proteins or peptides in the circulation. [123,154]
NP properties such as size and surface charge strongly influence their effect on the immune system. Particle size is especially important for biodistribution. Particles smaller than 200 nm can move rather easily through blood and lymph and can reach spleen and lymph nodes directly only hours after *i.v.* injection. In contrast, particles with a size larger than 200 nm up to some micrometers accumulate in the spleen but require internalisation and active transport by APC to reach the lymph nodes. [123,154,155] Moreover, it was suggested that smaller particles tend to be taken up by DC whereas larger particles are preferentially engulfed by Mϕ. [156] The surface properties of NP further impact biodistribution and circulation half-life. An often undesired effect of hydrophobic particles is their recognition by the reticulo-endothelial system (RES) which rapidly eliminates such particles from blood circulation. Shielding the particle surface with the hydrophilic and non-ionic polyethylene glycol (PEG) is commonly used to counteract interactions with the RES. "PEGylation" can significantly increase the half-life in the circulation. [157] Apart from trafficking, the surface charge influences also uptake and the type of response launched by the APC. Cationic NP seem to be internalised to a higher extent due to interactions with the negatively charged cell membrane [158,159] and are more associated with pro-inflammatory responses [154,160]. Anionic particles are less immunogenic and different groups managed to induce tolerance using NP with a ζ-potential in the range of -40 to -70 mV. [154,160–164]

Different basic materials are used to generate tolerognic NP, namely metals, lipids and polymers.
Yeste *et al.* designed gold particles loaded with antigen and the aryl hydrocarbon receptor (AhR) ligand ITE. By promoting Treg development these particles were able to suppress EAE and diabetes [165,166]. Another example for metal NP are iron oxide NP that present disease-relevant pMHC complexes. pMHC I-NP were able to induce $CD8^+$ T cell tolerance and to control diabetes [167] while pMHC II-NP were demonstrated to provoke Tr1 responses that were beneficial in different mouse models [168]. Notwithstanding that

pMHC-NP are a sophisticated approach, clinical translation will be difficult since detailed knowledge of relevant antigen epitopes and broadly usable MHC alleles is necessary. And moreover, metal NP cannot be fully degraded and accumulation might cause toxicities.
Liposomes are a well-known delivery system that can be trimmed by its phospholipid composition. The composition impacts basic properties like loading and uptake but can also be used for functionalisation.[154] PS is characteristically expressed on the surface of apoptotic cells and thus might support tolerance.[64,65] This feature was utilised to generate peptide-loaded PS liposomes that protected mice from developing diabetes.[169]
Polystyrene particles (also known as latex beads) are often used in early experimental studies since they are comparably easy to handle. As such, Getts *et al.* illustrated that negatively-charged, peptide-coupled polystyrene particles can prevent EAE and reduce disease burden. Interestingly, only 500 nm particles but not larger particles (1.75 μm and 4.5 μm) induced convincing immunosuppression.[170]
A more feasible polymer which is also suitable for clinical use is poly(lactic-co-glycolic acid) (PLGA). PLGA is biodegradable in the sense that it can be hydrolised to the natural metabolites lactic acid and glycolic acid and has a good safety profile. The formulation of PLGA-NP can be adjusted for different types of drugs and different drug release kinetics.[171–174] Thus, PLGA is approved by the FDA and EMA as drug delivery system in a couple of clinical applications.[175] Concerning the treatment of autoimmune disease, PLGA-NP with different properties, coating and loading are explored in preclinical studies. NP can contain immunomodulators in addition to the antigen to ensure a tolerogenic outcome. A rather stable approach is the encapsulation of antigen in combination with the mTOR inhibitor rapamycin. EAE was inhibited by NP combining rapamycin with either peptide or protein administered *via* different routes. Even when co-administered with Tol- like receptor (TLR) 7/8 agonists, these NP kept their immunosuppressive capacity.[176–178] Nevertheless, rapamycin is a drug with several adverse effects. These side effects might be reduced to some extent by encapsulation and hence restriction to certain cell populations, but in general the tolerogenic delivery of antigen without the need for additional drugs seems more appealing. More physiological immunomodulators could be one alternative to rapamycin. Roberts *et al.* ameliorated EAE by attaching PS to the surface of peptide-loaded NP in adaptation to apoptotic cells[179] and others incorporated recombinant IL-10 into the NP to achieve similar results[180]. Besides, it might even be possible to use antigen alone. Intravenous administration of negatively-charged NP loaded with antigen alone was sufficient to transfer antigen-specific tolerance in models of MS, T1D and graft rejection.[160–164,170,181,182] The potential mechanisms employed by these NP include specific targeting to marginal zone Mϕ but also conveying a tolerogenic phenotype to both Mϕ and DC resulting in anergy as well as Treg induction. However, the comprehensive mechanism for the observed immunosuppression is not yet clarified. Especially in the light of studies that showed no suppressive capacity[176] or even immun-

ogenic responses [183–186] to NP with antigen alone, it is important to define the distinct NP properties preceding the divergent outcomes. Although the underlying mechanism is not fully elucidated, this type of antigen-associated carboxylated NP is now tested in a phase I clinical trial for celiac disease (NCT03486990). In this context, the NP are termed tolerogenic immune-modifying particles (TIMP) and are loaded with the antigen gliadin

1.4 Annexins

The superfamily of annexins consists of thirteen members with one pseudogene (annexin A12) amongst them that does not result in a translated protein. The C-terminal part of annexins consists of four similar repeats and includes Ca^{2+} binding sites. Regardless of only 45-55 % amino acid identity, the core domain is evolutionary conserved with respect to its secondary and tertiary structure. In contrast, the N-terminal domain is unique to each family member. [187]

Annexin A1 (AnxA1) was initially described as a mediator in glucocorticoid responses assisting the resolution of inflammation. [188–190] Beyond this intracellular effect, it is now known that AnxA1 can also act as an extracellular mediator. Under steady state conditions AnxA1 resides in the cytosol. However, upon apoptosis it is translocated to the cell surface with kinetics similar to those of PS [80,191] suggesting a broader immunosuppressive role.
Many regulatory functions were attributed to the N-terminus of AnxA1 which is cleaved by extracellular proteases following externalisation which gives rise to a number of differently sized peptides. [192–195] These peptides can serve as chemoattractants for phagocytes and also enhance their phagocytic function. [196,197] Furthermore, the AnxA1 N-terminus was identified as ligand for the formyl peptide receptor (FPR)1 and FPR2 and as such to inhibit monocyte and neutrophil function and migration. [198,199]
Although most research on the anti-inflammatory function of AnxA1 focused onf FPR signalling, AnxA1 can also exert inhibitory functions *via* a second, FPR-independent mechanism. Full-length AnxA1 in the presence of FPR inhibitors or the AnxA1 core domain (Anx) alone transfer a tolerogenic phenotype to APC. [80,82,200]
AnxA1 was recognised as immune regulator, but $AnxA1^{-/-}$ mice show no signs of spontaneous autoimmunity. Redundancy between the members of the annexin family may be the reason for the inconspicuous phenotype. Annexin A5 and annexin A13 are translocated to the surface of early apoptotic cells and modulate DC maturation similar to AnxA1. [82,201,202] Above all, the suppressive capacity of AnxA1 on DC could be attributed to the conserved core domain. [80,82] Thus, general function of annexins as mediators of the apoptotic cell intrinsic immunosuppression can be assumed.
Besides the broad acceptance of AnxA1 being inhibitory at the level of APC, the effects on

T cells are controversial. AnxA1 deficient T cells were described to be both hypo-[203] and hyperproliferative[204]. Moreover, the induction of inflammatory conditions in AnxA1$^{-/-}$ mice also yielded contradictory results.[204–206] Delineating the effects of AnxA1 *in vivo* is complicated since yet unknown T cell-intrinsic AnxA1 effects can neither be ruled out nor separated from direct or indirect (APC-mediated) extracellular effects on T cells.

In humans, there are no known correlations of genetic defects in annexins that are causative for disease. This may be due to redundant function of annexins and the unlikeliness of spontaneous mutations in all or several annexins.
Nonetheless, increased levels of AnxA1 cleavage products were found in patients with fragile X syndrome, Weber-Christian disease, familial Mediterranean fever, cystic fibrosis and other lung diseases[192,207–209] whereas diminished serum levels of AnxA1 were reported for patients with uveitis and MS[206,210]. Furthermore, α-AnxA1 autoantibodies were detected in patients with rheumatoid arthritis, inflammatory bowel disease and systemic lupus erythematosus but so far no correlation with disease severity could be established.[211–214] α-AnxA1 autoantibodies may actually be a simple by-product generated in course of the disease. Neutrophil extracellular traps (NET) are normally a mechanism of innate immune defence. However, they are also associated with the production of α-DNA autoantibodies and aberrant protein modification. AnxA1 has been found to be abundant in NETs where it is also citrullinated. Citrullinated proteins are common targets of autoantibodies in several autoimmune disease, so AnxA1 does not seem to have a disease-related role in this context.[215]

1.5 Aim of the study

Apoptotic cells have intrinsic anti-inflammatory properties and maintain peripheral tolerance. Engulfment of apoptotic cells results in an immunologically silent presentation of their cargo by inducing an inhibitory phenotype in the phagocyte. Since apoptotic cells of an healthy individual mainly comprise self-antigens, this process is essential to avoid autoimmune reactions. However, the underlying mechanisms by which apoptotic cell-mediate immunosuppression are still largely unknown.

Our group previously found that several members of the annexin protein family are translocated to the surface of early apoptotic cells and hypothesised that the evolutionary conserved annexin core domain (Anx) is a mediator of apoptotic cell-mediated tolerance. Recombinant Anx antagonises Toll-like receptor signalling and impairs DC activation.

Hence, Anx is a potential tool to induce immunosuppression in an antigen-specific manner. Current therapies for autoimmune disease universally dampen the immune system and are thus accompanied by severe side effects. Restricting the suppressive treatment to the relevant self-antigens and inhibiting self-reactive immune responses by an endogenous mediator such as Anx could improve tolerability in patients suffering from autoimmune disease.

The aim of this study is to develop a vehicle that combines an antigen of interest and Anx to allow the delivery of the antigen in a tolerogenic context. We hypothesise that the combination of Anx with an antigen in a particulate structure induces antigen-specific immunosuppression. In order to test this hypothesis, Anx and the model-antigen Ova were coupled to polystyrene beads and PLGA nanoparticles. This study investigated the ability of the Anx-coated particles to affect DC phenotype and to modulate Ova-specific T cell responses. Furthermore, the function of Anx-coated particles was compared to soluble Anx and its known tolerogenic properties.

In summary, this study aims to develop a particle-based delivery system using Anx to promote antigen-specific tolerance and to investigate the underlying mechanisms of Anx-induced tolerance.

2 Materials

2.1 Chemicals and Reagents

2.1.1 Chemicals

Chemicals were purchased from Serva, Sigma-Aldrich or Roth.

2.1.2 Reagents

Reagent	**Company**
7AAD	Sigma-Aldrich
AKP	BD Becton Dickinson GmbH
Alexa Fluor 546 Phalloidin	Life Technologies
BCIP/NTP	Sigma-Aldrich
CFSE	Sigma-Aldrich
CpG ODN 1668	Biomol
DCFDA	Life Technologies
dNTPs (10 mM)	Life Technologies
DPBS	Life Technologies
Western Lightning Plus-ECL	PerkinElmer
FluoSpheres Sulfate Microspheres, 1 μm	Life Technologies
GeneAmp 10x PCR Buffer and $MgCl_2$	Life Technologies
Hoechst 34580	Life Technologies
MulV reverse transcriptase (50 U/μl)	Life Technologies
PageRuler Plus Prestained Protein Ladder	Thermo Scientific
PMA	Sigma-Aldrich
Poly(I:C)	InvivoGen
Power SYBR Green PCR Master Mix)	Applied Biosystems
RNAse Inhibitor (20 U/μl)	Life Technologies
Trolox	Th. Geyer

2.1.3 Commercial Kits

Kit	Company
EasySep Mouse CD4+ T Cell Isolation Kit	STEMCELL Technologies
FoxP3 Fixation/ Permeabilization Kit	eBioscience
mouse IL-6 OptEIA ELISA Set	BD Becton Dickinson GmbH
mouse IL-2 OptEIA ELISA Set	BD Becton Dickinson GmbH
mouse IFN-γ OptEIA ELISA Set	BD Becton Dickinson GmbH
Murine IL-12 Standard ABTS ELISA Kit	PeproTech
RNAqueous-Micro Total RNA Isolation Kit	Thermo Scientific (Ambion)

2.2 Buffers and solutions

Buffer/Solution	Composition	
ACK buffer pH 7.2	150 mM	Ammoniumchloride (NH_4Cl)
	10 mM	Kaliumhydrogencarbonate ($KHCO_3$)
	1 mM	EDTA
		ddH_2O
Blocking buffer (Western blot)	5 % (w/v)	skim milk powder
		TBS-T
Citrate buffer 0.1 M pH 5.0	30 mM	citric acid monohydrate
	70 mM	natrium citrate dihydrate
		ddH_2O
Coating buffer pH 9.6 (BD ELISA)	100 mM	Natriumhydrogencarbonate ($NaHCO_3$)
	34 mM	Natriumcarbonate (Na_2CO_3)
		ddH_2O
ELISA wash buffer	0.05 % (v/v)	Tween 20
		TBS
FC buffer	10 % (v/v)	rat serum
	10 % (v/v)	FCS
		PBS
OPD	50 ml	Citrate buffer
	1	OPD tablet

Phosphate Buffered Saline PBS pH 7.4	137 mM 8.1 mM 2.7 mM 1.5 mM 	Natriumchloride (NaCl) Dinatriumhydrogenphosphate (Na_2HPO_4) Kaliumchloride (KCl) Kaliumdihydrogenphosphate (KH_2PO_4) ddH_2O
PBS-T	0.05 % (v/v) 	Tween 20 PBS
Reducing Sample buffer 5x for Western Blot	50 % (v/v) 25 % (v/v) 10 % (w/v) 50 mM 0.25 mg/ml 	glycerol β -Mercaptoethanol SDS Tris pH 6.8 bromphenol blue ddH_2O
Resolving Gel (SDS-PAGE)	24 mM 5 % (w/v) 0.1 % (w/v) 0.1 % (w/v) 0.1 % (v/v) 	Tris-HCl pH 6.8 acrylamide SDS APS TEMED dH_2O
SDS Running Buffer	25 mM 0.19 M 1 % (w/v) 	Tris Glycine SDS dH_2O
Semi Dry Transfer Buffer pH 9.2	48 mM 39 mM 0.04 % (w/v) 10 % (v/v) 	Tris Glycine SDS Methanol ddH_2O
Stacking Gel (SDS-PAGE)	37.5 mM 10 % (w/v) 0.1 % (w/v) 0.03 % (w/v) 0.1 % (v/v) 	Tris-HCl pH 8.8 acrylamide SDS APS TEMED dH_2O

Stemcell buffer	1 mM 2 % (v/v)	EDTA FCS PBS
Tris-buffered Saline TBS pH 7.5	50 mM 150 mM	Tris-HCl pH 7.5 NaCl dH_2O
TBS-T	0.05 % (v/v)	Tween 20 TBS
Trypan blue 0.4 %	0.4 % (w/v) 0.1 % (v/v)	Trypan blue Natriumazide PBS

2.3 Culture Media and Supplements

Medium/Supplement	**Company/Composition**
DC medium	RPMI 1640, 10 % FCS, 20 ng/ml rmGMCSF
ELISpot medium	RPMI 1640, 1 % PenStrep, 2 % mouse serum
Fetal Calf Serum (FCS)	Sigma-Aldrich
Mouse Serum	Linaris
Penicillin Streptomycin 10'000U/ml	Life Technologies
Polymyxin B	Abcam
Rat Serum	Milteny Biotec
rmGMCSF	Immunotools
RPMI 1640 Medium	Sigma-Aldrich
1 % medium	RPMI 1640, 1 % (v/v) FCS
10 % medium	RPMI 1640, 10 % (v/v) FCS

2.4 Biologic material

2.4.1 Cell lines

Name	**Description**
JE6.1	human T cell line (ATCC TIB-152)

2.4.2 Mouse strains

Name	**Description**
C57BL/6C57	C57 Black 6 (wild type)
OT-II	B6.Cg-Tg(TcraTcrb)425Cbn/J

2.5 Antibodies

If not stated otherwise all antibodies are directed against mouse proteins.

2.5.1 ELISpot Antibodies

Antibody	Use	Dilution	Company
α-IL-2	capture	1:200	BD Becton Dickinson
α-IL-2-Biotin	detection	1:250	BD Becton Dickinson

2.5.2 Labelled Antibodies

Antigen target	Fluorophore	Clone	Dilution	Provider
Anx1	APC	mAx550	1:500	Heiko Weyd, DKFZ
CD4	APC-Cy7	GK1.5	1:200	Biolegend
CD4	PE	H129.19	1:200	BD Pharmingen
CD11c	APC	N418	1:150	Biolegend
CD40	PE	3/23	1:150	Biolegend
CD40	PE-Cy7	3/23	1:150	Biolegend
CD44	PE-Cy7	IM7	1:150	Biolegend
CD69	APC	H1.2F	1:150	Biolegend
CD73	APC	TY/11.8	1:150	Biolegend
CD80	FITC	16-10A1	1:150	eBioscience
CD85k (ILT3)	PE	H1.1	1:150	Biolegend
CD86	FITC	GL1	1:150	eBioscience
CD90.1 (Thy1.1)	PE	OX-7	1:200	BD Pharmingen
CD90.1 (Thy1.1)	PerCP-Cy5.5	OX-7	1:200	Biolegend
CD157 (CTLA-4)	PE-Cy7	UC10-4B9	1:150	Biolegend
CD223 (Lag3)	APC	C9B7w	1:150	Biolegend
CD273 (PD-L2)	FITC	122	1:150	eBioscience
CD274 (PD-L1)	PE-Cy7	10F.9G2	1:150	Biolegend
CD275 (ICOSL)	PE	HK5.3	1:150	Biolegend
CD279 (PD-1)	PE-Cy7	RMP1-30	1:150	Biolegend
CD366 (Tim-3)	PE	B8.2C12	1:150	Biolegend
FoxP3	APC	FJK-16s	1:50	eBioscience
FR4	PE	12A5	1:150	Biolegend
I-A/I-E(MHC-II)	PerCP-Cy5.5	M5/114.15.2	1:150	eBioscience

2.5.3 Western Blot Antibodies

Antibody	Dilution	Provider
mouse α-Anx1 (mAx550)	1:1000	Heiko Weyd, DKFZ
mouse α-Flag M2	1:10,000	Sigma-Aldrich
mouse α-Ova	1:1000	Santa Cruz
goat α-mouse-IgG-HRP	1:10,000	Santa Cruz
goat α-mouse-IgG2b-HRP	1:10,000	Southern Biotech

2.5.4 Stimulation Antibodies

Antigen target	Clone	Dilution	Company
CD3e	1 45-2C11	1:400	BD Biosciences
CD28	E18	1:400	BioLegend
CD40	FGK4.5		BioXcell

2.6 Proteins, Peptides and Oligonucleotides

2.6.1 Proteins

Protein	Provider
murine annexin core domain (Flag-tagged)	Fatmire Bujupi, DKFZ
DQ-Ovalbumin	Life Technologies
EndoGrade Ovalbumin	Hyglos

2.6.2 Peptides

Peptide name	Protein sequence	Company
ISQ	ISQAVHAAHAEINEAGR	InvivoGen
SIINF	SIINFEKL	eBioscience
SIY	SIYRYYGL	Peptide Specialty Laboratories

2.6.3 qPCR Primer

Gene target	Forward Primer 5'→ 3'	Reverse Primer 5'→ 3'
Cblb	ATGTCCCTCCTCGGCTTT	GAGACAATTTGCTAATGGACCAG
Egr2	GCCAAGGCCGTAGACAAAATC	CCACTCCGTTCATCTGGTCA
GRAIL	AATTTCACGGTGCCCACGGTTTGG	ATTGCAACAATGTCCCCAGACCC
HMBS	GAGTCTAGATGGCTCAGATAGCATGC	CCTACAGACCAGTTAGCGCACATC
HPRT	GAGGAGTCCTGTTGATGTTGCCAG	GGCTGGCCTATAGGCTCATAGTGC
IDO	GCCTCCTATTCTGTCTTATGCAG	CGAGGAAGAAGCCCTTGTC
IL-2	AAAAGCTTTCAATTGGAAGATGCT	TTGAGGGCTTGTTGAGATGA
IL-27p28	CTGTTGCTGCTACCCTTGCTT	CACTCCTGGCAATCGAGATTC
Maf	AGCAGAAGAGGCGGACCCTGAAAA	GCCGTTGCTCACCAGCTTCTCGTATT
SOCS1	CTGCGGCTTCTATTGGGGAC	AAAAGGCAGTCGAAGGTCTCG
SOCS3	ATGGTCACCCACAGCAAGTTT	TCCAGTAGAATCCGCTCTCCT

2.7 Consumables

Consumable	Company
BD Trucount tubes	BD Becton Dickinson GmbH
Cell culture plates and dishes	TPP
Costar® ELISA Plate 96 well clear flat bottom half area, high binding polystyrene	Corning
Costar® 50 ml reagent reservoir	Corning
EASYstrainer 40 μm sterile	Greiner Bio-one
FACS tubes	BD Becton Dickinson GmbH
IP clear plates 0.45 μl MSIPS4510 hydrophob high protein binding immobilion-P membrane sterile	Merck Millipore
LoBind microcentrifuge tubes	Eppendorf
Nitrocellulose membrane Amersham Protran 0.45 NC	GE Healthcare
Lab-Tek Chamber Slide, 8 wells, Permanox	Sigma-Aldrich
PCR tubes, flat lid, 100 μl	Starlab
Reaction tubes 1.5 ml/2 ml	Eppendorf

2.8 Instruments

Instrument	Company
CTL ImmunoSpot Reader	Cellular Technology Limited
FacsCanto II flow Cytometer	BD Becton Dickinson
GloMax-Multi Detection System	Promega
Chemi-Smart 5100	Peqlab
Microplate Reader Model 680	BioRad
Microplate Washer 405 TS	BioTek Instruments
Microscope brightfield	Carl Zeiss Microscopyy
Molecular Imager GelDoc XR+	BioRad
NanoDrop ND-1000 spectrophotometer	Peqlab
pH meter ProfiLine pH 3210	WTW
PowerPac HC	Biorad
Thermal Cycler C1000	BioRad
Thermomixer Comfort	Eppendorf
Trans-Blot® SD Semi-Dry Transfer Cell	BioRad
UV-Stratalinker	Stratagene

2.9 Software

Software	**Company**
ChemiCapt 5000 Imaging Software	Vilber Lourmat
FacsDiva	BD Becton Dickinson
Flow Jo	FlowJo LLC
GraphPad Prism version 6	GraphPad Software
ImageJ (Fiji)	Wayne Rasband, NIH
ImmunoSpot SC Suit	Cellular Technology Limited
LaTeX	Leslie Lamport, LaTex Project Team
Microplate Manager version 5.2.1	BioRad
Microsoft Office	Microsoft
Zen 2012 version 8.1	Carl Zeiss Microscop

3 Methods

3.1 Organ and cell Isolation

3.1.1 Bone marrow-derived dendritic cells - BMDC

Leg bones (tibia and fibia) of wt mice were dissected and bone marrow was flushed into PBS. The bone marrow cells in the suspension were then separated from other tissue by filtering through a 40 μm strainer. The cells were pelleted for 5 min at 1500 rpm and 4 °C and then resuspended in 3 ml ACK-buffer to lyse remaining erythrocytes. After 40 s the reaction was stopped by adding 40 ml 10 % medium. Following a washing step with 10 % medium, the cells were counted and adjusted to 0.5×10^6/ml in DC medium and seeded into a 24-well plate (1 ml/well). Bone marrow cells are differentiated into DC in DC medium over 7 d. DC medium was fully replaced with fresh medium after 2 days and partly replaced (500 of 1000 μl) after 4 days of differentiation.

3.1.2 Splenocytes and CD4$^+$ T cells

Spleens from OT-II mice were harvested and mashed through a 40 μm strainer. The cells were pelleted for 15 min at 1500 rpm and 4 °C and then resuspended in ACK-buffer to lyse remaining erythrocytes. After 1.5 min the reaction was stopped by filling up with 10 % medium. After centrifugation (15 min, 1500 rpm, 4 °C) splenocytes can be resuspended in 10 % medium for preactivation or in Stemcell buffer for further CD4$^+$ T cell isolation.

CD4$^+$ T cell were isolated using the EasySep mouse CD4$^+$ T cell isolation kit according to manufacturer's protocol. In brief, 1×10^8/ml splenocytes were incubated for 10 min with 50 μl rat serum and 50 μl negative selection cocktail per ml cell suspension. Then, 75 μl isolation beads per ml cell suspension were added. After 2.5 min the solution was filled up to a total volume of 10 ml with Stemcell buffer. The tube was placed into a EasySep magnet to separate T cells from other cells in the suspension. The cleared T cell solution was transferred to a new tube.

Subsequently, T cells were labelled with CFSE. First, cell suspension was adjusted to 2×10^7/ml in PBS and mixed with an equal volume of CFSE solution (1:15000 in PBS). Following 20 min incubation in the dark, the staining reaction was stopped by adding one volume of FCS. After 2 min at RT, the tube was filled up with ice cold 10 % medium and incubated for another 5 min on ice. Finally, the cells were washed 2 times with 1 % medium.

3.2 Cell Biology

3.2.1 Apoptosis induction

Apoptotic cells were generated by seeding 1×10^6/ml JE6.1 in a 6-well plate with a total volume of 2.5 ml/well and irradiation with 75 μJ UV-C. Irradiated cells were incubated at 37 °C for at least 2.5 h before they were used in further assays.

3.2.2 BMDC suppression assay

BMDC which were differentiated for 7 days were seeded in a 96-well plate (flat-bottom) at 0.75×10^5 cells/well in 175 μl 1 % medium supplemented with polymyxin B (PmxB) (final conc. 50 μg/ml). PmxB was added to avoid unspecific TLR4 stimulation by LPS and to rule out endotoxin tolerance. After 1 h resting at 37 °C, 50 μl treatment (e.g. Anx or beads) were added. In the case of apoptotic cell treatment, 3×10^5 apoptotic JE6.1 (aJ) were added 5 h after BMDC seeding. BMDC are incubated with treatments for 8 h (4 h for aJ) and then stimulated with 25 μl CpG (final conc. 20 nM). The response of BMDC to the different treatments was analysed by flow cytometry (FC), gene expression (qRT-PCR) and cytokine secretion (ELISA) on day 1 or day 2 after stimulation.

3.2.3 T cell suppression assay

For the analysis of T cell responses, BMDC were differentiated and treated as described in 3.1.1 and 3.2.2. On day 2 after BMDC stimulation, 0.5×10^6 CFSE labelled $CD4^+$ T cells were added per well. The preparation and staining of $CD4^+$ T cells from OT-II mice is described in 3.1.2. Following 2 days of co-culture, 60 μl/well supernatant were taken for IL-2 analysis and substituted with fresh 1 % medium. After a total of 5 days of co-culture, the media including the T cells was transferred into a round-well 96-well plate and centrifuged at 10 min at 1500 rpm. The supernatants were used to measure IFN-γ secretion while the cell pellet was further processed for FC analysis.

3.2.4 T cell preactivation

Spleens from OT-II mice were prepared as described in 3.1.2. Splenocytes were then seeded in a cell culture flask at a concentration of 1×10^7/ml in 10 % medium and stimulated with α-CD3 [1 μg/ml] and α-CD28 [0.5 μg/ml]. After over night incubation with the stimulatory antibodies, cells were washed and transferred to a new flask with fresh 10 % medium. Splenocytes were then rested for another 3 days, with addition of further fresh media if necessary, before $CD4^+$ T cells were isolated as described in 3.1.2. The activation status of the T cells was monitored by measuring the expression of CD69, CD44 and CD62L *via* FC before and after stimulation as well as after T cell isolation.

3.2.5 ROS assay

BMDC, differentiated for 6-7 days were seeded in a 48-well plate (flat-bottom) with 1×10^5 cells/well in 1 % medium supplemented with polymyxin B (final concentration: 50 μg/ml). After 1 h incubation at 37 °C, the treatment (e.g. Anx or Beads) or the positive control PMA [10 ng/ml] was added. Following 1.5 h of incubation with the treatment, the ROS-sensitive dye DCFDA was added in a final concentration of 5 μM. After a total of 2 h of treatment including 30 min DCFDA incubation, the cells were harvested by rinsing the wells and transferring the cell suspension into tubes or a round-bottom 96-well plate, to facilitate pelleting by centrifugation. From the harvesting step onwards, cells need to be kept on 4 °C to avoid further (unspecific) ROS production. Optionally the cells can be incubated with the ROS scavenger Trolox [final conc 25 μM] for 10 min before harvesting, to further exclude unspecific ROS production. The harvested cells were pelleted (5 min, 1500 rpm (plates) or 5000 rpm (tubes)), washed once with PBS and finally resuspended in FC buffer (optionally including Trolox). ROS production was then measured by assessing the fluorescent signal of processed DCFDA by FC.

3.2.6 DQ-Ovalbumin Assay

Antigen processing was analysed using a commercially available Ova that is labelled with a processing sensitive dye (DQ-Ova). BMDC were seeded and treated as described in 3.2.2. The treatment included soluble DQ-Ova and Beads coupled with DQ-Ova instead of unlabelled Ova. For each experiment, two similar plates were prepared in order to incubate one plate at 4 °C as background control while the other one was incubated at 37 °C to allow uptake and processing. After 4 h incubation, cells were harvested and analysed *via* FC.

3.3 Molecular Biology

3.3.1 Immunoassays

3.3.1.1 Enzyme Linked Immunosorbent Assay - ELISA

Generally, ELISA was performed according to manufacturer's protocol. This brief description is referring to the BD OptEIA kits.
Half-area plates were coated with 50 μl capture antibody solution per well and incubated over night at 4 °C. Plates were washed 3 times with TBS-T and then blocked with 100 μl PBS/10 % FCS for 1 h at RT. After blocking, plates were washed 3 times and 50 μl assay supernatant (if necessary diluted in PBS/10 % FCS) were loaded in duplicates for 2 h at RT. Following 5 times washing, 50 μl of detection antibody solution including streptavidin were added to the wells and incubated for 1 h. Plates were then washed 7 times and incubated with developing solution (OPD + H_2O_2 (1:1000)) in the dark. The colour

reaction was stopped with 25 μl 3N H_2SO_4 when desired intensity of the highest standard sample was reached. Cytokine secretion represented by colour intensities was measured at 490 nm absorbance with a microplate reader (BioRad).

3.3.1.2 Enzyme Linked Immunospot Assay - EliSpot

Membranes of the ELISpot-plates were activated by short incubation with 50 μl 70 % EtOH. Plates were washed with 200 μl PBS and then incubated with 100 μl coating antibody in PBS at 4 °C over night. After washing with PBS, the plates were blocked with ELISpot-medium at 37 °C for at least 1 h. After blocking, splenocytes in ELISpot-medium were seeded into the plate with 1.5×10^6/well. The cells were then stimulated with peptides [2 μM] or stimulation antibodies [50 μg/ml] over night. On the following day, the supernatants were taken and stored for additional ELISA. The plate was washed 5 times with PBS-T and once with PBS before 100 μl detection antibody in PBS was added and incubated for 2 h at RT. The plate was washed again 4 times with PBS and 100 μl Streptavidin-AKP solution (1:500 in PBS) was added for 30 min. Following 4 washes with PBS the plate was developed for 3 min in the dark using 100 μl BCPT/NBT solution. The developing reaction was stopped by rinsing the plate with dH_2O. The plate was dried and analysed using ImmunoSpot CTL machine and software.

3.3.1.3 Flow cytometry - FC

For the analysis of surface molecules, cells were first blocked for 10 min in FC buffer and then incubated with the desired mixture of labelled antibodies for 20 min on ice. After washing with PBS/10 % FCS, the cells could be analysed by flow cytometry or further processed for additional intracellular staining.
Intracellular staining of FoxP3 was performed using the eBioscience fixation and permeabilisation kit according to manufacturer's protocol. Briefly, surface stained cells were fixed for 20 min with Fix/Perm buffer followed by one washing step with PBS and two washing steps with permeabilisation buffer. Cells were then incubated for 15 min in permeabilisation buffer containing 2 % rat serum and subsequently α-FoxP3-PE was added for 25 min. Afterwards, the cells were washed with permeabilisation buffer and then resuspended in FC buffer. During and after staining, cells were kept at 4 °C.

3.3.1.4 Microscopy

BMDC which were differentiated for 6 days were seeded in a 8-well chamber slides at 9×10^4 cells/well in 200 μl 1 % medium supplemented with polymyxin B (final conc. 50 μg/ml). After 1 h resting at 37 °C, 50 μl beads [7.5×10^6/ml] were added. BMDC were incubated over night with the beads before they were fixed and stained for microscopy.
For the staining, cells were rinsed with PBS and then fixed for 15 min at RT with 4 % para-

formaldehyde. Following washing with 1 ml PBS, cells were then permeabilised by 10 min incubation in 0.1 % Triton X-100 and afterwards washed with PBS. Cells were blocked in 2 % BSA in PBS over night at 4 °C . After washing with PBS, cells were stained with Hoechst and Phalloidin (1:400 in 2 % BSA/PBS). The stained cells were washed with PBS and embedded with Mowiol.

3.3.1.5 Western Blot

Western blot was used to analyse the binding of Ova and Anx to the surface of latex beads. In order to elute proteins from the bead surface, beads were boiled at 95 °C in reducing sample buffer for 15 min. The protein elution was subjected to SDS-PAGE (10 % gels run at 120 V). Separated proteins were blotted onto a nitrocellulose membrane in a BioRad Trans-blot semi-dry cell for 30 min at 15 V. Membranes were then shortly washed with TBS-T and blocked with 5% milk powder in TBS-T for at least 30 min. For protein detection, membranes were incubated with primary antibodies (diluted in TBS-T/1 % BSA/N_3) over night at 4 °C followed by 3 times 5 min washing with TBS-T and 1 h incubation with the secondary antibody at RT. After another 3 times 5 min washing with TBS-T the membrane was developed using ECL detection reagent and recorded with the Chemi-Smart 5100 System.

3.3.2 mRNA quantification

3.3.2.1 RNA preparation

RNA was extracted using the ambion RNAqueous micro kit following manufacturer's protocol. In short, cell pellets were lysed by vortexing in 100 μl lysis buffer. After adding 50 μl EtOH, the lysates were transferred to the provided columns and centrifuged for 15 s at 13000 rpm, 4 °C. The column membranes were washed once with 180 μl wash solution I and twice with 180 μl wash solution II. The membranes were then dried by centrifugation for 1 min at 13000 rpm, 4 °C. Deviating from the recommendation of the manufacturer, RNA was eluted in a total volume of 15 μl in two rounds from membranes using preheated elution buffer (75 °C). RNA concentration was determined by spectrophotometry.

3.3.2.2 Quantitative Real-Time PCR - qRT-PCR

For gene expression analysis, 500 - 800 μg RNA was reverse transcribed into cDNA by mixing 11.7 μl RNA solution with 14.3 μl mastermix as shown in tab. 1 and performing a PCR with the programme shown in tab. 2.

Table 1: RT-PCR Mastermix 1x master mix for RT-PCR

Component	Volume
$MgCl_2$ [25 mM]	5.2 µl
10 x PCR Buffer	2.6 µl
dNTPs [10 mM]	2.6 µl
OligodT [100 pmol/µl]	1.3 µl
RNAse Inhibitor [20 U/µl]	1.3 µl
MulV transcrpitase [50 U/µl]	1.3 µl

Table 2: RT-PCR programme PCR programme for RT-PCR

Temperature	Time
25 °C	10 min
42 °C	45 min
95 °C	5 min
8 °C	∞

For the qPCR (programme see tab. 3), the cDNA (2 µl) was added to a mix of 7.5 µl SYRB green master mix, 1.5 µl primer mix [5 µM stocks] and 4 µl H_2O. Gene expression was evaluated using ΔΔCt method.

Table 3: qPCR programme PCR programme for qPCR

Temperature	Time	
50 °C	2 min	
60 °C	10 min	
95 °C	15 s	40 x
60 °C	1 min	

3.4 in vivo experiments

For the analysis of Ova-specific responses *in vivo*, OT-II T cells (2×10^6/mouse) were prepared and labelled as described in 3.1.2 and then *i.v.* injected into wt mice. On the following day (d0) mice were treated with beads or controls by *i.v.* injection. Six days after treatment, mice were sacrificed and spleens and in some cases lymph nodes were isolated analogous to 3.1.2. Both splenocytes and lymphocytes were analysed by FC while only splenocytes were plated and restimulated for cytokines analysis (see 3.3.1).

3.5 Particles

3.5.1 Bead preparation

Here, only the final and optimised protocol is described. More details and differential conditions are illustrated in the supplementary results

Beads harbouring Anx and Ova were generated using sulfate fluospheres as basis. These latex beads have a diameter of 1 µm and proteins can be attached by passive adsorption. Bead coating was performed at a bead concentration of 0.4 % solids (2000×10^6 beads/266 µl). First, Ova [2 ng/10^6 beads] was diluted in DBPS in protein lowbind tubes and a sample

was taken to monitor the input before coating. Beads were then added and the tubes were rotated over night at 4 °C. Coated beads were then pelleted (5 min, 13000 rpm, 4 °C) and supernatant was kept to monitor how much of the input was bound to the beads. The beads were then washed two more times before they were equally split into at least two tubes. In one tube the beads were resolved in DPBS/1 % mouse serum and rotated over night at 4 °C for blocking and then used as control Ova-beads (OB). Meanwhile, the second batch of Ova-coated beads was additionally coated with Anx by rotation over night at 4 °C and washed three times. Again, samples from before and after coating were kept to monitor coating efficiency. Finally, Ova-Anx-beads (OAB) were blocked over night in DPBS/1 % mouse serum. All coated beads were stored in DPBS/1 % mouse serum at 4 °C.
The ratio between Ova and Anx was calculated with the number of molecules that should attach to the beads assuming 100 % efficiency. This means that OAB 20 should harbour 20-fold more Anx molecules than Ova molecules. For OAB 20 this would translate to 2 ng Ova/10^6 beads and 29,7 ng Anx/10^6 beads.

3.5.2 Bead analysis

Beads were analysed after production to control successful coating but also regularly and prior the every experiments to ensure stable binding and to monitor bead concentrations. The bead production was initially controlled by western blot analysis as described in 3.3.1.5. However, this type of analysis was rather indirect and could be improved by using FITC-labelled Ova which allowed analysis by fluorescence measurements. For FC analysis the beads were diluted 1:100 and stained with α-Anx-APC. FC analysis provided fluorescence intensity measures for Ova and Anx per bead and hence visualised protein binding in general. Furthermore, it allowed to control stability of coating of the same bead charge over time and also to compare coating between different bead charges. However, quantification was not possible with this method. In order to quantify the amount of Ova on the beads and also to analyse the input and output samples that were obtained during the production, fluorescence was measured with a plate reader (GloMax, blue filter (excitation 490 nm)). Using a standard curve of Ova-FITC, the amount of Ova-FITC in the samples from the bead production and in a defined volume of bead solution could be calculated. Combining this measurement with a bead count (as described in the next paragraph), allows quantification of Ova-FITC per bead and accordingly coating efficiency.
Bead quality and concentration was controlled prior to every experiment to ensure similar bead numbers and consequently similar amounts of antigen for cell treatment. The bead concentration was determined by counting the beads with TruCount tubes. These tubes contain a pellet with a defined number of labelled beads. Solving this pellet in a defined volume allows to calculate which sample volume was measured with FC and hence allows

the correlation of the number of events measured by FC with a volume. In addition to the counting prior to the assay, samples from the bead solutions prepared for cell treatment were analysed post assay using the GloMax plate reader as described above to control once more whether cells received similar amounts of Ova.

3.5.3 Nanoparticles

Nanoparticles (NP) were produced by Nanovex Biotechnologies S.L.. The nanoparticles were made of poly(D,L-lactide-co-glycolide) (PLGA) with a L/G ratio of 50:50 and surface modification with PEI. Ova was encapsulated in the NP while Anx was covalently bound to PEI on the NP surface. ONP were characterised with a diameter of 222.4 nm, a ζ-potential of 45.2 mV and 0.5 μg Ova/mg NP. OANP were characterised with a diameter of 247.7 nm, a ζ-potential of 19.9 mV, 0.5 μg Ova/mg NP and 6.7 μg Anx/mg NP corresponding to a molecule ratio of 1:18 (Ova:Anx).

4 Results

4.1 Effects of soluble Anx on BMDC cytokine secretion

Annexins and in particular the annexin A1 core domain (Anx) was recently described to have tolerogenic functions.[80,82] To further analyse the tolerogenic capacity of Anx on BMDC, an *in vitro* suppression assay including apoptotic JE6.1 cells (aJ) as positive control was established (fig. 3A). As expected, cytokine suppression by aJ was observed in all performed experiments. Representative examples of IL-12 (fig. 3B) and IL-6 (fig. 3C) production show that aJ are able to keep the cytokine production at the baseline level of untreated cells or even repress it to undetectable levels. For unstimulated BMDC, Anx showed a suppressive activity comparable to aJ. Upon BMDC stimulation of the BMDC, Anx was however not as potent as aJ. Nonetheless, Anx reduced IL-6 secretion signific-

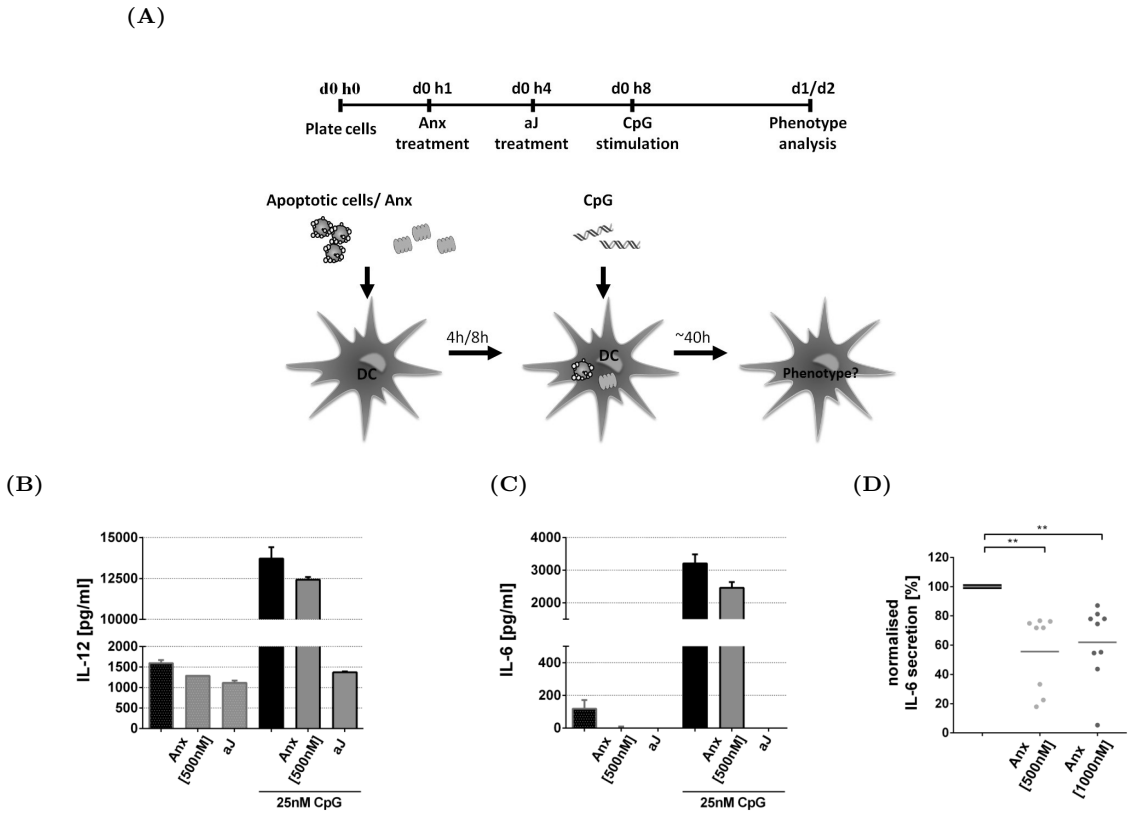

Figure 3: Suppression BMDC cytokine production following incubation with apoptotic cells or Anx. (A) BMDC were pre-treated with apoptotic JE6.1 cells (aJ) or Anx for 4 h and 8 h, respectively, before they were stimulated with CpG. (B+C) BMDC were pre-treated as illustrated in A and either left unstimulated or stimulated with CpG as indicated. Cytokine secretion was analysed *via* ELISA using supernatants (SN) that were collected after 2 days. (D) Nine individual experiments were summarised by normalising the IL-6 secretion to the IL-6 concentration in the supernatants of cells only stimulated with CpG, without pre-treatment (reference condition). The different Anx concentrations were analysed in separate experiments, however equally normalised to their respective reference condition. Significance was calculated using paired t-test (* $p<0.05$, ** $p<0.01$, *** $p<0.001$).

antly to approximately 60 % of the response seen in BMDC stimulated with CpG in the absence of any pre-treatment (fig. 3D).

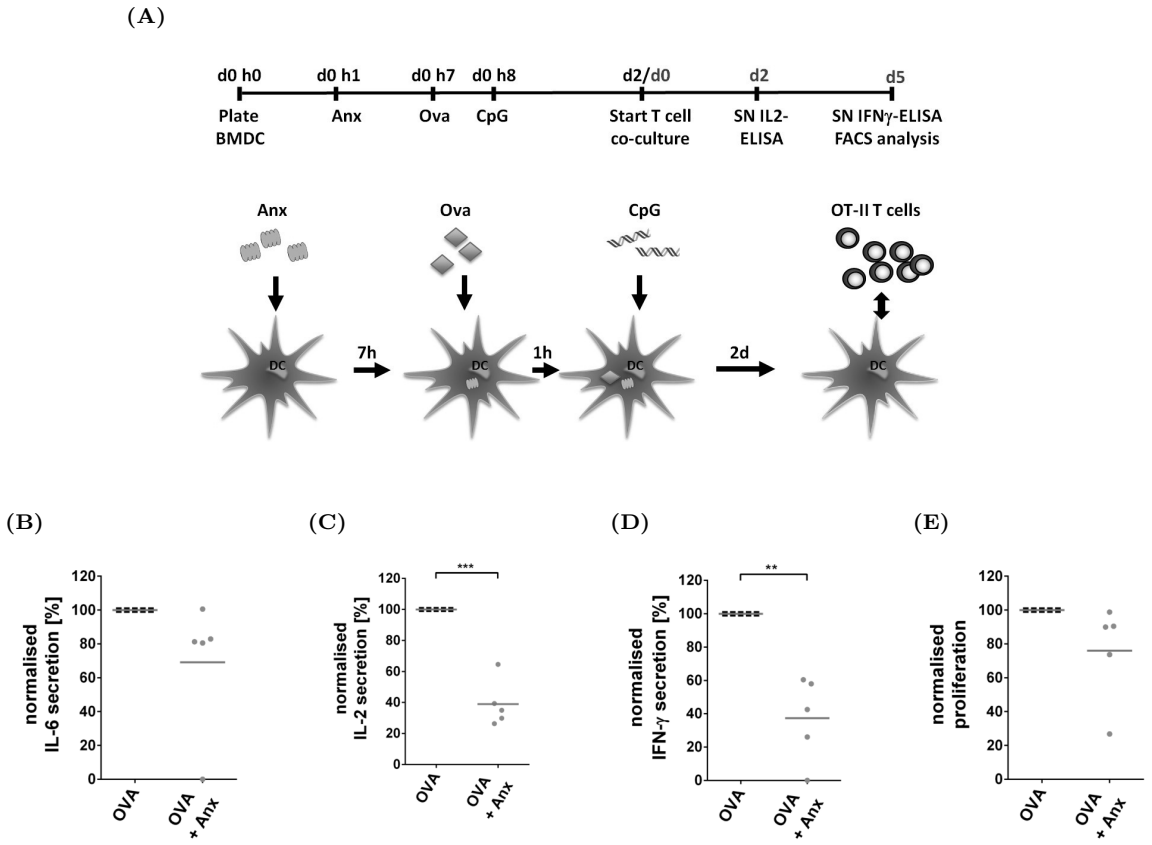

Figure 4: Reduction of Ova-specific T cell stimulation following pre-incubation with soluble Anx. (A) BMDC were pre-incubated for 7 h with Anx [1000 nM] before Ova [10 μg/ml] and, 1 h later, CpG were added. 2 days after treatment of the BMDC, CFSE-labelled OT-II T cells were added and co-cultured for a total of 5 days before the T cells were harvested for FC analysis. Supernatants for cytokine analysis were collected before T cells were added and on day 2 and day 5 of co-culture. (B) BMDC were treated as illustrated in A and supernatants collected before T cells were added were used to measure IL-6 production from BMDC. (C) Following 2 days of co-culture IL-2 production was analysed *via* ELISA. (D) Following 5 days of co-culture, IFN-γ production was measured *via* ELISA. (E) T cells were harvested after 5 days of co-culture and proliferation of the cells was determined by dilution of CFSE measured in FC. (B-E) show summaries of 5 independent experiments each normalised to their respective control (response to Ova alone). Significance was calculated using paired t-test (* $p<0.05$, ** $p<0.01$, *** $p<0.001$).

4.2 Effects of soluble Anx and Anx-beads on antigen-specific T cell responses

DC reside in the centre of the immune system and shape T cell responses.[9] Hence, the Anx-mediated inhibition of inflammatory cytokine secretion from DC was hypothesised to influence T cell responses as well. This hypothesis was investigated by expanding the BMDC suppression assay with Ova as antigen and Ova-specific $CD4^+$ T cells (OT-II T cells).

4.2.1 Effects of soluble Anx on Ova-specific T cell responses

The OT-II system was used to evaluate whether BMDC pre-incubation with soluble Anx as seen in figure 3 can influence T cell responses. Induction of OT-II T cell responses requires presentation of the relevant antigen Ova by BMDC. For this reason, the BMDC suppression assay was adjusted by adding recombinant Ova to the Anx-pretreated BMDC 1 h prior to CpG stimulation (fig. 4A). Additionally, the assay was expanded by co-culturing the pre-treated BMDC with CFSE-labelled OT-II T cells which were analysed for cytokine production and proliferation.
The suppression of IL-6 illustrated in figure 3D was maintained in the presence of Ova (fig. 4B). BMDC incubated with Ova and stimulated with CpG provoked a T_H1-like response in OT-II T cells represented by secretion of IL-2 and IFN-γ. Pre-incubation with soluble Anx resulted in a strong reduction of the Ova-specific cytokine response (fig. 4C, 4D) as well as in decreased proliferation (fig. 4E). These results indicate that the tolerogenic function of Anx on BMDC is transferred to $CD4^+$ T cells.

4.2.2 Effects of Anx-beads on Ova-specific T cell responses

The regulatory functions of Anx might be valuable for the development of antigen-specific therapies for autoimmune disease. Anx and Ova as antigen were coupled to polystyrene beads in order to investigate the modulatory capacity of Anx in an antigen-specific context. Details about the bead production and characterisation can be found in 3.5.1 and the supplementary results. Briefly, beads are coated either with Ova alone as reference beads (OB) or coated with Ova and Anx (OAB). All beads are coated with equal amounts of Ova. If not indicated otherwise, Anx is coated in 20-fold excess. To analyse how the T cell response is influenced by the beads, the suppression assay was performed similar to the assays with soluble Anx and is schematically shown in figure 5A. A titration experiment (n=3) with the beads was performed to determine an appropriate bead concentration (fig. 5B-5D). 14×10^6 beads/ml triggered T cell responses that were detectable but not yet in a plateau and thus this concentration was used for further experiments. Figure 5B-5D shows that T cell responses could be inhibited by Anx-bead treatment of BMDC. This

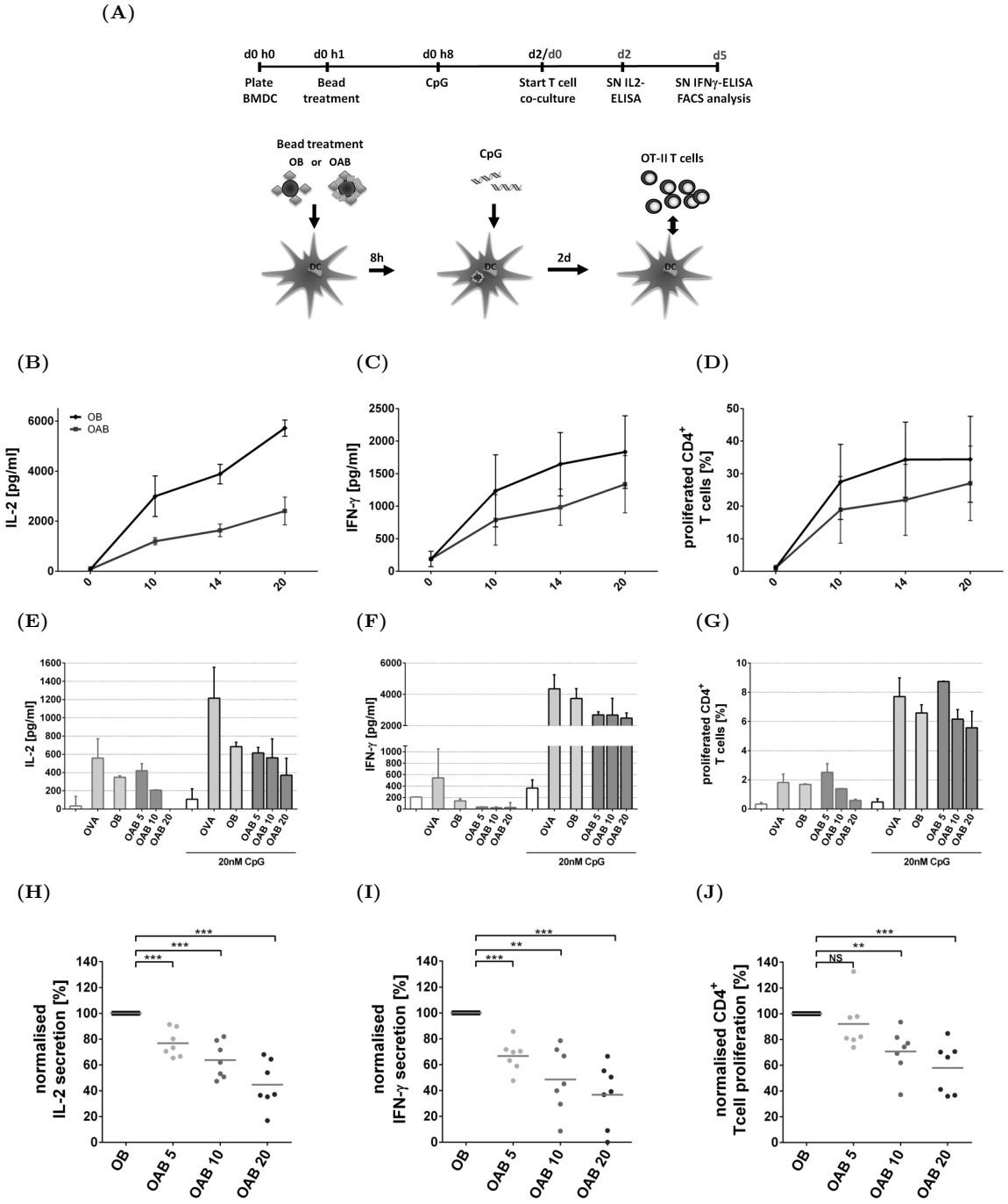

Figure 5: Attenuation of Ova-specific T cell stimulation by Ova-Anx-beads. (A) BMDC were incubated with beads coated with Ova (OB) or OVA and Anx (OAB) before they were stimulated with CpG. CFSE-labelled OT-II T cells were added and co-cultured for 5 days before the T cells were harvested to analyse proliferation by FC. Supernatants for cytokines analysis were collected before T cells were added (for IL-6) and on day 2 (for IL-2) and day 5 (for IFN-γ) of co-culture. (B-D) summarise T cell responses to ascending bead concentrations of 3 independent experiments. (E-J) illustrate the response to increasing amounts of Anx on the bead surface. (E-F) exemplifies the raw data of one experiment including treatment with soluble Ova as positive control and the responses in absence and presence of CpG stimulation. (H-J) show the summary of 7 independent experiments, each individually normalised to the response to the control beads (OB). Significance was calculated using paired t-test (* $p<0.05$, ** $p<0.01$, *** $p<0.001$).

inhibitory effect is further depicted with a representative experiment using OAB with different Anx concentrations (fig. 5E-5G). Beads were coated with a 5-fold (OAB 5), 10-fold (OAB 10) or 20-fold (OAB 20) excess of Anx molecules in relation to Ova molecules. Figure 5E-5G illustrate that T cell responses were decreased in Anx-concentration-dependent manner following co-culture with unstimulated and CpG-stimulated BMDC. This suppressive effect compared to the response to beads with Ova alone was observed reproducibly with a mean reduction of IL-2 secretion to 44.6 % (fig. 5H), mean reduction of IFN-γ secretion to 36.7 % (fig. 5I) and mean reduction of proliferation to 57.9 % (fig. 5J) referring to the highest Anx concentration.

4.2.3 Specificity of the Anx-bead effects

Several control experiments were performed to validate that the suppressive capacity of the Anx-beads shown in figure 5 is mediated specifically by the presence of Anx on the bead surface. First, it was examined whether the beads show any toxicity and whether the beads show any coating-related toxicity. Two separate experiments showed that the beads did not negatively influence BMDC viability irrespective of the coating and the amount of Anx on the bead surface (fig. 6A). T cell viability could be affected by the beads in two different ways: either directly by potentially remaining beads in the culture that have not been taken up by BMDC or indirectly by effects mediated through the bead-treated BMDC. However, no bead-induced cell death of T cells was detected in two independent experiments (fig. 6B). Viability was analysed in experiments performed in parallel with suppression assays, suggesting that inhibited T cell responses are not associated with increased cell death.

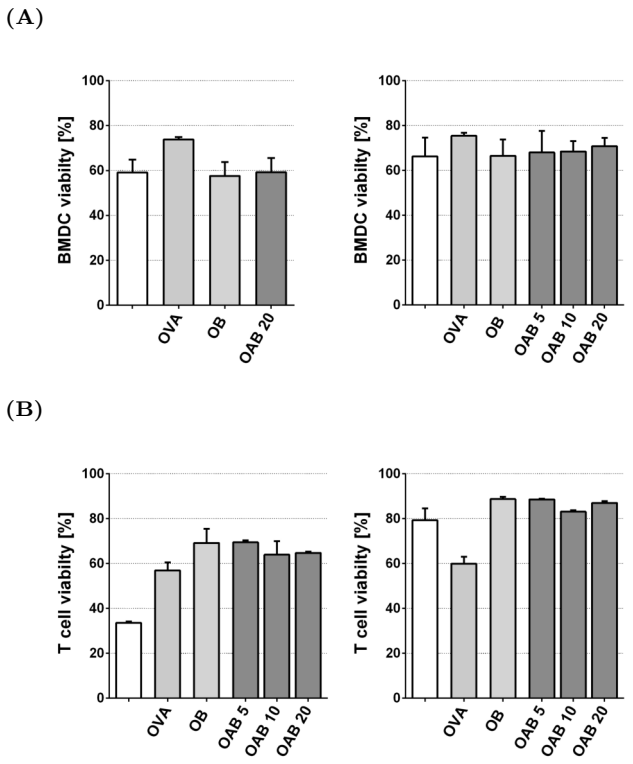

Figure 6: Viability of BMDC and T cells is not impaired by beads. Cell viability was analysed using 7-AAD staining to determine the percentage of living cells in the whole cell population. (A) BMDC were pre-incubated with Ova [10 μg/ml] or beads [14 x 10^6/ml] prior to CpG stimulation. 2 days after treatment, BMDC were harvested and stained for CD11c and with 7-AAD to measure dead cells in the $CD11c^+$ compartment. (B) OT-II T cells were harvested after 5 days of co-culture with pre-treated BMDC and stained for CD4 and with 7-AAD to measure cell death in the $CD4^+$ compartment.

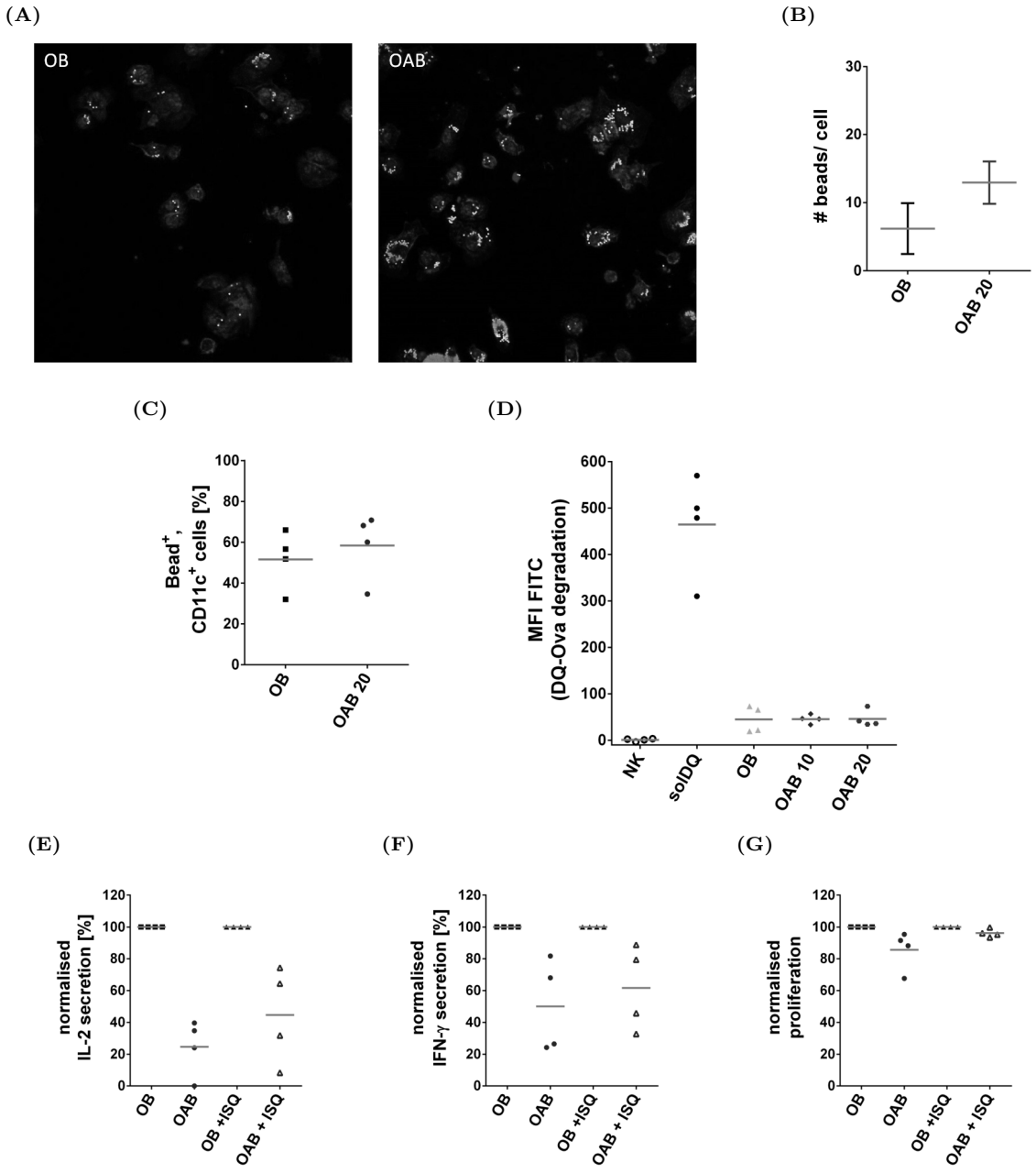

Figure 7: Bead uptake, Ova processing and Ova presentation are not significantly altered by Anx. (A+B) BMDC were incubated over night with beads [7.5×10^6/ml] and then fixed and stained for microscopy. Representative images of the bead uptake by BMDC are shown in A (yellow: beads; blue: hoechst, red: phalloidin) and the number of beads per cell quantified over 17 images per condition is shown in B. (C) BMDC were pre-treated treated with fluorescent beads [14×10^6/ml] and stimulated with CpG. 2 days later, BMDC were harvested, stained for CD11c and their bead content was analysed by FC. Dots represent independent experiments. (D) BMDC were incubated with soluble DQ-Ova [10 μg/ml] or beads coated with DQ-Ova ± Anx for 3 h at 37°C and 4°C in parallel. Cells were then harvested and Ova degradation was evaluated in FC. The background as determined by the signal measured at 4°C was subtracted in each of the 4 independent experiments. (E-G) BMDC were pre-treated as described for C and co-cultured with CFSE-labelled OT-II T cells. For the indicated conditions, ISQ [0,005 μM] was added at least 30 min prior to the T cells. (E) After 2 days of co-culture, IL-2 production was analysed by ELISA. (F) After 5 days of co-culture, IFN-γ production was measured by ELISA. (G) and proliferation of harvested T cells was determined by FC (G). To allow direct comparison, results were normalised to OB or OB + ISQ, respectively.

Next, the uptake of the beads by BMDC was analysed by microscopy (fig. 7A, 7B) and FC (fig. 7C). A yellow fluorescent variant of the polystyrene beads was used to visualise phagocytosed beads. Due to the strong fluorescent signa of the yellow bead variant, BMDC were treated over night with a reduced bead concentration before they were fixed and stained for microscopy. Nuclei and beads were counted separately to calculate the average number of beads per cell for each image. The summary of the images of one experiment demonstrate similar bead content in cells incubated with either OB or OAB (fig. 7B). Uptake was additionally analysed 2 days following bead treatment using the assay setup described in figure 5A by measuring what proportion of $CD11c^+$ cells were positive for the fluorescent signal of the beads (fig. 7C). The number of beads taken up per cell could not be estimated because the fluorescent signal of the beads was too high. Nevertheless, the FC analysis supports the microscopy data in figure 7B demonstrating that Anx-coating did not significantly alter uptake of the beads. These results exclude that the reduced T cell responses described above caused by reduced availability of Ova in the BMDC.

Anx might influence Ova processing and presentation, which could lead to less antigen presentation and hence less T cell activity. An Ova protein variant which is coupled to a processing sensitive dye (DQ-Ova) was utilised to evaluate processing in absence and presence of Anx. DQ is quenched as long as the protein is intact but upon degradation to smaller peptides the dye emits a fluorescent signal. Processing of DQ-Ova was neither affected by the presence of 10-fold nor 20-fold excess of Anx on the bead surface (fig. 7D). Presentation of Ova in the context of MHC II is difficult to measure directly due to the lack of an antibody recognising the Ova-MHC II complex. ISQ was added to BMDC prior to co-culture with OT-II T cells to indirectly assess whether T cell responses are reduced due to differential antigen presentation or due to active modulation of the T cell by the DC. The Ova peptide ISQ can be loaded into MHC II directly from the outside of the cell and is independent of uptake and processing [216]. The external loading with ISQ can override any potential difference in antigen presentation on BMDC following bead incubation. As illustrated in figure 7E-7G, T cell responses were similarly decreased by OAB as compared to OB in absence and presence of ISQ. It should be noted that the addition of ISQ did increase the T cell response which may account for differences in the suppression. The stimulatory effects of ISQ are not represented in the graphs since the response was normalised to the respective controls. Figure 7 demonstrates that T cells are actively modulated by BMDC-intrinsic mechanisms induced by Anx-coated beads and not by differences in antigen presentation.

4.3 Effects of soluble Anx and Anx-beads on BMDC phenotype

Anx attenuates T cell responses in soluble and particulate form. This is however an indirect effect on T cells mediated through the bead-treated BMDC. How the beads modulate the BMDC phenotype is addressed in the following sections.

4.3.1 T cell suppression in the context of BMDC cytokine suppression

Based on the initial finding that soluble Anx can repress the secretion of inflammatory cytokines (fig. 3), it can be hypothesised that the altered cytokine profile modulates the T cell response. However, in one experiment soluble Anx failed to suppress IL-6 production in BMDC while the inhibitory effect on T cell level was maintained (fig. 8A-8D). Furthermore, suppression of IL-6 or IL-12 secretion was never observed for bead-bound Anx (fig. 8E, 8F) despite the fact that T cell responses were diminished in all corresponding experiments (fig. 5). This indicates, that in contrast to soluble Anx, bead-bound Anx is not capable of suppressing inflammatory BMDC cytokines. Moreover, this data shows that T cell inhibition is independent of BMDC cytokine suppression.

While decreased inflammatory cytokine levels were negligible for the modulation of T cell responses, anti-inflammatory cytokines and mediators might be involved. IL-10 and TGF-β secretion by BMDC was not detectable 2 days following Anx or bead

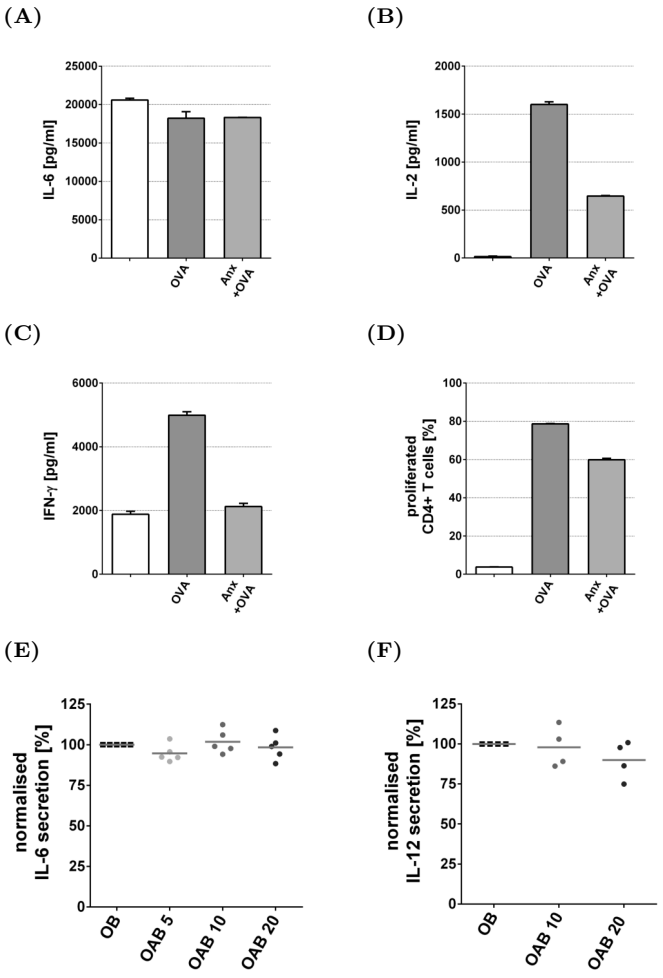

Figure 8: Diminished T cell responses are independent of BMDC cytokine suppression. (A-D) BMDC were pre-incubated for 7 h with Anx [1000 nM] before Ova [10 μg/ml] and 1 h later CpG were added. CFSE-labelled OT-II T cells were added and co-cultured for 5 days before the T cells were harvested to evaluate proliferation by FC (D). Supernatants for cytokines analysis were collected before T cells were added (A) and on day 2 (B) and day 5 of co-culture (D). (A-D) show results from a single experiment with triplicates for every condition. (E+F) BMDC were pre-incubated with beads an then stimulated with CpG. 2 days later supernatants were collected for ELISA. The data was normalised to the control-beads (OB) and corresponds to the data shown in figure 5H-5J.

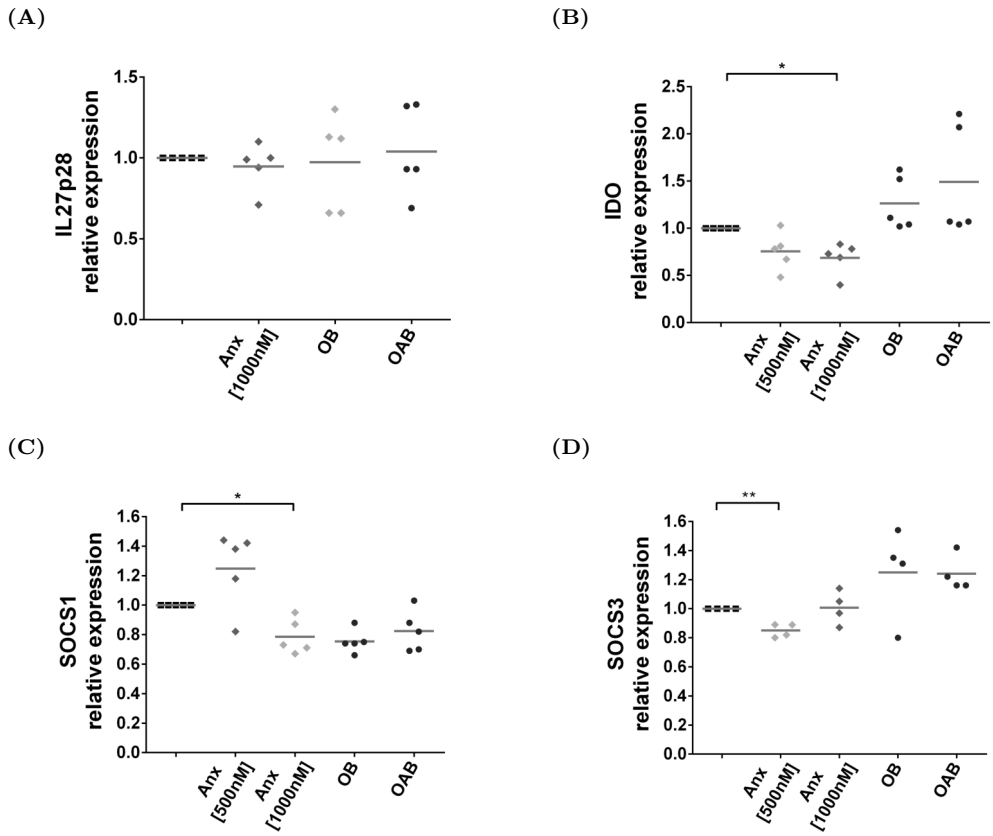

Figure 9: Expression of IL27, IDO, SOCS1 and SOCS3 was not modulated by Anx. BMDC were incubated with soluble Anx or beads [14×10^6/ml] for 4 h before cells were harvested. RNA was extracted from the cell lysates and analysed by qRT-PCR. Gene regulation was assessed with the ΔΔCT method and using HMBS as reference gene. The lower Anx concentration (500 nM) was analysed in separate experiments but equally normalised to their respective reference condition. Experiments were performed in parallel to T cell suppression assays. Dots indicate independent experiments and significance was calculated using paired t-test of log2 transformed data (* $p<0.05$, ** $p<0.01$, *** $p<0.001$).

treatment (data not shown). Additional anti-inflammatory cytokines and mediators were analysed on mRNA level. While T cell suppression was observed in parallel, neither the IL-27 subunit IL27p28 nor IDO was upregulated by Anx or Anx-beads (fig. 9A, 9B). SOCS1 and SOCS3 are known negative regulators in DC.[76] Besides regulating the response to exogenous cytokines they are also downstream targets of modulatory receptors and thus a potential target of Anx. However, gene expression of SOCS1 and SOCS3 was not altered by Anx in soluble or particulate form (fig. 9C, 9D).

The impact of soluble mediators was further examined by washing the BMDC prior to co-culture with OT-II T cells. Exchanging the BMDC medium before the T cells are added removes all soluble mediators secreted by BMDC in response to the beads. Figure 10 shows T cell responses to washed BMDC in a representative experiment. The lack of soluble factors like pro-inflammatory cytokines produced by the BMDC in response to CpG leads to a reduced T cell activity independent of any pre-treatment. Nevertheless, the suppression of T cell cytokine secretion and proliferation by OAB is sustained indicating

that Anx-mediated T cell suppression does not rely on the cytokine profile of BMDC.

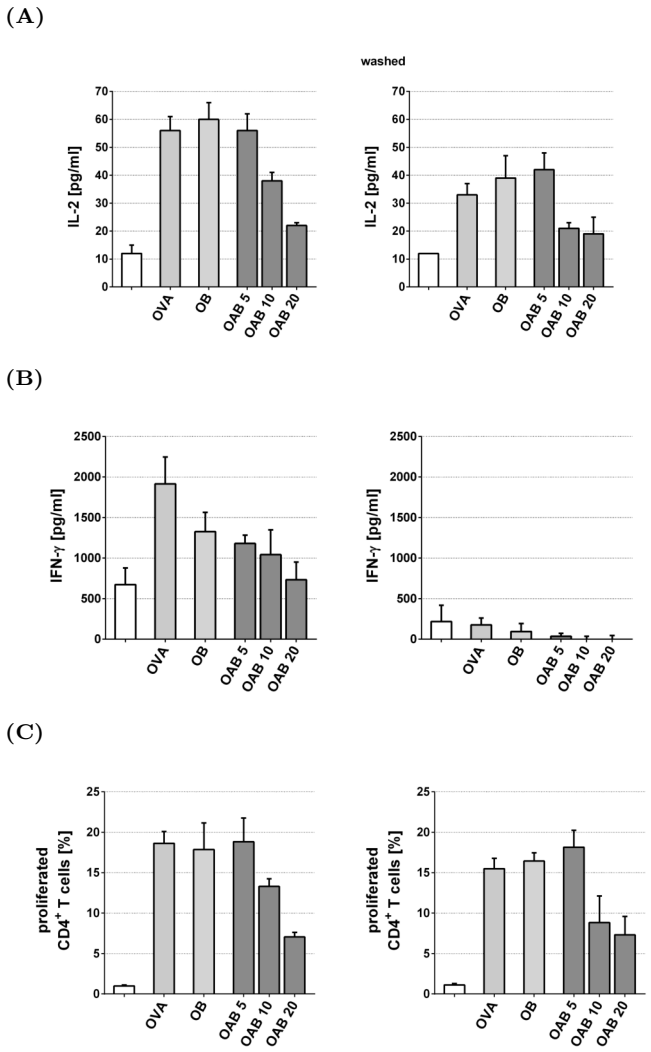

Figure 10: Soluble mediators have a minor role for T cell suppression by beads. BMDC were incubated with beads before they were stimulated with CpG. 2 days after the treatment, CFSE-labelled OT-II T cells were either added directly (left panel) or BMDC were washed before the OT-II T cells were added (right panel). (A) IL-2 production was measured after 2 days of co-culture. (B) IFN-γ production was measured after 5 days of co-culture. (C) Proliferation was measured after 5 days of co-culture.

4.3.2 Effects on BMDC surface marker expression

Anx-mediated T cell suppression might be induced in cell-cell contact-dependent manner, hence, the surface expression of co-stimulatory and co-inhibitory molecules on BMDC was analysed. Apoptotic cells attenuated the activation-induced upregulation of MHC II and the co-stimulatory molecules CD40 and CD86 (fig. 11A-11D). Neither 500 nM nor 1000 nM soluble Anx was able to reproduce this effect (fig. 11E-11G). Interestingly, apoptotic cells also impaired the upregulation of the co-inhibitory molecule PD-L1 (fig. 11D). A slight decrease in PD-L1 expression was also seen in BMDC pre-incubated with 1000 nM Anx but the effect was not significant (fig. 11G). The surface expression of additional stimulatory and inhibitory molecules, including CD80, ICOSL, PD-L2 and ILT3, was ex-amined on BMDC. None of analysed markers were affected by soluble Anx (fig. 11H-11K).

The surface marker panel used in figure 11 was also analysed following pre-incubation with beads (fig. 12). The bead material itself influences the expression of BMDC surface markers. Both OB- and OAB-treated BMDC showed a more stimulatory phenotype than non-bead-treated BMDC with increased MHC II, CD40, CD86 and CD80 levels (fig. 12A-12C, 12G) and decreased PD-L1 and ILT3 levels (fig. 12D, 12F). Although a slight increase in CD40, PD-L2 and ICOSL expression was detected in OAB-treated BMDC (fig. 12B, 12E, 12H), none of the analysed markers were altered significantly in OAB-treated com-

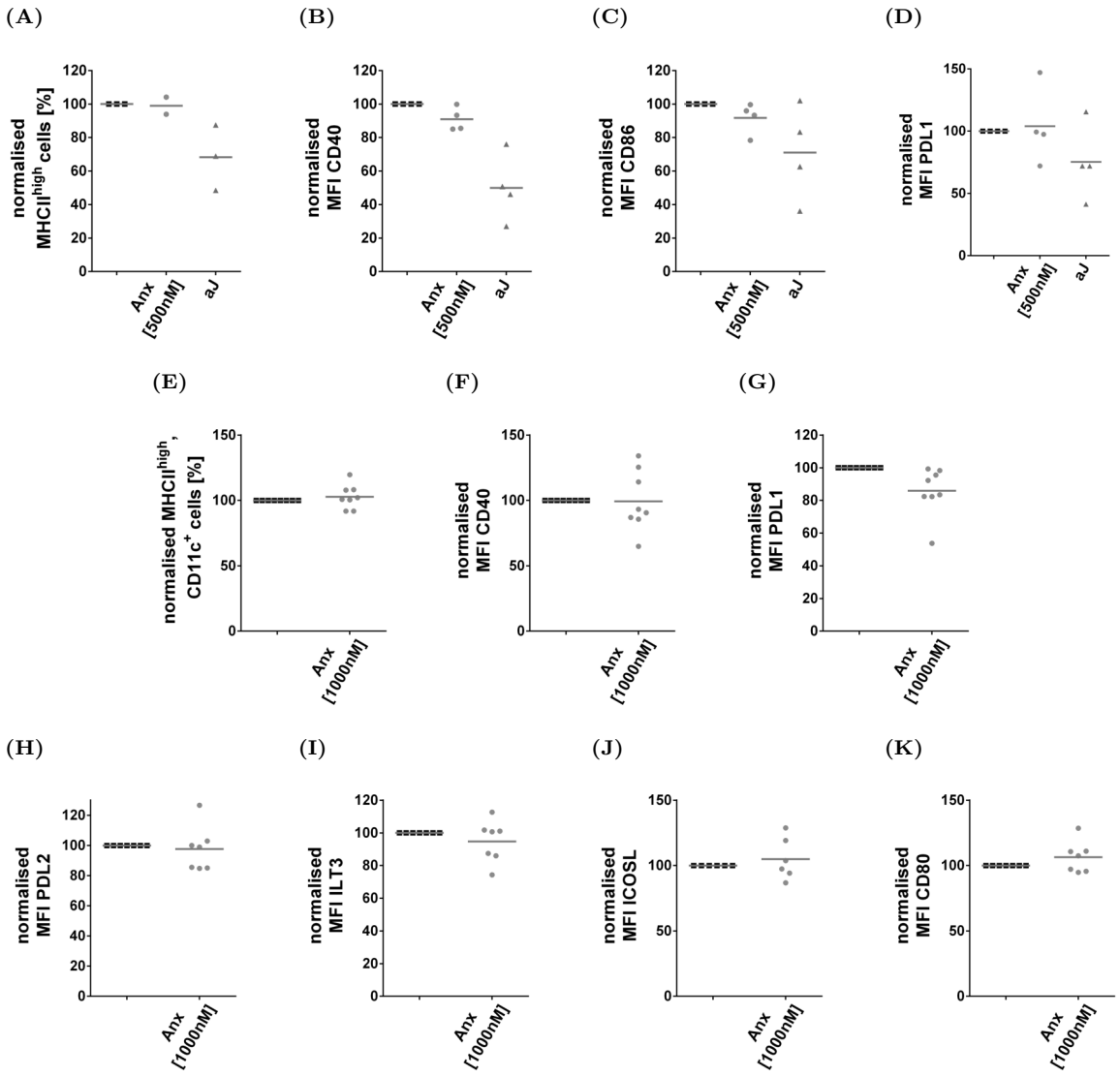

Figure 11: Alterations in BMDC surface marker expression by apoptotic cells and soluble Anx. BMDC were pre-incubated with Anx or apoptotic JE6.1 cells (aJ) and stimulated with CpG. On the following day (E-K) or after 2 days (A-D), BMDC were harvested and stained for FC analysis. Surface marker expression is shown for pre-gated $CD11c^+$ BMDC with each dot representing an independent experiment.

pared to OB-treated BMDC.

4.3.3 Effects on ROS production

Reactive oxygen species (ROS) were long considered to be harmful. However, in the last decade ROS like H_2O_2 were recognised as important modulators of diverse signalling pathways. Furthermore, ROS are implicated in T cell hyporesponsiveness. [217,218] Whether Anx can cause ROS production was investigated using DCFDA, a molecule that becomes fluorescent upon oxidation. Soluble Anx induced ROS production in BMDC peaking 2 h after treatment (fig. 13A). In In contrast to an oxidative burst as seen after PMA treatment, Anx provoked a low ROS signal (mean 25.8 % specifc MFI increase) which is

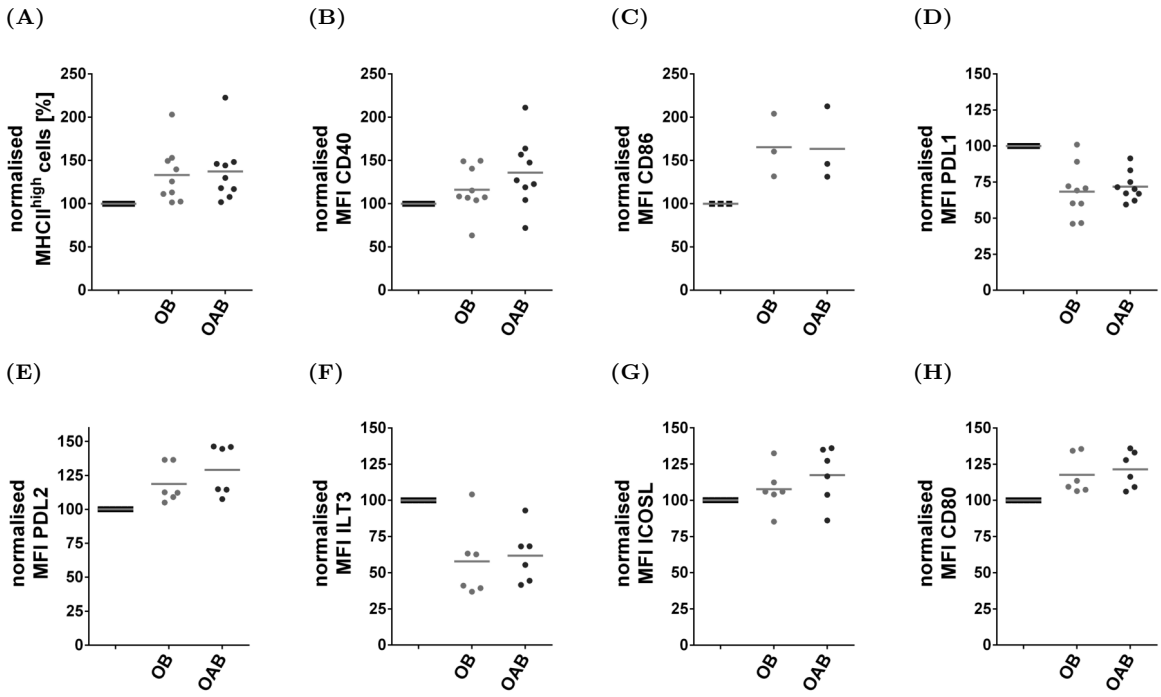

Figure 12: Alterations in BMDC surface marker expression by beads. BMDC were pre-incubated with beads before and stimulated with CpG. On the following day, BMDC were harvested and stained for FC analysis. T cell suppression was analysed in parallel. Surface marker expression is shown for pre-gated $CD11c^+$ BMDC with each dot representing an independent experiment.

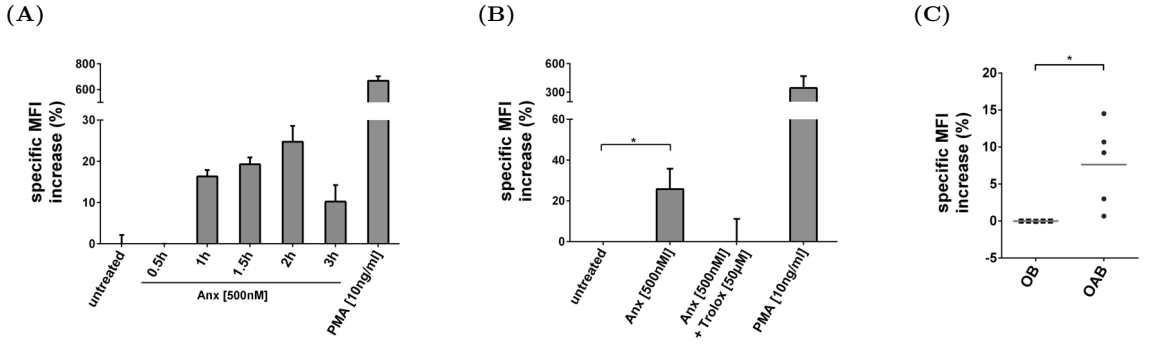

Figure 13: ROS production is increased by soluble Anx and Anx-beads. BMDC were treated with the listed substances for 2 h (or as indicated) and incubated with DCFDA in the last 30min of the treatment. ROS production is shown relative to untreated cells or a reference condition. (A) Kinetic of the Anx-induced ROS production measured in triplicates. (B) Summary of 4 independent experiments including pre-treatment with the ROS scavenger Trolox 10 min prior to the addition of Anx. (C) BMDC were treated with beads [14×10^6/ml] and ROS production normalised to control-beads (OB). Dots indicate independent experiments. Significance was calculated using paired t-test (* $p<0.05$, ** $p<0.01$, *** $p<0.001$).

suitable to modulate signalling without killing the cell [219]. The Anx-induced ROS was specifically blocked by the ROS scavanger Trolox (fig. 13B). Beads did also induce ROS production and despite the increased background ROS in OB-treated cells, the signal was further elevated with OAB (fig. 13C). This data shows that both soluble and bead-bound Anx induce ROS generation which might have modulatory effects on BMDC and T cells.

4.4 Effects of soluble Anx and Anx-beads on T cell phenotype

Soluble Anx and Anx-beads modulate Ova-specific T cell responses as demonstrated in the previous figures. The following section addresses the T cell phenotype and the potential mode of tolerance induced by Anx-treated BMDC.

4.4.1 Effects on T cell cytokine production

The T cell cytokine profile provides information about the T cell subtype. The presentation of Ova by BMDC (unstimulated as well as CpG-stimulated) results in differentiation of OT-II T cells into T_H1 cells, characterised by IFN-γ secretion. Alternative differentiation or conversion into T_H2 cell was not observed, since IL-4 was neither detectable in untreated nor bead-treated conditions (data not shown). Reduced production of IL-2, IFN-γ (fig. 5) and TNF-α (fig. 14A), a pro-inflammatory cytokine involved in the pathogenesis of asthma and allergy, indicates that Anx-beads attenuate pro-inflammatory cytokine responses from T cells. Whether T cells additionally gained anti-inflammatory functions was investigated by measuring secretion of IL-10 and TGF-β, which are associ-

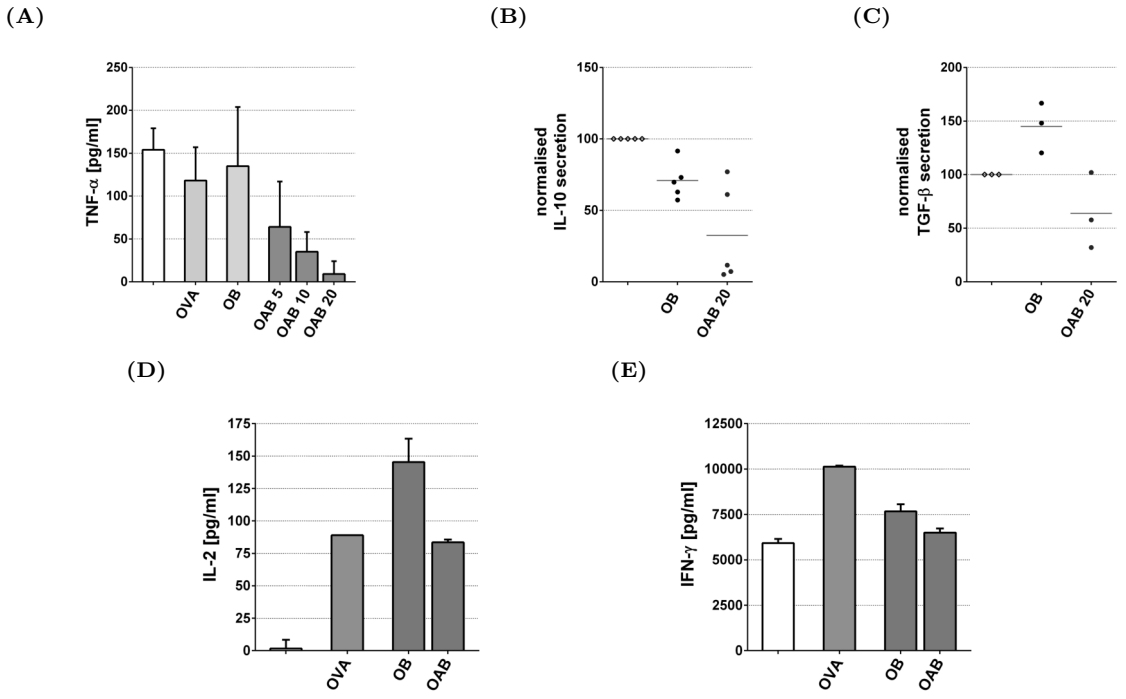

Figure 14: Global T cell cytokine suppression by Anx-beads. (A-C) BMDC were pre-incubated with Ova or beads prior to stimulated with CpG. CFSE-labelled OT-II T cells were co-cultured with treated BMDC for 5 days and cytokine production was measured by ELISA. (A) TNF-α production was evaluated in triplicates.(B+C) Cytokine production was normalised to the non-pre-treated but CpG-stimulated condition and summarised with each dot representing an independent experiment. (D+E) BMDC were pre-incubated with Ova or beads prior to stimulated with CpG. Activated OT-II T cells were co-cultured with treated BMC and cytokine production was measured after 2 days (D) or 5 days (E) by ELISA. D + E show results from one experiment, performed with triplicates for each condition.

ated with regulatory T cell subtypes (fig. 14B, 14C). IL-10 and TGF-β levels were low in OT-II T cells following co-culture with BMDC and pre-treatment with Anx-beads further diminished the secretion of these cytokines (fig. 14B, 14C). These results suggest a global suppression of cytokine production including both pro- and anti-inflammatory cytokines. Furthermore, cytokine secretion was also found to be inhibited in preliminary experiments with pre-activated T cells (fig. 14). Co-culturing bead-treated BMDC with OT-II T cells that were pre-activated with αCD3/αCD28 resulted in reduced IL-2 and IFN-γ levels as exemplified in figure 14D and 14E.

4.4.2 Effects on T cell surface marker expression

Although anti-inflammatory cytokines like IL-10 or TGF-β are common mediators of tolerance, regulatory T cell subsets utilise several effector mechanisms in addition to these cytokines. For instance, FoxP3$^+$ Treg are described to rely on contact-dependent mechanisms rather than cytokine secretion.[107,108] Hence, tolerogenic properties including the expression of FoxP3 and co-inhibitory molecules were investigated. Activation of OT-II T cells by BMDC treated with soluble Ova or beads decreased the proportion of FoxP3$^+$ cells and Anx-beads were neither able to initiate FoxP3 expression nor to prevent the

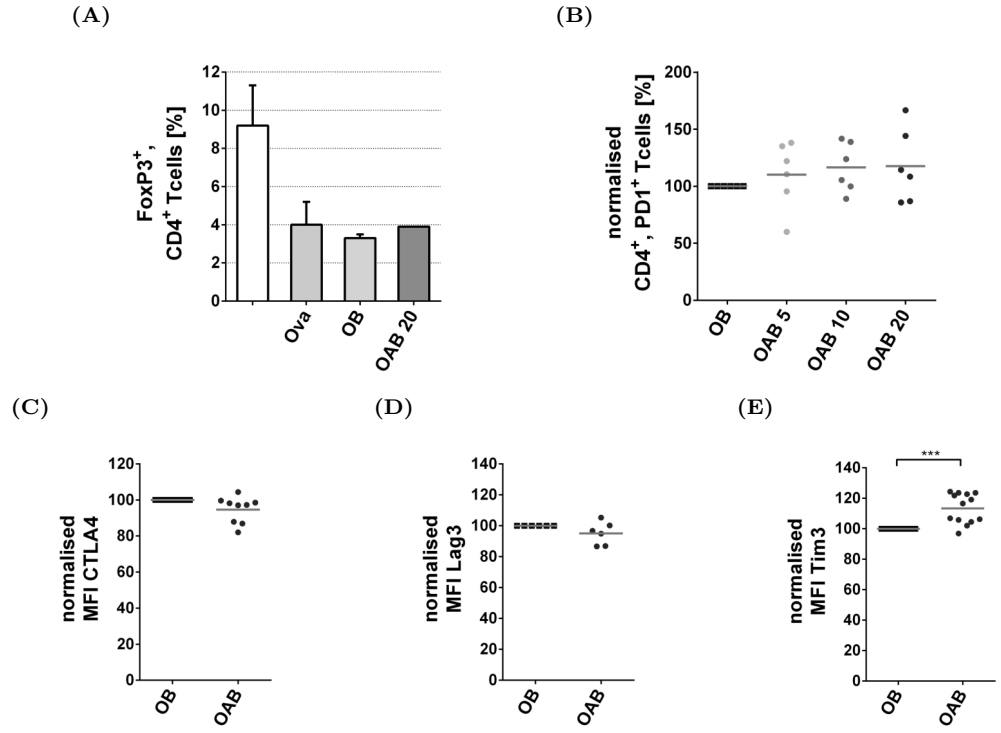

Figure 15: Anti-inflammatory marker are scarcely influenced by Anx-beads. BMDC were pre-incubated with Ova or beads prior to stimulated with CpG. CFSE-labelled OT-II T cells were co-cultured with treated BMDC. (A) Following 7 days of co-culture, T cells were harvested and analysed for FoxP3 expression by FC. The bars show mean and SD of 2 independent experiments. (B-E) Following 5 days of c-culture, T cells were harvested, stained for the indicated surface molecules and analysed by FC. MFIs of each experiment were normalised to the MFI of the respective reference condition (OB). Significance was calculated using paired t-test (* $p<0.05$, ** $p<0.01$, *** $p<0.001$).

activation-related reduction in FoxP3 expression (fig. 15A).

A variety of co-inhibitory receptors affect tolerance induction and maintenance. PD-1 and CTLA-4 are crucial for peripheral tolerance while Tim-3 and Lag-3 are often described to cooperate with other molecules to support tolerance. Thus, these receptors might also contribute to Anx-bead mediated effects on T cells. However, the surface expression of PD-1, CTLA-4 and Lag-3 was not modulated in OT-II T cells following co-culture with Anx-bead-treated BMDC (fig. 15B-15D). Tim-3 was significantly modulated by Anx-beads (fig. 15E). The average increase in the MFI of Tim-3 in the $CD4^+$ T cell compartment was 13.3 %. It should however be noted that only a small subset of maximally 20 % of OT-II T cells were Tim-3 positive.

4.4.3 Evaluation of anergy-related characteristics

T cell tolerance is often described in three categories: T cell deletion, T cell anergy and Treg cells. Anergy is a state of unresponsiveness, mainly described by attenuated prolifer-

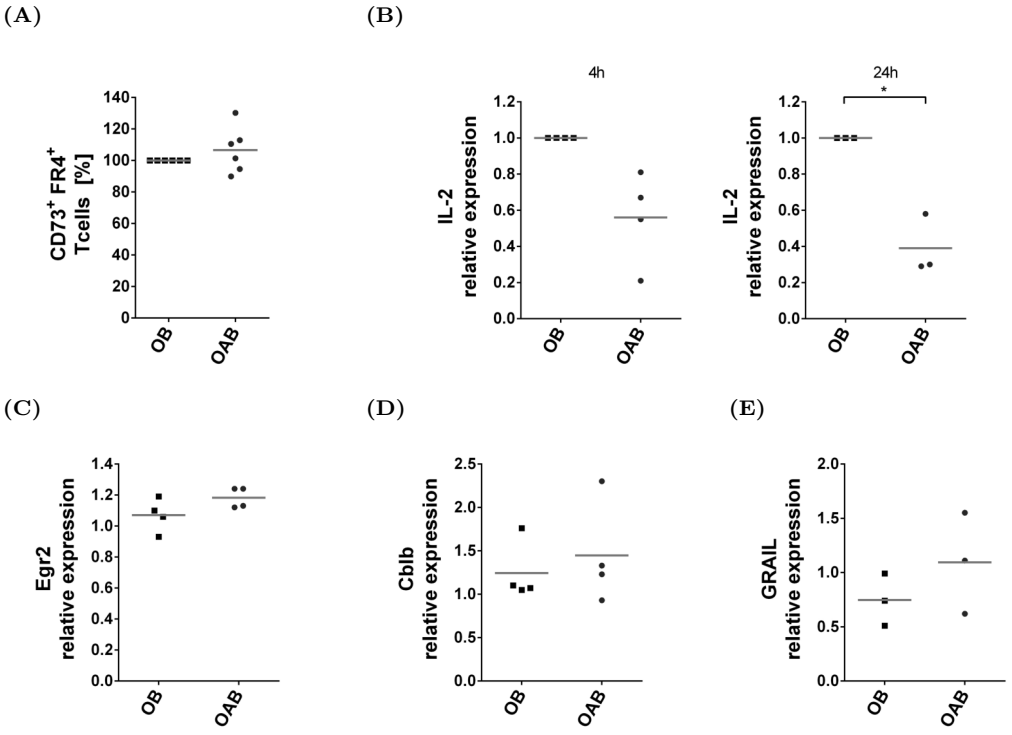

Figure 16: An anergic phenotype is only partly observed in Anx-bead treated T cells. BMDC were pre-incubated with Ova or beads prior to stimulated with CpG. CFSE-labelled OT-II T cells were co-cultured with treated BMDC. (A) Following 5 days of co-culture, T cells were harvested, stained for the indicated surface molecules and analysed by FC. Each experiment was normalised to the respective reference (OB). (B-E) If not stated otherwise, T cells were harvested after 4 h of co-culture to analyse gene expression *via* qRT-PCR using HPRT as reference gene. (B) IL-2 expression was analysed after 4h (left) and 24h (right) and is shown relative to the expression in the OB condition. (C-E) Expression of the indicated genes is illustrated relative to the expression of T cells co-cultured with non-pre-treated but CpG-stimulated BMDC. Dots indicate independent experiments and significance was calculated using paired t-test of log2 transformed data (* $p<0.05$, ** $p<0.01$, *** $p<0.001$).

ation and cytokine production.[87] These properties were observed in OT-II T cells following co-culture with Anx-treated BMDC (fig. 4, fig. 5). In order to test the hypothesis that Anx-beads induce T cell anergy, additional markers associated with an anergic phenotype were analysed (fig. 16).

Some publications describe a anergic T cell population *in vivo* which is double-positive for CD73 and FR4 surface marker expression.[105,220] Anx-bead treatment did not result in a significant increase of the $CD73^+$, $FR4^+$ subpopulation in OT-II T cells *in vitro* (fig. 16A). A hallmark of anergy is impaired IL-2 transcription.[87,221] In addition to reduced IL2 secretion demonstrated in figure 5, co-culture of T cells with Anx-bead treated BMDC led to significantly decreased IL-2 mRNA expression after 24 h (fig. 16B). The same trend was observed after 4 h. IL-2 transcription requires both TCR and CD28 signalling. The lack of co-stimulation *via* CD28 results in an alternative transcription programme including Egr2 expression which in turn enhances the expression Cblb and GRAIL. All three mentioned factors are implicated in T cell anergy[87,221,222] and were thus analysed in OT-II T cells 4 h after co-culture with bead-treated BMDC (fig. 16C-16E). The increase in expression of Egr2, Cblb and GRAIL following Anx-bead treatment is not significant and quantitatively not comparable with gene expression profiles of anergic T cells found in literature[98,99,101,102,223,224]. Similarly, soluble Anx mediated a decrease in IL-2 transcription while the other anergy-associated genes tested were unaffected (fig. S6).

4.5 *In vivo* effects of Anx-beads

Anx-beads were able to suppress T cell responses *in vitro* and it was investigated whether this effect can be reproduced *in vivo*.
Mice were first treated with the control-beads (OB) to estimate an appropriate bead concentration for further *in vivo* experiments (fig. 17A). 6 days after treatment, the

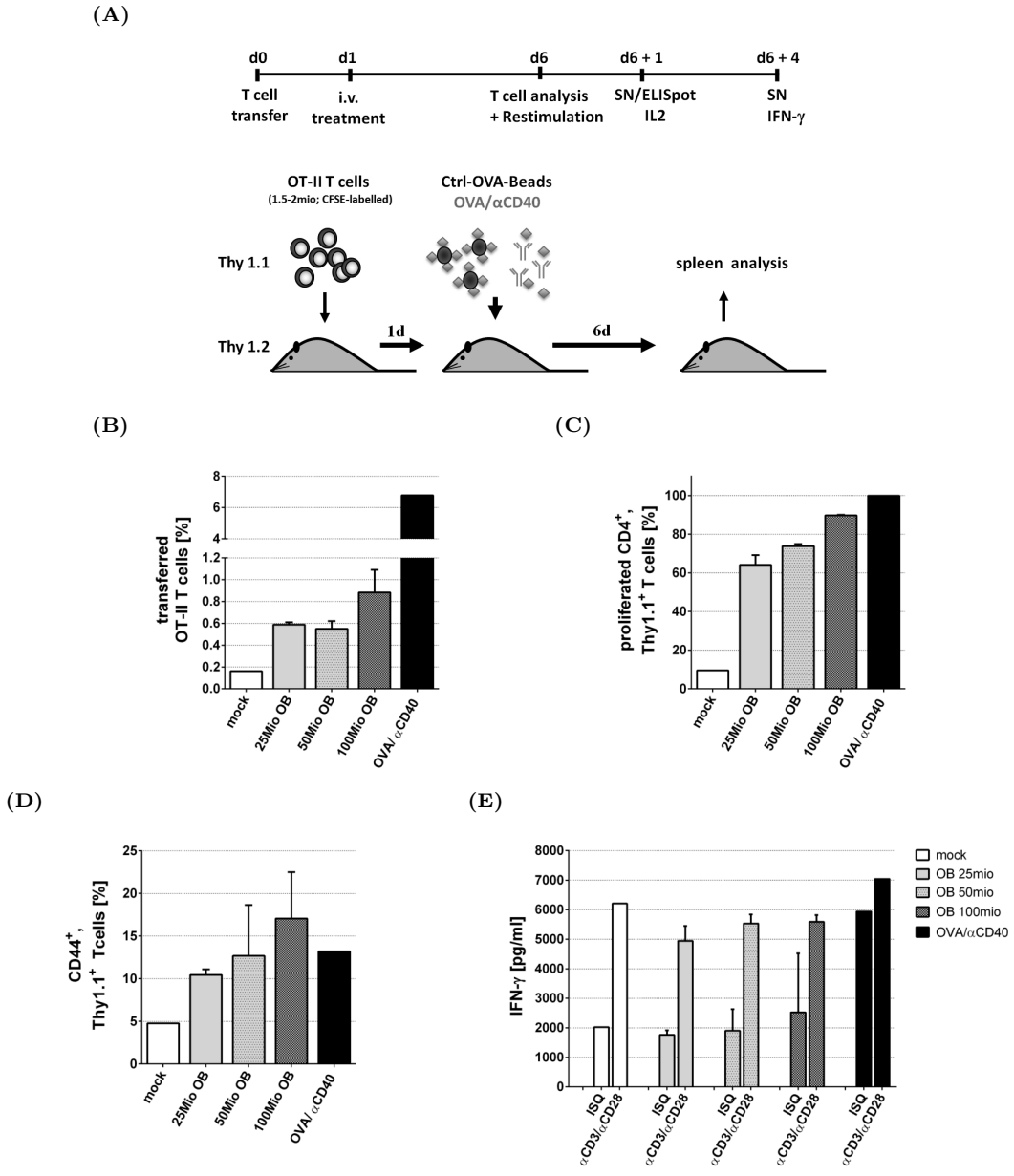

Figure 17: T cell proliferation *in vivo* is induced by control-beads in a concentration dependent manner. 1.5×10^6 CFSE-labelled OT-II T cells were transferred into wt mice one day prior to *i.v.* injection of PBS (mock), the indicated amounts of beads or 500 μg Ova/50 μg αCD40. 6 days after treatment mice were sacrificed to analyse T cell responses in the spleen. Mean and SD of 2 mice are shown for the bead treatments. (A-D) Splenocytes were isolated, stained and analysed by FC. (E) Splenocytes were restimulated with the relevant Ova-peptide ISQ or stimulatory antibodies for 4 days before supernatants (SN) were analysed by ELISA. Graphs show baseline-subtracted cytokine secretion

transferred OT-II T cell comprised 0.59 - 0.88 % of the CD4$^+$ T cells in the spleens of bead-treated mice, showing that OB caused an active response to Ova compared to the mock treatment (PBS) with only 0.16 % OT-II T cells (fig. 17B). 25×10^6 beads per mouse were sufficient to induce proliferation in 64.1 % of the transferred T cells *in vivo* whereas 100×10^6 beads per mouse induced proliferation in almost all (89.8 %) transferred T cells (fig. 17C). In line with the proliferation, the expression of the activation marker CD44

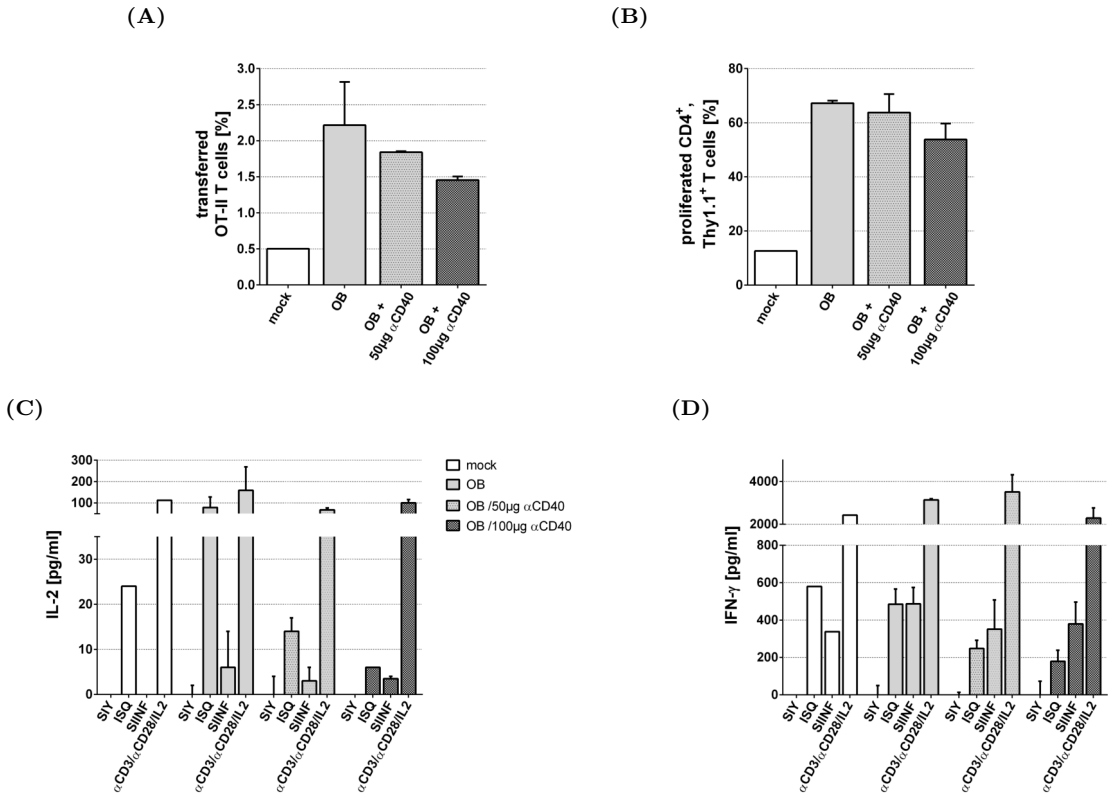

Figure 18: Co-stimulation with αCD40 was not sufficient to induce antigen-specific cytokine responses *in vivo*. 2×10^6 CFSE-labelled OT-II T cells were transferred into wt mice one day prior to *i.v.* injection of with the PBS (mock) or 50×10^6 OB with the indicated amounts of αCD40. 5 days after treatment mice were sacrificed to analyse T cell responses in the spleen. Mean and SD of 2 mice are shown for all treatments except the mock treatment. (A-B) Splenocytes were isolated, stained and analysed by FC. (D) Splenocytes were restimulated with mock-peptide (SIY), Ova-peptides (ISQ, SIINF) or stimulatiory antibodies (α-CD3/α-CD28) for 2 days (IL-2) or 4 days (IFN-γ) before supernatants were analysed by ELISA. Graphs show baseline-subtracted cytokine secretion

was enhanced with increasing bead concentrations (fig. 17D). This T cell activation was however not reflected in IFN-γ secretion upon *ex vivo* restimulation. The antigen-specific response to the Ova peptide ISQ in T cells from bead-treated mice was comparable to the baseline IFN-γ secretion from T cells from mock-treated mice. Only the positive control treatment with Ova/αCD40 resulted in increased Ova-specific IFN-γ secretion (fig. 17E). These results indicate that the control-beads alone may not be sufficient to provoke a complete T cell responses *in vivo* including both proliferation and cytokine production. In order to complement the T cell activation *in vivo*, αCD40 was co-administered with

the beads. However, αCD40 had no additive effect on the T cell response induced by OB (fig. 18). Contrary to the expectations, the response was decreased in the presence of αCD40 and IFN-γ secretion following *ex vivo* restimulation remained below the levels of the mock treated mouse). Antigen-specific secretion of IL-2 above the mock level was detected from mice treated with OB alone (fig. 18C).
Despite the insufficient cytokine responses seen in figure 17 and 18, Anx-beads were used *in vivo* to compare the effects of OB and OAB (fig. 19). Similar proliferation and cytokine secretion were observed in response to OB and OAB (fig. 19C-19E). The absolute number of OT-II T cells per spleen was reduced from an average of $3.2\,\mathrm{x}\,10^4$ cells after OB treatment to an average of $1.9\,\mathrm{x}\,10^4$ cells after OAB treatment (fig. 19B).
The effect of OB and OAB on T cells *in vivo* was further investigated in the presence of co-stimulation by polyI:C (fig. 19F-19J). The absolute number and the percentage of OT-II T cells in the spleen 6 days after treatment was decreased in mice treated with OAB compared to mice treated with OB (fig. 19F, 19G) while proliferation was similar (fig. 19H). Deviating from the previous experiment, IL-2 production was higher in the OAB-treated mice compared to the OB-treated mice. However, the high variance within the groups hinders data interpretation (fig. 19I). The co-administration of polyI:C raised the IFN-γ secretion from $CD4^+$ T cells of OB-treated mice above the level of mock mice (fig. 19J). The average of IFN-γ secretion in response to ISQ was 154 pg/ml in OB-treated mice and 43.7 pg/ml in OAB-treated mice. Although no clear Anx-mediated effects were observed, this experiment showed that bead treatment in the presence of polyI:C can provoke potent T cell responses. The secretion of IL-2 and IFN-γ in response to the MHC I-peptide SIINFEKL demonstrates that Ova-specific $CD8^+$ T cells from the endogenous T cell population of the mice were expanded (fig. 19I, 19J).

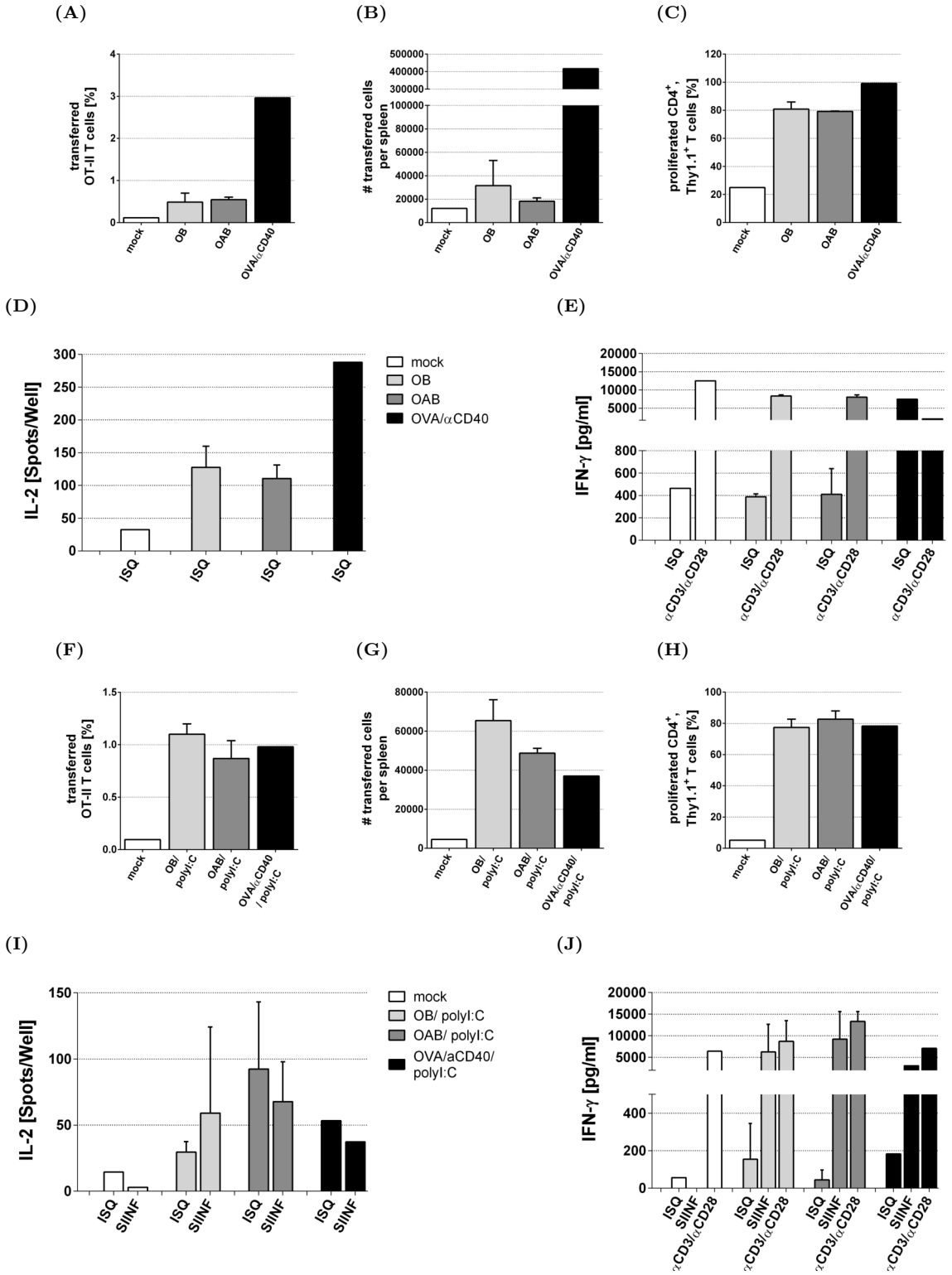

Figure 19: Anx-beads induce similar responses as control-beads *in vivo*. 1.5×10^6 CFSE-labelled OT-II T cells were transferred into wt mice one day prior to *i.v.* injection of with PBS (mock), 50×10^6 beads, 250 μg Ova/50 μg αCD40 (A-E) or 100 μg Ova/50 μg αCD40 (F-J). If indicated, treatment was supplemented with 25 μg polyI:C. 6 days after treatment mice were sacrificed to analyse T cell responses in the spleen. Mean and SD of 3 mice are shown for the bead treatments. (A-C; F-H) Splenocytes were isolated, stained and analysed by FC. TruCount tubes were used to calculate the number of transferred cells. (D-E; I-J) Splenocytes were restimulated with Ova-peptides (ISQ, SIINF) or stimulatiory antibodies (α-CD3/α-CD28) over night for IL-2 analysis or for 4 days for IFN-γ analysis. Graphs show baseline-subtracted cytokine secretion

4.6 Effects of Anx-nanoparticle on BMDC and T cells

Polystyrene beads are a tool often used in preliminary studies for a proof of concept since they are commercially available and protein coating to such beads is easier compared to protein coating to particles of other material. Nevertheless, polystyrene beads are not applicable for therapeutic use in patients. Thus, the suppressive antigen delivery mediated by Anx needs to be translated to particles of appropriate material. PLGA is a FDA-approved polymer widely used as nanoparticulate carrier. In collaboration with

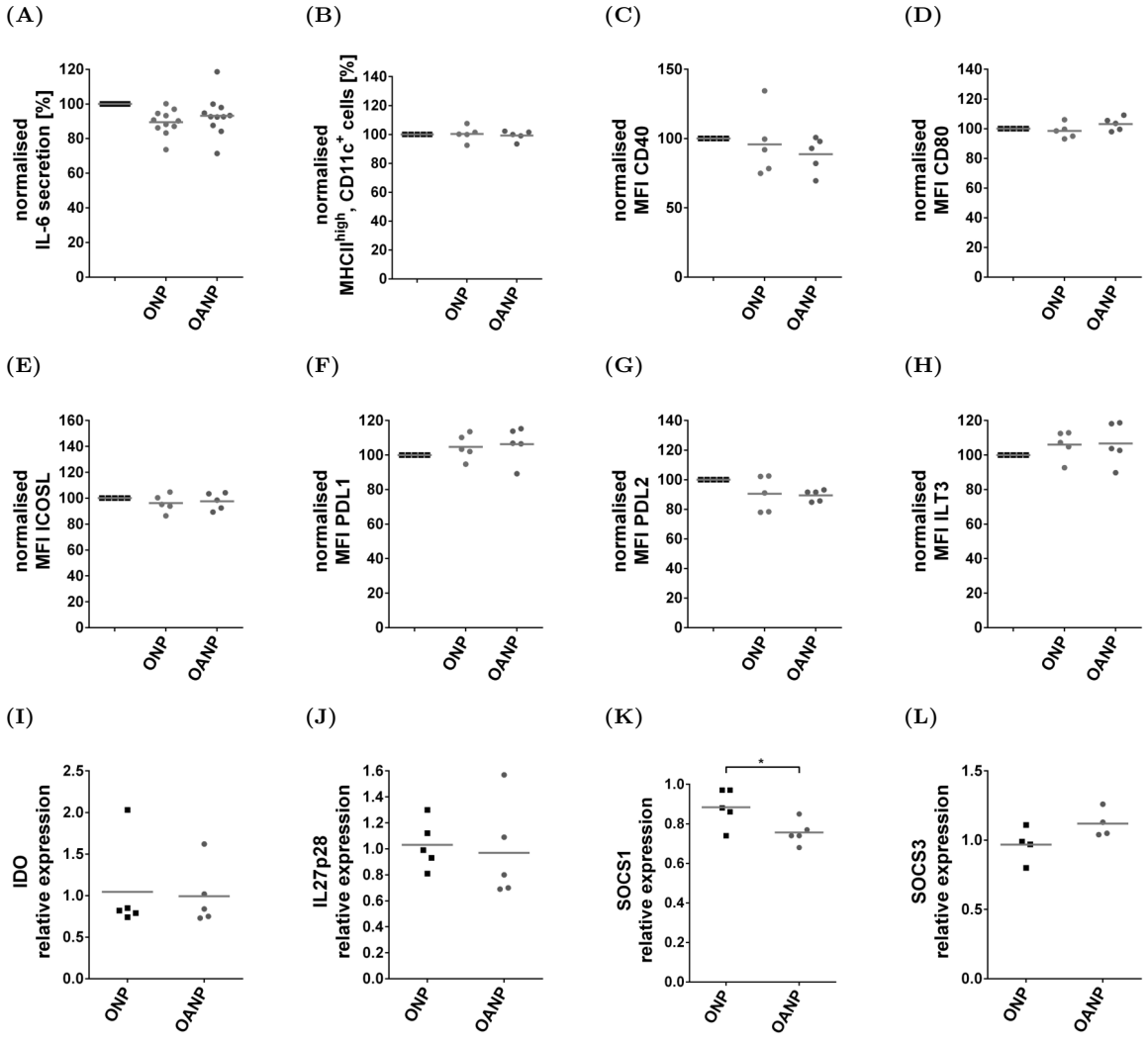

Figure 20: Nanoparticle show only minor effects on BMDC phenotype. BMDC were pre-incubated with NP [1 μg/ml] and stimulated with CpG. (A) Supernatants were collected 1-2 days after treatment to analyse IL-6 secretion by ELISA. (B-H) 1 day after treatment, BMDC were harvested and stained for FC analysis. Surface marker expression is shown for pre-gated CD11c^{+} BMDC. (A-H) show results normalised to the non-pre-treated but CpG-stimulated condition for each experiment. (I-L) RNA lysates collected 4 h after treatment were analysed by qRT-PCR. Gene regulation was assessed using HMBS as reference gene and the $\Delta\Delta$CT method. Results were normalised to the non-pre-treated but CpG-stimulated condition. Dots indicate independent experiments and significance was calculated using paired t-test of log2 transformed data (* $p<0.05$, ** $p<0.01$, *** $p<0.001$)

Nanovex Biotechnologies, PLGA-NP were generated which encapsulate Ova (ONP) and in addition have Anx covalently attached to their surface (OANP).
First, the effects of the NP on BMDC were investigated in suppression assays analogous to those used with soluble Anx or beads (fig. 3A). In high concentrations, NP themselves suppressed IL-6 production independent of the NP loading (data not shown). This phenomena was also observed with polystyrene beads (fig. S5A-S5B). The working concentrations used for beads and NP were adjusted to cause minimal unspecific BMDC cytokine suppression. IL-6 secretion was comparable after pre-treatment with ONP or OANP (fig. 20A). Furthermore, Anx-NP had no anti-inflammatory effect on BMDC at the level of surface molecule expression (fig. 20B-20H). Irrespective of Anx presence, CD40 and PD-L2 expression was slightly decreased (fig. 20C, 20G) whereas PD-L1 and ILT3 expression was slightly increased (fig. 20F, 20H) suggesting different basic properties of polystyrene and PLGA particles. At the level of gene transcription, NP did not significatnly modulate IDO, IL-27 and SOCS3. SOCS1 was significantly regulated by OANP but the relevance of this effect is questionable.
Second, the effects of NP on T cell responses were analysed. Titrations, illustrated by a representative experiment in figure 21A-21D, demonstrated a NP concentration-dependent T cell activation. The suppressive activity of Anx-beads on IL-2, IFN-γ and proliferation, was not reproduced with Anx-NP (fig. 21B-21G). Furthermore, no increase in the mRNA expression of anergy-related genes with OANP was detected (fig. 21H-21J). Interestingly, the control-NP themselves upregulated the expression of Egr2, Cblb and GRAIL to about 1.5-fold but the presence of Anx seemed to counteract this effect.
In summary, the generated Anx-NP have no inhibitory function and a refinement of the NP properties may be necessary to promote the desired Anx-mediated suppression.

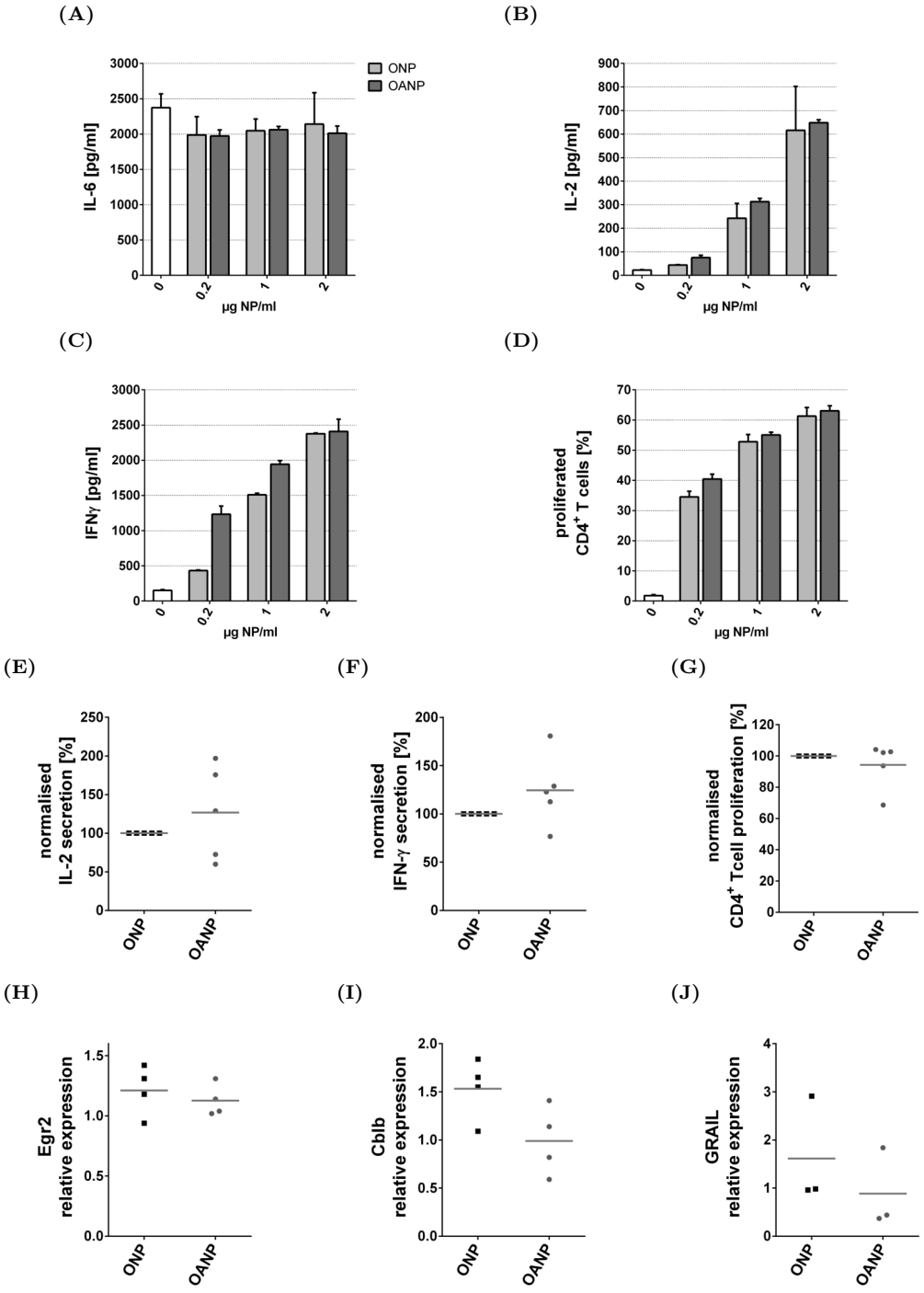

Figure 21: Attenuation of Ova-specific T cell stimulation was not reproduced by Anx-NP. BMDC were pre-incubated with Ova or beads prior to stimulated with CpG. CFSE-labelled OT-II T cells were co-cultured with treated BMDC. (A) IL-6 production was measured before T cells were added.(B+E) IL-2 production was measured after 2 days of co-culture. (C+F) IFN-γ production was measured after 5 days of co-culture. (D+G) Proliferation was evaluated by CFSE dilution measured after 5 days of co-culture. (A-D) show a representative titration experiment performed with triplicates for each condition. (E-F) show a summary of experiments performed with 1 μg NP/ml normalised to the control-NP (ONP). (H-J) T cells were harvested after 4 h of co-culture with BMDC treated with 1 μg NP/ml. Gene expression was analysed via qRT-PCR using HPRT as reference gene. Expression of the indicated genes is illustrated relative to the expression of T cells co-cultured with non-pre-treated but CpG-stimulated BMDC.Dots indicate independent experiments.

5 Discussion

Apoptotic cells are essential for the maintenance of peripheral tolerance and to prevent autoimmunity.[67,225,226] The uptake of apoptotic cells induces a tolerogenic phenotype in phagocytes and thus antigens associated with apoptotic cells (mainly self-antigens) are presented in a tolerogenic context.[65] Due to this regulatory function, apoptotic cells were recognised as a vehicle to promote antigen-specific immunosuppression. The reinfusion of endogenous cells that were fixed with antigen and rendered apoptotic *ex vivo* was shown to ameliorate autoimmune disease in mice and is also investigated in patients.[145,146,149,227] The adoptive transfer of cells in a clinical setting is however challenging and a synthetic antigen delivery system that mimicks the properties of apoptotic cells would be favourable. Although the mechanisms underlying apoptotic cell-mediated tolerance are incompletely understood, several suppressive mediators of apoptotic cells were characterised[79,225,226] and could be utilised to engineer apoptotic cell-like vehicles. Our group identified the annexin protein family as such a mediator and demonstrated that the evolutionary conserved core domain of annexin contributes to the anti-inflammatory effects of apoptotic cells.[80,82] This study examined Anx as a tool to induce antigen-specific immunosuppression. Particles harbouring Anx and the model-antigen Ova were generated using either polystyrene or PLGA as basic material. The modulatory effects on Ova-specific T cell responses of these Anx-particles as well as of soluble Anx were investigated on DC and $CD4^+$ T cell level.

5.1 Anx affecting DC phenotype and DC response to TLR challenge

AnxA1 was previously described to modulate APC responses to TLR challenge.[80,82,200,228] In line with these reports, figure 3 demonstrated that pre-incubation with soluble Anx inhibits IL-6 and IL-12 secretion from BMDC.

The suppression of inflammatory cytokines is an indirect readout of the inhibitory activity of Anx including pre-incubation and CpG stimulation. The steady-state cytokine secretion of BMDC is low and TLR stimulation raises the activity of BMDC to facilitate cytokine detection. In spite of apoptotic cells being potent immunosuppressors in steady-state and inflammatory conditions[72,73], it was shown that the inhibition of TLR responses was most pronounced when DC were co-cultured with apoptotic cells 3 h prior to TLR stimulation[229]. Furthermore our group observed that cytokine repression by AnxA1 required pre-incubation.[230] Accordingly, in all experiments presented in this study, BMDC were incubated with Anx or aJ prior to CpG stimulation.

Soluble Anx interferes with TLR induced cytokine secretion but the effector mechanism leading to the suppression of pro-inflammatory cytokines are elusive. SOCS proteins are

well-known regulators of cytokine signalling and target the downstream-signalling of different TLRs [231,232]. The inhibition or lack of SOCS1 or SOCS3 was shown to result in enhanced cytokine responses [231,233]. Alterations in SOCS activity is thus a candidate effector mechanism of Anx. However, neither soluble nor particulate Anx modulated the expression of SOCS1 or SOCS3 in BMDC analysed 4 h after treatment (fig. 9C, 9D). Similar results were obtained from BMDC incubated with Anx for 8 h and 24 h (data not shown). Nevertheless, it can not be excluded that a regulation of these genes occurred at time points not covered in this analysis. Interestingly, SOCS3 is reported to be upregulated by apoptotic cells and by an N-terminal peptide of AnxA1 (Ac2-26) leading to phosphorylation of STAT3 [228]. Full-length AnxA1 also induced SOCS3 expression in human monocytes-derived DC, but this upregulation was shown to be dispensable for cytokine suppression. [230] The discrepancy between the present study and the indicated literature on SOCS3 regulation can be explained by the use of different cell types from different species and by the use of different annexin proteins/peptides. Pupjalis *et al.* described the effect on SOCS3 specifically for the N-terminus of AnxA1 [228] and the work of Jahndel *et al.* used the full-length AnxA1 including this N-terminus [230] whereas the present study utilised the core domain of AnxA1 excluding effects of the N-terminus. Nevertheless, STAT3 phosphorylation in response to Anx should be examined to confirm that the core domain does not influence SOCS3 activity.

NF-κB is a master regulator of gene transcription and is amongst others associated with cell activation and pro-inflammatory responses e.g. to TLR stimulation. Many regulatory pathways result in inhibition of NF-κB. AnxA1 was shown to reduce phsphorylation of the NF-κB subunit p65 and to decrease binding of NF-κB to DNA [80,230]. This effect was not validated for the core domain, yet, and the signalling events upstream of NF-κB regulation need to be further analysed. Apoptotic cells mediate NF-κB inhibition by a variety of pathways including SOCS, and PPARγ signalling [73,228,234,235]. While SOCS1 and SOCS3 could not be associated with Anx in the present study, PPARγ is an interesting candidate target for Anx and should be investigated. Another candidate target for Anx is Nr4a1 which is a nuclear receptor described to inhibit NF-κB activity and IL-12 induction. Nr4a1 interacts with TRAF6 and binds to p65 preventing NF-κB-DNA binding [236].

A second comprehensive pathway involved in signal transduction of many receptors is the Ca^{2+}-calcineurin-NFAT axis. PRRs like TLR4 or the C-type lectin dectin-1 activate calcineurin which modulates pro- and anti-inflammatory cytokine responses. [237] Interestingly, calcineurin inhibition, e.g. by tacrolimus, was associated with reduced [238–240] as well as with increased cytokine responses [241,242]. In addition to the impact on cytokine secretion, Ca^{2+} signalling plays a role in DC development and maturation. GM-CSF is a NFAT target and calcineurin impairment was associated with an anti-inflammatory or immature DC phenotype. [243–245] Hence, calcineurin and NFAT activity should be analysed

to further elucidate the mode of action of Anx.

Tolerance induction involves the combination of several signals that determine the type of immune response. Reduced levels of pro-inflammatory cytokines can be one of these signals but are not sufficient to induce immunosuppression.Thus, it was investigated whether Anx specifically antagonises TLR signalling or whether it has a broader effect on the BMDC phenotype.
Figure 3B and 3C exemplify that Anx attenuated IL-6 and IL-12 secretion in the absence of TLR-stimulation with CpG which demonstrates that Anx activity is not restricted to TLR signalling. We hypothesised that Anx causes a tolerogenic phenotype in BMDC. Tolerogenic DC are not strictly defined and the characteristics of DC that exert immunosuppressive functions vary between different studies. Nonetheless, tolerogenic DC are commonly described to express anti-inflammatory mediators and to show an immature phenotype. [43,66]
Anx did not enhance IL-10 and TGF-β secretion or alter IDO expression (data not shown, fig. 9B) which are the most prominently described soluble anti-inflammatory mediators. Moreover, the inhibitory surface molecules PD-L1, PD-L2 and ILT3 were not upregulated by Anx, either (fig. 11D, 11G-11I, fig. 12D-12F). PD-L1 was upregulated by AnxA1 in human PBMC [80,230] whereas Linke *et al.* showed no regulation of PD-L1 by AnxA1, AnxA5 or AnxA13 in mouse BMDC [82]. The latter is in line with the results in figure 11D,11G and 12D. Interestingly, apoptotic cells did not upregulate PD-L1 but prevented stimulation-induced upregulation of PD-L1 in this system (fig. 11D). An immature phenotype is characterised by low expression of co-stimulatory molecules. In accordance with the literature [77–79,246,247], figure 11A-11D showed that MHC II, CD40, CD80 and CD86 levels remained low following TLR stimulation when BMDC were pre-treated with apoptotic cells. However, Anx pre-treatment did not significantly modulate the expression of these markers in the same experimental setting (fig. 11A-11F, 11K, fig. 12A-12C, 12H). Contrary to these results, Linke *et al.* reported downregulation of CD80 and CD86 by AnxA1, AnxA5 and AnxA13 [82]. This discrepancy may be due to the use of different mouse strains and annexin protein preparations.
In the present study, Anx failed to preserve an immature phenotype in BMDC following TLR challenge. Nonetheless, Anx might still induce tolerogenic DC with an semi-mature phenotype. A number of studies reported immunosuppressive activity by DC which express enhanced levels of co-stimulatory molecules [45,48,50,248,249]. For instance, Menges *et al.* reported that DC treated with the pro-inflammatory cytokine TNF-α have a mature phenotype but generate only low amounts of cytokines. In spite of the maturation, these DC cause T cell tolerance and ameliorate EAE. [249] Moreover, it was appreciated that a certain degree of DC maturation is beneficial to induce T cell tolerance. Immature DC efficiently endocytose antigens whereas antigen processing and presentation is more ef-

ficient in mature DC. Thus, increased MHC II levels can support the interaction of DC and T cells in an anti-inflammatory context. Further examples are CCR7 which allows migration of the DC to reach the relevant T cells and CD40 which promotes DC survival in a positive feedback loop. [45,118,250]

This study is the first to show that Anx provokes ROS production in BMDC (fig. 13). In contrast to the PMA-induced oxidative burst, the ROS signal in response to Anx is low suggesting a role of ROS as signalling mediator [219].
ROS, especially H_2O_2, can modulate a variety of signalling pathways and cellular processes like pagosomal acidification which is a requisite for the cross-presentation of antigens [251]. H_2O_2 is relatively stable and thus it can act over short distances between cells and can even cross cell membranes to act in paracrine and autocrine manner. Furthermore, it is an ubiquitous signalling messenger by selectively oxidising proteins. [217,218,252] Cysteins are the main targets of H_2O_2 but only specific cysteins in coordination with other adjacent amino acid can react with H_2O_2 in a process called sulfenylation. Similar to phosphorylation, sulfenylation leads to post-translational modifications which influence protein conformation and activity. [252–254] As such, ROS affects transcription factors like NF-κB and AP-1. [255] The regulation of NF-κB by Anx might be mediated by ROS similar to the reduced NF-κB activity in neutrophils treated with H_2O_2 observed by Zmijewski *et al.* [256].
The impact of ROS for anti-inflammatory immune responses was emphasised in context with NADPH oxidase 2 (NOX2) which is the major cellular source of H_2O_2 and signalling ROS in immune cells. [257] Impaired function of NOX2 was associated with exacerbated autoimmune disease in rodent models of arthritis and MS. [258–261] In addition, NOX2-dependent ROS generated by myeloid-derived suppressor cells (MDSC) acts as feedback to maintain the MDSC in an undifferentiated state and also supports the immunosuppressive properties of MDSC. [262,263] Preliminary experiments showed that both soluble and particulate Anx generate ROS via NOX2 (personal communication Kevin Bode, DKFZ Heidelberg) and we hypothesise that the tolerogenic effects of Anx are at least partly mediated by ROS.

5.2 Comparison of soluble and particulate Anx

This study examined the effects of Anx in soluble and particulate form. The type of Anx presentation had minor influence on ROS production (fig. 13) and surface molecule expression (fig. 11, fig. 12) while suppression of IL-6 and IL-12 was only observed with soluble Anx (fig. 3) and not with Anx-particles (fig. 8E, 8F, fig. 20A).
Particulate structures are generally thought to be pro-inflammatory and inflammasome activation was described e.g. for bacteria and synthetic particle preparations [264–266]. IL-1β

which is produced in response to inflammasome activation was not detectable in supernatants of BMDC treated with OB or OAB (data not shown). The polystyrene bead preparations did however increase the expression of co-stimulatory surface markers and decreased the expression of co-inhibitory molecules independent of Anx (fig. 12). It can be speculated that these pro-inflammatory effects of the bead material override the anti-inflammatory effects of Anx on BMDC cytokine production. However, the control-beads were not observed to enhance IL-6 or IL-12 secretion in the presence and absence of CpG stimulation (fig. S5C-S5D) and initial bead titration experiments showed a reduction in pro-inflammatory cytokine responses with increasing bead-concentration independent of Anx (fig. S5A-S5B). Moreover, both soluble Anx and Anx-beads were able to suppress Ova-specific T cell responses (fig. 4, fig. 5) demonstrating an anti-inflammatory function of bead-bound Anx. Thus, it is unlikely that intrinsic inflammatory bead properties account for the lack of cytokine suppression by Anx-beads.

An alternative explanation for the divergent effect of soluble Anx and Anx-beads on BMDC cytokine regulation may be an altered interaction with potential receptors and hence different downstream signalling. The geometry of a ligand can modulate signal intensity and can even lead to different signalling outcomes. For instance, phagocytic receptors work cooperatively to achieve phagocytosis and to efficiently induce signalling. NFAT activation was found to be a shared endpoint in the signalling of diverse phagocytic receptors.[267] Furthermore, single receptors can signal distinctively depending on ligand properties like affinity and duration of ligand-receptors interaction. The immunoreceptor tyrosine-based activation motif (ITAM) domain, e.g. present in C-type lectin receptors, is sensitive to the nature of the ligand. High avidity ligands which are often patriculate lead to complete phosphorylation of the domain and recruitment of Syk resulting in an inflammatory response. On the contrary, low avidity ligands can lead to hypophosphorylation of the ITAM domain and recruitment of phosphatases *via* SH2 resulting in inhibitory signalling.[268–272] Beyond the differences of soluble and particulate ligands, the distinct form of particulation can influence the response. PS was complexed in different particles to promote anti-inflammatory responses. Interestingly, the comparison of equally loaded liposomes, cylindrical PLGA-particles and rod-shaped PLGA-particles revealed superior function of PS in rod-shaped particles.[179]

The receptor or receptors of the annexin core domain have not been identified, yet. Nonetheless, it can be speculated that Anx induces different signalling axes for BMDC cytokine suppresssion and T cell suppression. Particulate presentation of Anx might enhance affinity or interaction duration at its receptor or alternatively incorporate additional receptors which counteract the effects on BMDC cytokines while the effects mediating T cell suppression are maintained.

5.3 Anx affecting DC-T cell interaction

Inhibition of the T cell responses was a shared result mediated by BMDC treated with soluble and particulate Anx (fig. 4, fig. 5) but the underlying mechanism still need to be elucidated.
IL-10, TGF-β and IDO, which are common regulatory mediators, were not detectable following Anx-treatment of BMDC (data not shown, fig. 9B). Moreover, washing BMDC prior to T cell co-culture suggests a minor role of soluble mediators for the suppressive outcome of BMDC/ T cell interaction (fig. 10). Although the production of soluble mediators after the media exchange cannot be excluded, this data implies that Anx exerts its function mainly in contact-dependent manner, which is in line with reports showing that the tolerogenic effects of apoptotic cells require cell-cell-contact [71,273].
BMDC/ T cell interactions include TCR stimulation by pMHC and co-stimulatory and co-inhibitory signals. Figure 7 showed that antigen presentation was not affected by Anx. The comparable phagocytosis (fig. 7A-7C) and Ova processing (fig. 7D) of control and Anx-beads in addition to the experiments with soluble Anx, in which Ova was separately delivered 7 h after Anx (fig. 4), indicate that T cell responses were not attenuated due to reduced antigen availability. Whether Ova was equally presented within the MHC could not be analysed directly. Anx did not cause changes in the overall expression of MHC II (fig. 11E, fig. 12A). Furthermore, extracellular loading of MHC II with Ova peptide after bead treatment demonstrated indirectly that Anx-mediated T cell suppression did not rely on altered antigen presentation but is rather caused by intrinsic alterations in BMDC (fig. 7E-7G).
As discussed in 5.1, the co-modulatory molecules CD40, CD80, CD86, PD-L1, PD-L2 and ILT3 were not targeted by Anx. ICOSL, which has a dual role as co-stimulatory and co-inhibitory molecule [34,35], was not significantly affected by Anx, either. However, a slight upregulation was observed in figure 12B. This trend probably plays no major role in the initiation of Anx-mediated T cell tolerance but it might contribute to secondary BMDC/ T cell interactions e.g. following a shift in the receptors involved in co-stimulation of T cells. In this context, it would be interesting to analyse the expression of ICOS and CD28 on the T cells.

Another modulator of the BMDC/ T cell interaction might be H_2O_2. When DC and T cell form an immunological synapse, the cells are in close contact so that DC-derived H_2O_2 could diffuse into the T cell [257]. Cemerski *et al.* demonstrated that neutrophil-derived ROS or treatment with H_2O_2 inhibited DNA synthesis in T cells resulting in reduced proliferation, NFAT activation and IL-2 production. ROS is however also described to positively influence T cell activation [274,275] but it should be noted that these reports include effects of T cell-intrinsic ROS. The level and location or source of ROS can impact the type

of modulation. Whether the Anx-dependent ROS production illustrated in figure 13 acts in an autocrine or paracrine way or both needs to be further investigated e.g. by using ROS scavengers or NOX2 inhibitors. Moreover, the ROS levels during BMDC/ T cell co-culture must be analysed since the present study only demonstrated ROS generation by BMDC shortly after Anx encounter.
In summary, Anx most likely exerts its regulatory function in a contact-dependent manner but the molecules and mechanisms involved could not be identified in this study.

5.4 Anx attenuates Ova-specific T cell responses

Anx-treated BMDC dampen T cell proliferation and cytokine production (fig. 4, fig. 5, fig. 14) indicating a shift in the T cell phenotype that might lead to T cell tolerance.
The deletion of autoreactive T cells is one type of T cell tolerance resulting from repeated antigen stimulation.[83] Since the T cell viability in the presented experiments remained at around 80 % and was not specifically altered by Anx-beads (fig. 6B), it is unlikely that Anx promotes $CD4^+$ T cell deletion *in vitro*.
The two other types of T cell tolerance, Treg and anergy, are both associated with increased expression of co-inhibitory receptors.[109,221] However, no Anx-mediated changes were observed in the surface expression of CTLA-4, PD1 and Lag-3 (fig. 15B-15D). CTLA-4 is internalised and recycled upon ligation leading to a rapid turnover and to an intracellular location of a high proportion of the protein[16,221]. Thus, the involvement of CTLA-4 in Anx-mediated effector mechanism cannot be definitely excluded until intracellular and/or mRNA levels of CTLA-4 are investigated. Moreover, the ratio of CTLA-4 and CD28 expression should be analysed. CTLA-4 binds the same ligands (CD80, CD86) as CD28 but with a higher affinity[16,17]. A downregulation of CD28 in combination with high levels of CD80/CD86 could enhance CTLA-4 activity irrespective of unaltered expression of CTLA-4 itself. A potential role of CTLA-4 could be further investigated using CTLA-4 blocking antibodies.
Tim-3 was described as negative regulator of T_H1 responses[22]. Figure 15E shows a significant but small increase in Tim-3 expression caused by Anx. Tim-3 was only expressed in a subpopulation of the cells (data not shown) and thus it seems unlikely that Tim-3 has a major role in the Anx-mediated T cell regulation. Nonetheless, the effect of Tim-3 blockade should be examined. Furthermore, Tim-3 should be assessed in the context of PD-1 since it is reported to act cooperatively with PD-1[22] and the effects on either of the co-receptors may be more pronounced in a double positive population. If Anx promotes the generation of a $Tim\text{-}3^+$, $PD1^+$ T cell population it would be interesting to separately investigate this population in more detail. Tim-3 could point to a regulatory T cell subset as it was observed to be upregulated in some $FoxP3^+$ Treg[22]. However, figure 15A illustrates that Anx-bead treated BMDC did not induce FoxP3 expression in T cells.

Anx did generally not seem to mediate the conversion into Treg cells *in vitro*. The different Treg subsets are characterised by FoxP3 expression, IL-10 secretion or TGF-β secretion. None of these properties were observed in T cells following co-culture with Anx-bead treated BMDC (fig. 14B-14C, fig. 15A).

While Treg cells are often characterised by functional mediators, anergy is mainly described by the lack of effector function [87,221]. The reduced proliferation and cytokine production, especially of IL-2, mediated by Anx (fig. 4, fig. 5, fig. 14) represents this basic definition leading to the hypothesis that Anx induces anergy. Anergic T cells develop upon suboptimal T cell stimulation like TCR signalling in the absence of co-stimulation [91,221,276]. The lack of CD28 signalling can result in an alternative gene programme including transcription of Cblb, GRAIL and Egr2 [87,94,98,101,102]. Egr2 is an early response gene that further promotes transcription of the mentioned E3 ubiquitin ligases and its mRNA expression was shown to be increased up to 100-fold in the first 3 h after TCR stimulation [95]. This anergy-related gene signature was not observed after 4 h (fig. 16C-16E) or 24 h (data not shown) of T cell co-culture with Anx-treated BMDC. A modulation at the protein level or of the activity of Cblb and GRAIL was not analysed and cannot be excluded.

A primary outcome of the signalling *via* NFAT in the absence of AP-1 is diminished IL-2 transcription which is also a hallmark of anergy [87]. In spite of the presence of co-stimulation (fig. 11, fig. 12) and the unaltered transcription levels of anergy-related genes (fig. 16C-16E), IL-2 transcription in T cells was markedly reduced by Anx-beads and soluble Anx (fig. 16B, fig. S6A). Activation and DNA-binding of both NFAT and AP-1 is required for IL-2 transcription and it should be further examined whether AP-1 translocation is impaired in Anx-dependent manner. In addition to NFAT and AP-1, a variety of other molecules and transcription factors are involved in the regulation of IL-2 transcription. For instance, RhoA, Ikaros and SATB1 counteract histone acetylation at the IL-2 promoter restricting its accessibility and thus inhibit IL-2 transcription. [277–279] microRNAs like miR146a can also interfere with IL-2 transcription. miR146a impairs AP-1 production [280] and is further described to downregulate Stat1 and to limit TRAF6 and IRAK signalling [281,282]. These examples illustrate that the identification of IL-2 transcription as an Anx-mediated effect unveils a plethora of potential targets.

In summary, Anx mediates neither T cell deletion nor Treg induction *in vitro* while it does mediate an anergy-like phenotype. However, not all properties associated with anergic T cells were observed in the treated T cells. A microarray analysis could help to further analyse the T cell phenotype and to identify molecules and pathways involved in the attenuation of the T cell response.

5.5 Anx-beads *in vivo*

The immunospressive capacity of Anx-beads illustrated *in vitro* needs to be confirmed *in vivo* to asses their potential value for future therapies.
In contrast to the *in vitro* data, Anx-beads did neither reduce proliferation nor cytokine production of OT-II T cells *in vivo* (fig. 19). The cytokine response was however difficult to evaluate. The treatment with control-beads did not result in sufficient IFN-γ secretion, even when administered in the presence of co-stimulatory agents (fig. 17E, fig. 18D, fig. 19E, 19J) and thus it was not feasible to detect a potential inhibition of IFN-γ. In spite of IL-2 levels above the baseline (set as the level in mock treated mice) (fig. 18C, fig. 19D, 19I), no clear conclusion could be drawn comparing the levels of IL-2 induced by control- or Anx-beads. Only two experiments with 3 mice per group each were performed with Anx-beads. Besides high variation especially in the experiment with polyI:C (fig. 19I), the two experiments showed contradicting trends. Figure 19D shows slightly decreased to similar levels of IL-2 in Anx-bead-treated mice compared to control-bead-treated mice, whereas figure 19I shows rather increased IL-2 production from mice treated with Anx-beads in the presence of polyI:C.
Proliferation alone is not a sufficient readout to determine the type of T cell response induced by the beads as initial proliferation is observed for inflammatory and tolerogenic T cell responses [88,283–285]. The absolute number of OT-II T cells detected in the spleen 6 days after treatment was lower in Anx-bead-treated mice compared to control-bead-treated mice (fig. 19B, 19G,). This might indicate T cell deletion but larger groups of mice are necessary to show whether this effect is significant. In addition, evaluation of later time points is necessary to validate T cell deletion. The latter is especially interesting since anergy can develop in parallel to deletion. While most of the T cells die after proliferation, the small population that survives was found to be anergic [88,283]. The experimental setup was modified to investigate late T cell phenotypes. Splenocytes were harvested 9 days after treatment or 3 days after a challenge with OVA/CpG given 10 days after the primary treatment (data not shown). However, only inadequate numbers of transferred OT-II T cells were detected in these experiments, even in mice treated with Ova/αCD40. These technical issues need to be solved to examine the longterm T cell response. Furthermore, the effects of beads on an established immune response should be investigated. Figure 14D-14E indicates that Anx-beads could diminish cytokine secretion from preactivated OT-II T cells, hence *in vivo* experiments in mice primed with Ova prior to bead treatment should be performed.
Anx-mediated T cell suppression was not observed in the presented *in vivo* experiments which may be due to the above discussed limitation in the experimental setup. Another possible reason for the diverging results *in vitro* and *in vivo* is the fact that the beads encounter different cell subsets. The function of the beads described *in vitro* was initiated

via BMDC, which are an artificial and heterogeneous cell population that has no exact counterpart *in vivo* [286–288]. Following *i.v.* injection, the beads are presumably taken up by splenic CD8α^+ DC and/or marginal zone macrophages [120,154]. Whether the beads affect these cell subsets similarly to BMDC is yet to be investigated.
A final conclusion about the tolerogenic potential of Anx-beads *in vivo* can not be drawn and further experiments including the use of adoptively transferred OT-II T cells and the stimulation of endogenous T cell populations are needed. And eventually, the beads must be analysed in pathologically relevant mouse models.

5.6 Anx-coated PLGA nanoparticles

PLGA was chosen as FDA-approved basis for the generation of an Anx-containing antigen delivery system to facilitate translation into a clinical setting. Anx-NP were encapsulated with Ova while Anx was covalently attached to the NP-surface. Although the ratio of Anx:Ova was similar on beads and NP, Anx-NP had no suppressive activity *in vitro* (fig. 20, fig. 21).
This lack of function may be caused by differential protein loading. Since NP-treated BMDC provoke OT-II T cell responses (fig. 21B-21G), it can be inferred that Ova encapsulation did not adversely affect protein integrity or availability of Ova. The coating of Anx was analysed and confirmed by Nanovex Biotechnologies. However, the conformation of Anx at the particle-surface is unknown. The covalent attachment might affect protein folding and could thus mask or disrupt the signalling-relevant domains of Anx. Whether the covalent binding of Anx interferes with its function is however difficult to test. On the one side, the molecular interaction partner and hence the corresponding binding site of Anx was not yet identified. Additionally, the spatial organisation of Anx on the particle-surface may effect efficient receptor-interaction [179]. On the other side, the anti-inflammatory capacity of Anx was mainly analysed with indirect assays which can be affected by many variables. The only direct readout identified so far is ROS production, hence ability of Anx-NP to induce ROS may reveal the functional status of the NP-coupled Anx.
Despite appropriate protein coating, the function of NP is highly influenced by general properties like size and charge which could antagonise immunosuppressive effects of Anx. Inflammatory as well as anti-inflammatory effects are reported for PLGA-NP encapsulated with antigen [154,160]. The NP used in the present study showed no intrinsic pro-inflammatory activity, since IL-6 secretion and the expression of maturation markers were not increased in BMDC by the control-NP treatment (fig. 20A-20D). Intrinsic anti-inflammatory properties were not observed, either (fig. 20F-20L) and thus the NP seem to be an inert verhicle.
Anx-NP failed to dampen T cell responses (fig. 21) but many variables could be adjusted

to improve the function of Anx-NP. Although even experts in the field admitted that it can be challenging to transfer a concept from one particle type to another and to reach optimal properties with PLGA-NP [154], PLGA-NP are a promising carrier system that is now clinically tested [182]. A number of studies reported a tolerogenic effect of PLGA-NP with negative ζ-potential [161–164] and thus a first attempt to improve Anx-NP could be the generation of negatively-charged Anx-NP.

5.7 Conclusion

This study describes a particle-based delivery system with the capacity to promote antigen-specific tolerance.

In vitro, polystyrene beads coated with Anx and the model antigen Ova induced an anergy-like phenotype represented by reduced proliferation, IFN-γ and IL-2 secretion. The most pronounced effects were observed on IL-2 production and could be attributed to attenuated IL-2 transcription. Impaired IL-2 transcription is a hallmark of anergy resulting from TCR stimulation in the absence of co-stimulation which in turn leads to an altered gene transcription programme. The anergy-associated genes analysed in this study were not regulated by Anx-beads and additional studies are needed to identify the mechanisms leading to reduced IL-2 transcription and to further characterise the induced T cell phenotype.

The outlined T cell suppression is a DC-mediated effect. The treatment of BMDC with Anx-beads did not result in a tolerogenic phenotype typically described by the secretion of anti-inflammatory cytokines and reduced expression of co-stimulatory markers and the distinct mechanisms used by the treated DC to regulate the T cell response remain elusive. However, this study revealed that the suppression of T cell responses is a Anx-mediated function which is independent of the inhibition of pro-inflammatory cytokines that was previously described and confirmed in the present study for soluble Anx. Furthermore, this study is the first to show that Anx induces ROS production in BMDC. Whether and how this ROS signal influences DC and the DC/T cell interaction needs to be further investigated.

The immunosuppressive function of the Anx-beads could not be validated *in vivo*, yet, and additional experiments are needed to delineate the effects of these beads under physiological conditions as well as in pathologically relevant models.

In addition to the polystyrene-beads, an alternative vehicle that is more suitable for clinical use was generated with the FDA-approved polymer PLGA. However, the Anx-NP examined in this study showed no immunosuppressive function. The properties of the PLGA-NP need to be improved to reproduce the effects observed with polystyrene-beads since the translation to a clinically relevant material is indispensable to develop an Anx-dependent tolerogenic antigen delivery system as a new therapeutic approach for

autoimmune disease.

References

1. Janeway C. A., J. & Medzhitov, R. Innate immune recognition. *Annu Rev Immunol* **20,** 197–216 (2002).

2. Geissmann, F., Manz, M. G., Jung, S., Sieweke, M. H., Merad, M. & Ley, K. Development of monocytes, macrophages, and dendritic cells. *Science* **327,** 656–61 (2010).

3. Sallusto, F. & Lanzavecchia, A. Efficient presentation of soluble antigen by cultured human dendritic cells is maintained by granulocyte/macrophage colony-stimulating factor plus interleukin 4 and downregulated by tumor necrosis factor alpha. *J Exp Med* **179,** 1109–18 (1994).

4. Sallusto, F., Cella, M., Danieli, C. & Lanzavecchia, A. Dendritic cells use macropinocytosis and the mannose receptor to concentrate macromolecules in the major histocompatibility complex class II compartment: downregulation by cytokines and bacterial products. *J Exp Med* **182,** 389–400 (1995).

5. Trombetta, E. S. & Mellman, I. Cell biology of antigen processing in vitro and in vivo. *Annu Rev Immunol* **23,** 975–1028 (2005).

6. Burgdorf, S., Kautz, A., Bohnert, V., Knolle, P. A. & Kurts, C. Distinct pathways of antigen uptake and intracellular routing in CD4 and CD8 T cell activation. *Science* **316,** 612–6 (2007).

7. Cooper, M. D. & Alder, M. N. The evolution of adaptive immune systems. *Cell* **124,** 815–22 (2006).

8. Tonegawa, S., Steinberg, C., Dube, S. & Bernardini, A. Evidence for somatic generation of antibody diversity. *Proc Natl Acad Sci U S A* **71,** 4027–31 (1974).

9. Reis e Sousa, C. Dendritic cells in a mature age. *Nat Rev Immunol* **6,** 476–83 (2006).

10. Bennett, S. R., Carbone, F. R., Karamalis, F., Flavell, R. A., Miller, J. F. & Heath, W. R. Help for cytotoxic-T-cell responses is mediated by CD40 signalling. *Nature* **393,** 478–80 (1998).

11. Freeman, G. J. *et al.* Engagement of the PD-1 immunoinhibitory receptor by a novel B7 family member leads to negative regulation of lymphocyte activation. *J Exp Med* **192,** 1027–34 (2000).

12. Tivol, E. A., Borriello, F., Schweitzer, A. N., Lynch, W. P., Bluestone, J. A. & Sharpe, A. H. Loss of CTLA-4 leads to massive lymphoproliferation and fatal multiorgan tissue destruction, revealing a critical negative regulatory role of CTLA-4. *Immunity* **3,** 541–7 (1995).

13. Waterhouse, P. *et al.* Lymphoproliferative disorders with early lethality in mice deficient in Ctla-4. *Science* **270,** 985–8 (1995).

14. Hodi, F. S. *et al.* Improved survival with ipilimumab in patients with metastatic melanoma. *N Engl J Med* **363,** 711–23 (2010).

15. Robert, C. *et al.* Pembrolizumab versus Ipilimumab in Advanced Melanoma. *N Engl J Med* **372,** 2521–32 (2015).

16. Rudd, C. E. & Schneider, H. Unifying concepts in CD28, ICOS and CTLA4 co-receptor signalling. *Nat Rev Immunol* **3,** 544–56 (2003).

17. Ikemizu, S. *et al.* Structure and dimerization of a soluble form of B7-1. *Immunity* **12,** 51–60 (2000).

18. Nishimura, H., Nose, M., Hiai, H., Minato, N. & Honjo, T. Development of lupus-like autoimmune diseases by disruption of the PD-1 gene encoding an ITIM motif-carrying immunoreceptor. *Immunity* **11,** 141–51 (1999).

19. Nishimura, H. *et al.* Autoimmune dilated cardiomyopathy in PD-1 receptor-deficient mice. *Science* **291,** 319–22 (2001).

20. Chen, L. Co-inhibitory molecules of the B7-CD28 family in the control of T-cell immunity. *Nat Rev Immunol* **4,** 336–47 (2004).

21. Parry, R. V. *et al.* CTLA-4 and PD-1 receptors inhibit T-cell activation by distinct mechanisms. *Mol Cell Biol* **25,** 9543–53 (2005).

22. Anderson, A. C., Joller, N. & Kuchroo, V. K. Lag-3, Tim-3, and TIGIT: Co-inhibitory Receptors with Specialized Functions in Immune Regulation. *Immunity* **44,** 989–1004 (2016).

23. Hannier, S., Tournier, M., Bismuth, G. & Triebel, F. CD3/TCR complex-associated lymphocyte activation gene-3 molecules inhibit CD3/TCR signaling. *J Immunol* **161,** 4058–65 (1998).

24. Gao, X. *et al.* TIM-3 expression characterizes regulatory T cells in tumor tissues and is associated with lung cancer progression. *PLoS One* **7,** e30676 (2012).

25. Sakuishi, K. *et al.* TIM3(+)FOXP3(+) regulatory T cells are tissue-specific promoters of T-cell dysfunction in cancer. *Oncoimmunology* **2,** e23849 (2013).

26. McMahan, R. H. *et al.* Tim-3 expression on PD-1+ HCV-specific human CTLs is associated with viral persistence, and its blockade restores hepatocyte-directed in vitro cytotoxicity. *J Clin Invest* **120,** 4546–57 (2010).

27. Wu, W., Shi, Y., Li, J., Chen, F., Chen, Z. & Zheng, M. Tim-3 expression on peripheral T cell subsets correlates with disease progression in hepatitis B infection. *Virol J* **8,** 113 (2011).

28. Jones, R. B. *et al.* Tim-3 expression defines a novel population of dysfunctional T cells with highly elevated frequencies in progressive HIV-1 infection. *J Exp Med* **205,** 2763–79 (2008).

29. Zhu, B. *et al.* Early growth response gene 2 (Egr-2) controls the self-tolerance of T cells and prevents the development of lupuslike autoimmune disease. *J Exp Med* **205,** 2295–307 (2008).

30. DeKruyff, R. H. *et al.* T cell/transmembrane, Ig, and mucin-3 allelic variants differentially recognize phosphatidylserine and mediate phagocytosis of apoptotic cells. *J Immunol* **184,** 1918–30 (2010).

31. Huang, Y. H. *et al.* CEACAM1 regulates TIM-3-mediated tolerance and exhaustion. *Nature* **517,** 386–90 (2015).

32. Arimura, Y. *et al.* A co-stimulatory molecule on activated T cells, H4/ICOS, delivers specific signals in T(h) cells and regulates their responses. *Int Immunol* **14,** 555–66 (2002).

33. Harada, Y. *et al.* A single amino acid alteration in cytoplasmic domain determines IL-2 promoter activation by ligation of CD28 but not inducible costimulator (ICOS). *J Exp Med* **197,** 257–62 (2003).

34. Akbari, O. *et al.* Antigen-specific regulatory T cells develop via the ICOS-ICOS-

ligand pathway and inhibit allergen-induced airway hyperreactivity. *Nat Med* **8,** 1024–32 (2002).

35. Ito, T. *et al.* Plasmacytoid dendritic cells prime IL-10-producing T regulatory cells by inducible costimulator ligand. *J Exp Med* **204,** 105–15 (2007).

36. Klein, L., Kyewski, B., Allen, P. M. & Hogquist, K. A. Positive and negative selection of the T cell repertoire: what thymocytes see (and don't see). *Nat Rev Immunol* **14,** 377–91 (2014).

37. Ohnmacht, C. *et al.* Constitutive ablation of dendritic cells breaks self-tolerance of CD4 T cells and results in spontaneous fatal autoimmunity. *J Exp Med* **206,** 549–59 (2009).

38. Mellanby, R. J. *et al.* TLR-4 ligation of dendritic cells is sufficient to drive pathogenic T cell function in experimental autoimmune encephalomyelitis. *J Neuroinflammation* **9,** 248 (2012).

39. Weir, C. R., Nicolson, K. & Backstrom, B. T. Experimental autoimmune encephalomyelitis induction in naive mice by dendritic cells presenting a self-peptide. *Immunol Cell Biol* **80,** 14–20 (2002).

40. Martin, D. A. *et al.* Autoimmunity stimulated by adoptively transferred dendritic cells is initiated by both alphabeta and gammadelta T cells but does not require MyD88 signaling. *J Immunol* **179,** 5819–28 (2007).

41. Van Brussel, I. *et al.* Tolerogenic dendritic cell vaccines to treat autoimmune diseases: can the unattainable dream turn into reality? *Autoimmun Rev* **13,** 138–50 (2014).

42. Vremec, D. *et al.* The surface phenotype of dendritic cells purified from mouse thymus and spleen: investigation of the CD8 expression by a subpopulation of dendritic cells. *J Exp Med* **176,** 47–58 (1992).

43. Jonuleit, H., Schmitt, E., Steinbrink, K. & Enk, A. H. Dendritic cells as a tool to induce anergic and regulatory T cells. *Trends Immunol* **22,** 394–400 (2001).

44. Friedman, S. L., Rockey, D. C., McGuire, R. F., Maher, J. J., Boyles, J. K. & Yamasaki, G. Isolated hepatic lipocytes and Kupffer cells from normal human liver: morphological and functional characteristics in primary culture. *Hepatology* **15,** 234–43 (1992).

45. Maldonado, R. A. & von Andrian, U. H. How tolerogenic dendritic cells induce regulatory T cells. *Adv Immunol* **108,** 111–65 (2010).

46. Steinman, R. M. The dendritic cell system and its role in immunogenicity. *Annu Rev Immunol* **9,** 271–96 (1991).

47. Banchereau, J. *et al.* Immunobiology of dendritic cells. *Annu Rev Immunol* **18,** 767–811 (2000).

48. Sporri, R. & Reis e Sousa, C. Inflammatory mediators are insufficient for full dendritic cell activation and promote expansion of CD4+ T cell populations lacking helper function. *Nat Immunol* **6,** 163–70 (2005).

49. Lutz, M. B. & Schuler, G. Immature, semi-mature and fully mature dendritic cells: which signals induce tolerance or immunity? *Trends Immunol* **23,** 445–9 (2002).

50. Torres-Aguilar, H. *et al.* Tolerogenic dendritic cells generated with different immunosuppressive cytokines induce antigen-specific anergy and regulatory properties in memory CD4+ T cells. *J Immunol* **184,** 1765–75 (2010).

51. Akbari, O., DeKruyff, R. H. & Umetsu, D. T. Pulmonary dendritic cells producing IL-10 mediate tolerance induced by respiratory exposure to antigen. *Nat Immunol* **2,** 725–31 (2001).

52. Wakkach, A., Fournier, N., Brun, V., Breittmayer, J. P., Cottrez, F. & Groux, H. Characterization of dendritic cells that induce tolerance and T regulatory 1 cell differentiation in vivo. *Immunity* **18,** 605–17 (2003).

53. Rubtsov, Y. P. & Rudensky, A. Y. TGFbeta signalling in control of T-cell-mediated self-reactivity. *Nat Rev Immunol* **7,** 443–53 (2007).

54. Levings, M. K., Sangregorio, R., Galbiati, F., Squadrone, S., de Waal Malefyt, R. & Roncarolo, M. G. IFN-alpha and IL-10 induce the differentiation of human type 1 T regulatory cells. *J Immunol* **166,** 5530–9 (2001).

55. Hunter, C. A. & Kastelein, R. Interleukin-27: balancing protective and pathological immunity. *Immunity* **37,** 960–9 (2012).

56. Iwata, M., Hirakiyama, A., Eshima, Y., Kagechika, H., Kato, C. & Song, S. Y. Retinoic acid imprints gut-homing specificity on T cells. *Immunity* **21,** 527–38 (2004).

57. Belladonna, M. L., Orabona, C., Grohmann, U. & Puccetti, P. TGF-beta and kynurenines as the key to infectious tolerance. *Trends Mol Med* **15,** 41–9 (2009).

58. Errico, A. Immunotherapy: PD-1-PD-L1 axis: efficient checkpoint blockade against cancer. *Nat Rev Clin Oncol* **12,** 63 (2015).

59. Vlad, G., Chang, C. C., Colovai, A. I., Berloco, P., Cortesini, R. & Suciu-Foca, N. Immunoglobulin-like transcript 3: A crucial regulator of dendritic cell function. *Hum Immunol* **70,** 340–4 (2009).

60. Gregori, S. *et al.* Differentiation of type 1 T regulatory cells (Tr1) by tolerogenic DC-10 requires the IL-10-dependent ILT4/HLA-G pathway. *Blood* **116,** 935–44 (2010).

61. Kim-Schulze, S. *et al.* Recombinant Ig-like transcript 3-Fc modulates T cell responses via induction of Th anergy and differentiation of CD8+ T suppressor cells. *J Immunol* **176,** 2790–8 (2006).

62. Suciu-Foca, N. *et al.* Soluble Ig-like transcript 3 inhibits tumor allograft rejection in humanized SCID mice and T cell responses in cancer patients. *J Immunol* **178,** 7432–41 (2007).

63. Abel, M. *et al.* Intrahepatic virus-specific IL-10-producing CD8 T cells prevent liver damage during chronic hepatitis C virus infection. *Hepatology* **44,** 1607–16 (2006).

64. Ravichandran, K. S. Beginnings of a good apoptotic meal: the find-me and eat-me signaling pathways. *Immunity* **35,** 445–55 (2011).

65. Steinman, R. M., Turley, S., Mellman, I. & Inaba, K. The induction of tolerance by dendritic cells that have captured apoptotic cells. *J Exp Med* **191,** 411–6 (2000).

66. Steinman, R. M., Hawiger, D. & Nussenzweig, M. C. Tolerogenic dendritic cells. *Annu Rev Immunol* **21,** 685–711 (2003).

67. Mueller, D. L. Mechanisms maintaining peripheral tolerance. *Nat Immunol* **11,** 21–7 (2010).

68. Scott, R. S. *et al.* Phagocytosis and clearance of apoptotic cells is mediated by MER. *Nature* **411,** 207–11 (2001).

69. Hanayama, R. *et al.* Autoimmune disease and impaired uptake of apoptotic cells in MFG-E8-deficient mice. *Science* **304,** 1147–50 (2004).

70. Kawane, K. *et al.* Chronic polyarthritis caused by mammalian DNA that escapes from degradation in macrophages. *Nature* **443,** 998–1002 (2006).

71. Voll, R. E., Herrmann, M., Roth, E. A., Stach, C., Kalden, J. R. & Girkontaite, I. Immunosuppressive effects of apoptotic cells. *Nature* **390,** 350–1 (1997).

72. Fadok, V. A., Bratton, D. L., Konowal, A., Freed, P. W., Westcott, J. Y. & Henson, P. M. Macrophages that have ingested apoptotic cells in vitro inhibit proinflammatory cytokine production through autocrine/paracrine mechanisms involving TGF-beta, PGE2, and PAF. *J Clin Invest* **101,** 890–8 (1998).

73. Cvetanovic, M. & Ucker, D. S. Innate immune discrimination of apoptotic cells: repression of proinflammatory macrophage transcription is coupled directly to specific recognition. *J Immunol* **172,** 880–9 (2004).

74. Kim, S., Elkon, K. B. & Ma, X. Transcriptional suppression of interleukin-12 gene expression following phagocytosis of apoptotic cells. *Immunity* **21,** 643–53 (2004).

75. Lucas, M. *et al.* Requirements for apoptotic cell contact in regulation of macrophage responses. *J Immunol* **177,** 4047–54 (2006).

76. Tassiulas, I., Park-Min, K. H., Hu, Y., Kellerman, L., Mevorach, D. & Ivashkiv, L. B. Apoptotic cells inhibit LPS-induced cytokine and chemokine production and IFN responses in macrophages. *Hum Immunol* **68,** 156–64 (2007).

77. Urban, B. C., Willcox, N. & Roberts, D. J. A role for CD36 in the regulation of dendritic cell function. *Proc Natl Acad Sci U S A* **98,** 8750–5 (2001).

78. Stuart, L. M., Lucas, M., Simpson, C., Lamb, J., Savill, J. & Lacy-Hulbert, A. Inhibitory effects of apoptotic cell ingestion upon endotoxin-driven myeloid dendritic cell maturation. *J Immunol* **168,** 1627–35 (2002).

79. Wallet, M. A. *et al.* MerTK is required for apoptotic cell-induced T cell tolerance. *J Exp Med* **205,** 219–32 (2008).

80. Weyd, H. *et al.* Annexin A1 on the surface of early apoptotic cells suppresses CD8+ T cell immunity. *PLoS One* **8,** e62449 (2013).

81. Ip, W. K. & Lau, Y. L. Distinct maturation of, but not migration between, human monocyte-derived dendritic cells upon ingestion of apoptotic cells of early or late phases. *J Immunol* **173,** 189–96 (2004).

82. Linke, B. *et al.* The tolerogenic function of annexins on apoptotic cells is mediated by the annexin core domain. *J Immunol* **194,** 5233–42 (2015).

83. Hughes, P. D., Belz, G. T., Fortner, K. A., Budd, R. C., Strasser, A. & Bouillet, P. Apoptosis regulators Fas and Bim cooperate in shutdown of chronic immune responses and prevention of autoimmunity. *Immunity* **28,** 197–205 (2008).

84. Rammensee, H. G., Kroschewski, R. & Frangoulis, B. Clonal anergy induced in mature V beta 6+ T lymphocytes on immunizing Mls-1b mice with Mls-1a expressing cells. *Nature* **339,** 541–4 (1989).

85. Steinbrink, K., Wolfl, M., Jonuleit, H., Knop, J. & Enk, A. H. Induction of tol-

erance by IL-10-treated dendritic cells. *J Immunol* **159,** 4772–80 (1997).

86. Steinbrink, K., Jonuleit, H., Muller, G., Schuler, G., Knop, J. & Enk, A. H. Interleukin-10-treated human dendritic cells induce a melanoma-antigen-specific anergy in CD8(+) T cells resulting in a failure to lyse tumor cells. *Blood* **93,** 1634–42 (1999).

87. Fathman, C. G. & Lineberry, N. B. Molecular mechanisms of CD4+ T-cell anergy. *Nat Rev Immunol* **7,** 599–609 (2007).

88. Rocha, B., Tanchot, C. & Von Boehmer, H. Clonal anergy blocks in vivo growth of mature T cells and can be reversed in the absence of antigen. *J Exp Med* **177,** 1517–21 (1993).

89. Pape, K. A., Merica, R., Mondino, A., Khoruts, A. & Jenkins, M. K. Direct evidence that functionally impaired CD4+ T cells persist in vivo following induction of peripheral tolerance. *J Immunol* **160,** 4719–29 (1998).

90. Schmitz, M. L. Activation of T cells: releasing the brakes by proteolytic elimination of Cbl-b. *Sci Signal* **2,** pe38 (2009).

91. Jenkins, M. K., Pardoll, D. M., Mizuguchi, J., Chused, T. M. & Schwartz, R. H. Molecular events in the induction of a nonresponsive state in interleukin 2-producing helper T-lymphocyte clones. *Proc Natl Acad Sci U S A* **84,** 5409–13 (1987).

92. Jenkins, M. K., Chen, C. A., Jung, G., Mueller, D. L. & Schwartz, R. H. Inhibition of antigen-specific proliferation of type 1 murine T cell clones after stimulation with immobilized anti-CD3 monoclonal antibody. *J Immunol* **144,** 16–22 (1990).

93. Groux, H., Bigler, M., de Vries, J. E. & Roncarolo, M. G. Interleukin-10 induces a long-term antigen-specific anergic state in human CD4+ T cells. *J Exp Med* **184,** 19–29 (1996).

94. Quill, H. & Schwartz, R. H. Stimulation of normal inducer T cell clones with antigen presented by purified Ia molecules in planar lipid membranes: specific induction of a long-lived state of proliferative nonresponsiveness. *J Immunol* **138,** 3704–12 (1987).

95. Zheng, Y., Zha, Y., Driessens, G., Locke, F. & Gajewski, T. F. Transcriptional regulator early growth response gene 2 (Egr2) is required for T cell anergy in vitro and in vivo. *J Exp Med* **209,** 2157–63 (2012).

96. Harris, J. E. *et al.* Early growth response gene-2, a zinc-finger transcription factor, is required for full induction of clonal anergy in CD4+ T cells. *J Immunol* **173,** 7331–8 (2004).

97. Li, S. *et al.* The transcription factors Egr2 and Egr3 are essential for the control of inflammation and antigen-induced proliferation of B and T cells. *Immunity* **37,** 685–96 (2012).

98. Safford, M. *et al.* Egr-2 and Egr-3 are negative regulators of T cell activation. *Nat Immunol* **6,** 472–80 (2005).

99. Bachmaier, K. *et al.* Negative regulation of lymphocyte activation and autoimmunity by the molecular adaptor Cbl-b. *Nature* **403,** 211–6 (2000).

100. Fang, D. & Liu, Y. C. Proteolysis-independent regulation of PI3K by Cbl-b-mediated ubiquitination in T cells. *Nat Immunol* **2,** 870–5 (2001).

101. Chiang, Y. J. *et al.* Cbl-b regulates the CD28 dependence of T-cell activation. *Nature* **403,** 216–20 (2000).

102. Anandasabapathy, N. *et al.* GRAIL: an E3 ubiquitin ligase that inhibits cytokine gene transcription is expressed in anergic CD4+ T cells. *Immunity* **18,** 535–47 (2003).

103. Su, L., Lineberry, N., Huh, Y., Soares, L. & Fathman, C. G. A novel E3 ubiquitin ligase substrate screen identifies Rho guanine dissociation inhibitor as a substrate of gene related to anergy in lymphocytes. *J Immunol* **177,** 7559–66 (2006).

104. Soares, L. *et al.* Two isoforms of otubain 1 regulate T cell anergy via GRAIL. *Nat Immunol* **5,** 45–54 (2004).

105. Kalekar, L. A. *et al.* CD4(+) T cell anergy prevents autoimmunity and generates regulatory T cell precursors. *Nat Immunol* **17,** 304–14 (2016).

106. Steinbrink, K., Graulich, E., Kubsch, S., Knop, J. & Enk, A. H. CD4(+) and CD8(+) anergic T cells induced by interleukin-10-treated human dendritic cells display antigen-specific suppressor activity. *Blood* **99,** 2468–76 (2002).

107. Thornton, A. M. & Shevach, E. M. Suppressor effector function of CD4+CD25+ immunoregulatory T cells is antigen nonspecific. *J Immunol* **164,** 183–90 (2000).

108. Jonuleit, H., Schmitt, E., Stassen, M., Tuettenberg, A., Knop, J. & Enk, A. H. Identification and functional characterization of human CD4(+)CD25(+) T cells with regulatory properties isolated from peripheral blood. *J Exp Med* **193,** 1285–94 (2001).

109. Sakaguchi, S. Regulatory T cells: key controllers of immunologic self-tolerance. *Cell* **101,** 455–8 (2000).

110. Weiner, H. L. Induction and mechanism of action of transforming growth factor-beta-secreting Th3 regulatory cells. *Immunol Rev* **182,** 207–14 (2001).

111. Roncarolo, M. G., Bacchetta, R., Bordignon, C., Narula, S. & Levings, M. K. Type 1 T regulatory cells. *Immunol Rev* **182,** 68–79 (2001).

112. Tadokoro, C. E. *et al.* Regulatory T cells inhibit stable contacts between CD4+ T cells and dendritic cells in vivo. *J Exp Med* **203,** 505–11 (2006).

113. Onishi, Y., Fehervari, Z., Yamaguchi, T. & Sakaguchi, S. Foxp3+ natural regulatory T cells preferentially form aggregates on dendritic cells in vitro and actively inhibit their maturation. *Proc Natl Acad Sci U S A* **105,** 10113–8 (2008).

114. Huang, C. T. *et al.* Role of LAG-3 in regulatory T cells. *Immunity* **21,** 503–13 (2004).

115. Apostolou, I. & von Boehmer, H. In vivo instruction of suppressor commitment in naive T cells. *J Exp Med* **199,** 1401–8 (2004).

116. Jonuleit, H., Schmitt, E., Schuler, G., Knop, J. & Enk, A. H. Induction of interleukin 10-producing, nonproliferating CD4(+) T cells with regulatory properties by repetitive stimulation with allogeneic immature human dendritic cells. *J Exp Med* **192,** 1213–22 (2000).

117. Hawiger, D. *et al.* Dendritic cells induce peripheral T cell unresponsiveness under steady state conditions in vivo. *J Exp Med* **194,** 769–79 (2001).

118. Kurts, C., Kosaka, H., Carbone, F. R., Miller, J. F. & Heath, W. R. Class I-restricted cross-presentation of exogenous self-antigens leads to deletion of autoreactive CD8(+) T cells. *J Exp Med* **186,** 239–45 (1997).

119. Adler, A. J. *et al.* CD4+ T cell tolerance to parenchymal self-antigens requires presentation by bone marrow-derived antigen-presenting cells. *J Exp Med* **187,** 1555–64 (1998).

120. Gharagozloo, M., Majewski, S. & Foldvari, M. Therapeutic applications of nanomedicine in autoimmune diseases: from immunosuppression to tolerance induction. *Nanomedicine* **11,** 1003–18 (2015).

121. Pescovitz, M. D. *et al.* Rituximab, B-lymphocyte depletion, and preservation of beta-cell function. *N Engl J Med* **361,** 2143–52 (2009).

122. Herold, K. C. *et al.* Teplizumab (anti-CD3 mAb) treatment preserves C-peptide responses in patients with new-onset type 1 diabetes in a randomized controlled trial: metabolic and immunologic features at baseline identify a subgroup of responders. *Diabetes* **62,** 3766–74 (2013).

123. Miller, S. D., Turley, D. M. & Podojil, J. R. Antigen-specific tolerance strategies for the prevention and treatment of autoimmune disease. *Nat Rev Immunol* **7,** 665–77 (2007).

124. Gaur, A., Wiers, B., Liu, A., Rothbard, J. & Fathman, C. G. Amelioration of autoimmune encephalomyelitis by myelin basic protein synthetic peptide-induced anergy. *Science* **258,** 1491–4 (1992).

125. Critchfield, J. M. *et al.* T cell deletion in high antigen dose therapy of autoimmune encephalomyelitis. *Science* **263,** 1139–43 (1994).

126. Smith, C. E., Eagar, T. N., Strominger, J. L. & Miller, S. D. Differential induction of IgE-mediated anaphylaxis after soluble vs. cell-bound tolerogenic peptide therapy of autoimmune encephalomyelitis. *Proc Natl Acad Sci U S A* **102,** 9595–600 (2005).

127. Xu, D., Prasad, S. & Miller, S. D. Inducing immune tolerance: a focus on Type 1 diabetes mellitus. *Diabetes Manag (Lond)* **3,** 415–426 (2013).

128. Luo, X., Herold, K. C. & Miller, S. D. Immunotherapy of type 1 diabetes: where are we and where should we be going? *Immunity* **32,** 488–99 (2010).

129. Bielekova, B. *et al.* Encephalitogenic potential of the myelin basic protein peptide (amino acids 83-99) in multiple sclerosis: results of a phase II clinical trial with an altered peptide ligand. *Nat Med* **6,** 1167–75 (2000).

130. Fontoura, P. & Garren, H. Multiple sclerosis therapies: molecular mechanisms and future. *Results Probl Cell Differ* **51,** 259–85 (2010).

131. Kappos, L. *et al.* Induction of a non-encephalitogenic type 2 T helper-cell autoimmune response in multiple sclerosis after administration of an altered peptide ligand in a placebo-controlled, randomized phase II trial. The Altered Peptide Ligand in Relapsing MS Study Group. *Nat Med* **6,** 1176–82 (2000).

132. Roep, B. O. *et al.* Plasmid-encoded proinsulin preserves C-peptide while specifically reducing proinsulin-specific CD8(+) T cells in type 1 diabetes. *Sci Transl Med* **5,** 191ra82 (2013).

133. Chang, Y. *et al.* DNA vaccination with an insulin construct and a chimeric protein binding to both CTLA4 and CD40 ameliorates type 1 diabetes in NOD mice. *Gene Ther* **12,** 1679–85 (2005).

134. Tang, Q. *et al.* In vitro-expanded antigen-specific regulatory T cells suppress autoimmune diabetes. *J Exp Med* **199,** 1455–65 (2004).

135. Scalapino, K. J., Tang, Q., Bluestone, J. A., Bonyhadi, M. L. & Daikh, D. I. Suppression of disease in New Zealand Black/New Zealand White lupus-prone mice by adoptive transfer of ex vivo expanded regulatory T cells. *J Immunol* **177,** 1451–9 (2006).

136. Tarbell, K. V. *et al.* Dendritic cell-expanded, islet-specific CD4+ CD25+ CD62L+ regulatory T cells restore normoglycemia in diabetic NOD mice. *J Exp Med* **204,** 191–201 (2007).

137. Zhou, X. *et al.* Instability of the transcription factor Foxp3 leads to the generation of pathogenic memory T cells in vivo. *Nat Immunol* **10,** 1000–7 (2009).

138. Komatsu, N. *et al.* Pathogenic conversion of Foxp3+ T cells into TH17 cells in autoimmune arthritis. *Nat Med* **20,** 62–8 (2014).

139. Marek-Trzonkowska, N. *et al.* Therapy of type 1 diabetes with CD4(+)CD25(high)CD127-regulatory T cells prolongs survival of pancreatic islets - results of one year follow-up. *Clin Immunol* **153,** 23–30 (2014).

140. Giannoukakis, N., Phillips, B., Finegold, D., Harnaha, J. & Trucco, M. Phase I (safety) study of autologous tolerogenic dendritic cells in type 1 diabetic patients. *Diabetes Care* **34,** 2026–32 (2011).

141. Jauregui-Amezaga, A. *et al.* Intraperitoneal Administration of Autologous Tolerogenic Dendritic Cells for Refractory Crohn's Disease: A Phase I Study. *J Crohns Colitis* **9,** 1071–8 (2015).

142. Benham, H. *et al.* Citrullinated peptide dendritic cell immunotherapy in HLA risk genotype-positive rheumatoid arthritis patients. *Sci Transl Med* **7,** 290ra87 (2015).

143. Bell, G. M. *et al.* Autologous tolerogenic dendritic cells for rheumatoid and inflammatory arthritis. *Ann Rheum Dis* **76,** 227–234 (2017).

144. Phillips, B. E., Garciafigueroa, Y., Trucco, M. & Giannoukakis, N. Clinical Tolerogenic Dendritic Cells: Exploring Therapeutic Impact on Human Autoimmune Disease. *Front Immunol* **8,** 1279 (2017).

145. Getts, D. R. *et al.* Tolerance induced by apoptotic antigen-coupled leukocytes is induced by PD-L1+ and IL-10-producing splenic macrophages and maintained by T regulatory cells. *J Immunol* **187,** 2405–17 (2011).

146. Luo, X. *et al.* ECDI-fixed allogeneic splenocytes induce donor-specific tolerance for long-term survival of islet transplants via two distinct mechanisms. *Proc Natl Acad Sci U S A* **105,** 14527–32 (2008).

147. Prasad, S., Kohm, A. P., McMahon, J. S., Luo, X. & Miller, S. D. Pathogenesis of NOD diabetes is initiated by reactivity to the insulin B chain 9-23 epitope and involves functional epitope spreading. *J Autoimmun* **39,** 347–53 (2012).

148. Smarr, C. B., Hsu, C. L., Byrne, A. J., Miller, S. D. & Bryce, P. J. Antigen-fixed leukocytes tolerize Th2 responses in

mouse models of allergy. *J Immunol* **187,** 5090–8 (2011).

149. Lutterotti, A. *et al.* Antigen-specific tolerance by autologous myelin peptide-coupled cells: a phase 1 trial in multiple sclerosis. *Sci Transl Med* **5,** 188ra75 (2013).

150. De Back, D. Z., Kostova, E. B., van Kraaij, M., van den Berg, T. K. & van Bruggen, R. Of macrophages and red blood cells; a complex love story. *Front Physiol* **5,** 9 (2014).

151. Pishesha, N. *et al.* Engineered erythrocytes covalently linked to antigenic peptides can protect against autoimmune disease. *Proc Natl Acad Sci U S A* **114,** 3157–3162 (2017).

152. Kontos, S., Kourtis, I. C., Dane, K. Y. & Hubbell, J. A. Engineering antigens for in situ erythrocyte binding induces T-cell deletion. *Proc Natl Acad Sci U S A* **110,** E60–8 (2013).

153. Grimm, A. J., Kontos, S., Diaceri, G., Quaglia-Thermes, X. & Hubbell, J. A. Memory of tolerance and induction of regulatory T cells by erythrocyte-targeted antigens. *Sci Rep* **5,** 15907 (2015).

154. Kishimoto, T. K. & Maldonado, R. A. Nanoparticles for the Induction of Antigen-Specific Immunological Tolerance. *Front Immunol* **9,** 230 (2018).

155. Bachmann, M. F. & Jennings, G. T. Vaccine delivery: a matter of size, geometry, kinetics and molecular patterns. *Nat Rev Immunol* **10,** 787–96 (2010).

156. Shao, K., Singha, S., Clemente-Casares, X., Tsai, S., Yang, Y. & Santamaria, P. Nanoparticle-based immunotherapy for cancer. *ACS Nano* **9,** 16–30 (2015).

157. Gref, R. *et al.* 'Stealth' corona-core nanoparticles surface modified by polyethylene glycol (PEG): influences of the corona (PEG chain length and surface density) and of the core composition on phagocytic uptake and plasma protein adsorption. *Colloids Surf B Biointerfaces* **18,** 301–313 (2000).

158. Foged, C., Brodin, B., Frokjaer, S. & Sundblad, A. Particle size and surface charge affect particle uptake by human dendritic cells in an in vitro model. *Int J Pharm* **298,** 315–22 (2005).

159. Vasir, J. K. & Labhasetwar, V. Quantification of the force of nanoparticle-cell membrane interactions and its influence on intracellular trafficking of nanoparticles. *Biomaterials* **29,** 4244–52 (2008).

160. McCarthy, D. P., Hunter, Z. N., Chackerian, B., Shea, L. D. & Miller, S. D. Targeted immunomodulation using antigen-conjugated nanoparticles. *Wiley Interdiscip Rev Nanomed Nanobiotechnol* **6,** 298–315 (2014).

161. Bryant, J. *et al.* Nanoparticle delivery of donor antigens for transplant tolerance in allogeneic islet transplantation. *Biomaterials* **35,** 8887–8894 (2014).

162. Hunter, Z. *et al.* A biodegradable nanoparticle platform for the induction of antigen-specific immune tolerance for treatment of autoimmune disease. *ACS Nano* **8,** 2148–60 (2014).

163. Kuo, R., Saito, E., Miller, S. D. & Shea, L. D. Peptide-Conjugated Nanoparticles Reduce Positive Co-stimulatory Expression and T Cell Activity to Induce Tolerance. *Mol Ther* **25,** 1676–1685 (2017).

164. McCarthy, D. P. *et al.* An antigen-encapsulating nanoparticle platform

for TH1/17 immune tolerance therapy. *Nanomedicine* **13,** 191–200 (2017).

165. Yeste, A., Nadeau, M., Burns, E. J., Weiner, H. L. & Quintana, F. J. Nanoparticle-mediated codelivery of myelin antigen and a tolerogenic small molecule suppresses experimental autoimmune encephalomyelitis. *Proc Natl Acad Sci U S A* **109,** 11270–5 (2012).

166. Yeste, A. *et al.* Tolerogenic nanoparticles inhibit T cell-mediated autoimmunity through SOCS2. *Sci Signal* **9,** ra61 (2016).

167. Tsai, S. *et al.* Reversal of autoimmunity by boosting memory-like autoregulatory T cells. *Immunity* **32,** 568–80 (2010).

168. Clemente-Casares, X. *et al.* Expanding antigen-specific regulatory networks to treat autoimmunity. *Nature* **530,** 434–40 (2016).

169. Pujol-Autonell, I. *et al.* Use of autoantigen-loaded phosphatidylserine-liposomes to arrest autoimmunity in type 1 diabetes. *PLoS One* **10,** e0127057 (2015).

170. Getts, D. R. *et al.* Microparticles bearing encephalitogenic peptides induce T-cell tolerance and ameliorate experimental autoimmune encephalomyelitis. *Nat Biotechnol* **30,** 1217–24 (2012).

171. Danhier, F., Ansorena, E., Silva, J. M., Coco, R., Le Breton, A. & Preat, V. PLGA-based nanoparticles: an overview of biomedical applications. *J Control Release* **161,** 505–22 (2012).

172. Lamprecht, A. *et al.* Biodegradable nanoparticles for targeted drug delivery in treatment of inflammatory bowel disease. *J Pharmacol Exp Ther* **299,** 775–81 (2001).

173. Horisawa, E. *et al.* Size-dependency of DL-lactide/glycolide copolymer particulates for intra-articular delivery system on phagocytosis in rat synovium. *Pharm Res* **19,** 132–9 (2002).

174. Costantino, L., Gandolfi, F., Tosi, G., Rivasi, F., Vandelli, M. A. & Forni, F. Peptide-derivatized biodegradable nanoparticles able to cross the blood-brain barrier. *J Control Release* **108,** 84–96 (2005).

175. Wang, Y., Qu, W. & Choi, S. H. FDA's Regulatory Science Program for Generic PLA/ PLGA-Based Drug Products. *American Pharmaceutical Review* **19** (2016).

176. Maldonado, R. A. *et al.* Polymeric synthetic nanoparticles for the induction of antigen-specific immunological tolerance. *Proc Natl Acad Sci U S A* **112,** E156–65 (2015).

177. Tostanoski, L. H. *et al.* Reprogramming the Local Lymph Node Microenvironment Promotes Tolerance that Is Systemic and Antigen Specific. *Cell Rep* **16,** 2940–2952 (2016).

178. Kishimoto, T. K. *et al.* Improving the efficacy and safety of biologic drugs with tolerogenic nanoparticles. *Nat Nanotechnol* **11,** 890–899 (2016).

179. Roberts, R. A. *et al.* Towards programming immune tolerance through geometric manipulation of phosphatidylserine. *Biomaterials* **72,** 1–10 (2015).

180. Cappellano, G. *et al.* Subcutaneous inverse vaccination with PLGA particles loaded with a MOG peptide and IL-10 decreases the severity of experimental autoimmune encephalomyelitis. *Vaccine* **32,** 5681–9 (2014).

181. Carambia, A. *et al.* Nanoparticle-based autoantigen delivery to Treg-inducing liver sinusoidal endothelial cells enables control of autoimmunity in mice. *J Hepatol* **62,** 1349–56 (2015).

182. Prasad, S. *et al.* Tolerogenic Ag-PLG nanoparticles induce tregs to suppress activated diabetogenic CD4 and CD8 T cells. *J Autoimmun* **89,** 112–124 (2018).

183. Demento, S. L. *et al.* Inflammasome-activating nanoparticles as modular systems for optimizing vaccine efficacy. *Vaccine* **27,** 3013–21 (2009).

184. Hanlon, D. J. *et al.* Enhanced stimulation of anti-ovarian cancer CD8(+) T cells by dendritic cells loaded with nanoparticle encapsulated tumor antigen. *Am J Reprod Immunol* **65,** 597–609 (2011).

185. Jones, D. H., Partidos, C. D., Steward, M. W. & Farrar, G. H. Oral delivery of poly(lactide-co-glycolide) encapsulated vaccines. *Behring Inst Mitt,* 220–8 (1997).

186. Partidos, C. D., Vohra, P., Jones, D., Farrar, G. & Steward, M. W. CTL responses induced by a single immunization with peptide encapsulated in biodegradable microparticles. *J Immunol Methods* **206,** 143–51 (1997).

187. Gerke, V. & Moss, S. E. Annexins: from structure to function. *Physiol Rev* **82,** 331–71 (2002).

188. Wallner, B. P. *et al.* Cloning and expression of human lipocortin, a phospholipase A2 inhibitor with potential anti-inflammatory activity. *Nature* **320,** 77–81 (1986).

189. Kim, S. W. *et al.* Inhibition of cytosolic phospholipase A2 by annexin I. Specific interaction model and mapping of the interaction site. *J Biol Chem* **276,** 15712–9 (2001).

190. Davidson, J., Flower, R. J., Milton, A. S., Peers, S. H. & Rotondo, D. Antipyretic actions of human recombinant lipocortin-1. *Br J Pharmacol* **102,** 7–9 (1991).

191. Arur, S. *et al.* Annexin I is an endogenous ligand that mediates apoptotic cell engulfment. *Dev Cell* **4,** 587–98 (2003).

192. Smith, S. F., Tetley, T. D., Guz, A. & Flower, R. J. Detection of lipocortin 1 in human lung lavage fluid: lipocortin degradation as a possible proteolytic mechanism in the control of inflammatory mediators and inflammation. *Environ Health Perspect* **85,** 135–44 (1990).

193. Lim, L. H., Solito, E., Russo-Marie, F., Flower, R. J. & Perretti, M. Promoting detachment of neutrophils adherent to murine postcapillary venules to control inflammation: effect of lipocortin 1. *Proc Natl Acad Sci U S A* **95,** 14535–9 (1998).

194. Vong, L. *et al.* Annexin 1 cleavage in activated neutrophils: a pivotal role for proteinase 3. *J Biol Chem* **282,** 29998–30004 (2007).

195. Rescher, U., Goebeler, V., Wilbers, A. & Gerke, V. Proteolytic cleavage of annexin 1 by human leukocyte elastase. *Biochim Biophys Acta* **1763,** 1320–4 (2006).

196. Maderna, P., Yona, S., Perretti, M. & Godson, C. Modulation of phagocytosis of apoptotic neutrophils by supernatant from dexamethasone-treated macrophages and annexin-derived peptide Ac(2-26). *J Immunol* **174,** 3727–33 (2005).

197. Scannell, M. *et al.* Annexin-1 and peptide derivatives are released by apoptotic cells and stimulate phagocytosis of apoptotic

neutrophils by macrophages. *J Immunol* **178,** 4595–605 (2007).

198. Walther, A., Riehemann, K. & Gerke, V. A novel ligand of the formyl peptide receptor: annexin I regulates neutrophil extravasation by interacting with the FPR. *Mol Cell* **5,** 831–40 (2000).

199. Perretti, M., Getting, S. J., Solito, E., Murphy, P. M. & Gao, J. L. Involvement of the receptor for formylated peptides in the in vivo anti-migratory actions of annexin 1 and its mimetics. *Am J Pathol* **158,** 1969–73 (2001).

200. Blume, K. E. *et al.* Cell surface externalization of annexin A1 as a failsafe mechanism preventing inflammatory responses during secondary necrosis. *J Immunol* **183,** 8138–47 (2009).

201. Perretti, M., Becherucci, C., Mugridge, K. G., Solito, E., Silvestri, S. & Parente, L. A novel anti-inflammatory peptide from human lipocortin 5. *Br J Pharmacol* **103,** 1327–32 (1991).

202. Liu, A. *et al.* Induction of dendritic cell-mediated T-cell activation by modified but not native low-density lipoprotein in humans and inhibition by annexin a5: involvement of heat shock proteins. *Arterioscler Thromb Vasc Biol* **35,** 197–205 (2015).

203. D'Acquisto, F., Paschalidis, N., Sampaio, A. L., Merghani, A., Flower, R. J. & Perretti, M. Impaired T cell activation and increased Th2 lineage commitment in Annexin-1-deficient T cells. *Eur J Immunol* **37,** 3131–42 (2007).

204. Yang, Y. H. *et al.* Deficiency of annexin A1 in CD4+ T cells exacerbates T cell-dependent inflammation. *J Immunol* **190,** 997–1007 (2013).

205. Paschalidis, N. *et al.* Modulation of experimental autoimmune encephalomyelitis by endogenous annexin A1. *J Neuroinflammation* **6,** 33 (2009).

206. Yazid, S. *et al.* Annexin-A1 restricts Th17 cells and attenuates the severity of autoimmune disease. *J Autoimmun* **58,** 1–11 (2015).

207. Akama, H., Tanaka, H. & Kawai, S. Possible mechanisms of glucocorticoid–unresponsive pyrexia. Defect in lipocortin 1? *Mater Med Pol* **27,** 75–8 (1995).

208. Sun, H. T., Cohen, S. & Kaufmann, W. E. Annexin-1 is abnormally expressed in fragile X syndrome: two-dimensional electrophoresis study in lymphocytes. *Am J Med Genet* **103,** 81–90 (2001).

209. Hayes, M. J. & Moss, S. E. Annexins and disease. *Biochem Biophys Res Commun* **322,** 1166–70 (2004).

210. Cristante, E. *et al.* Identification of an essential endogenous regulator of blood-brain barrier integrity, and its pathological and therapeutic implications. *Proc Natl Acad Sci U S A* **110,** 832–41 (2013).

211. Goulding, N. J. *et al.* Autoantibodies to recombinant lipocortin-1 in rheumatoid arthritis and systemic lupus erythematosus. *Ann Rheum Dis* **48,** 843–50 (1989).

212. Stevens, T. R., Smith, S. F. & Rampton, D. S. Antibodies to human recombinant lipocortin-I in inflammatory bowel disease. *Clin Sci (Lond)* **84,** 381–6 (1993).

213. Kretz, C. C. *et al.* Anti-annexin 1 antibodies: a new diagnostic marker in the serum of patients with discoid lupus erythematosus. *Exp Dermatol* **19,** 919–21 (2010).

214. Bastian, B. C., Nuss, B., Romisch, J., Kraus, M. & Brocker, E. B. Autoantibodies to annexins: a diagnostic marker for cutaneous disorders? *J Dermatol Sci* **8,** 194–202 (1994).

215. Bruschi, M., Petretto, A., Vaglio, A., Santucci, L., Candiano, G. & Ghiggeri, G. M. Annexin A1 and Autoimmunity: From Basic Science to Clinical Applications. *Int J Mol Sci* **19** (2018).

216. Rotzschke, O., Falk, K., Stevanovic, S., Jung, G., Walden, P. & Rammensee, H. G. Exact prediction of a natural T cell epitope. *Eur J Immunol* **21,** 2891–4 (1991).

217. Belikov, A. V., Schraven, B. & Simeoni, L. T cells and reactive oxygen species. *J Biomed Sci* **22,** 85 (2015).

218. Gough, D. R. & Cotter, T. G. Hydrogen peroxide: a Jekyll and Hyde signalling molecule. *Cell Death Dis* **2,** e213 (2011).

219. Ushio-Fukai, M. Compartmentalization of redox signaling through NADPH oxidase-derived ROS. *Antioxid Redox Signal* **11,** 1289–99 (2009).

220. Martinez, R. J. *et al.* Arthritogenic self-reactive CD4+ T cells acquire an FR4hiCD73hi anergic state in the presence of Foxp3+ regulatory T cells. *J Immunol* **188,** 170–81 (2012).

221. Schwartz, R. H. T cell anergy. *Annu Rev Immunol* **21,** 305–34 (2003).

222. Whiting, C. C., Su, L. L., Lin, J. T. & Fathman, C. G. GRAIL: a unique mediator of CD4 T-lymphocyte unresponsiveness. *Febs j* **278,** 47–58 (2011).

223. Parish, I. A. *et al.* The molecular signature of CD8+ T cells undergoing deletional tolerance. *Blood* **113,** 4575–85 (2009).

224. Heissmeyer, V. *et al.* Calcineurin imposes T cell unresponsiveness through targeted proteolysis of signaling proteins. *Nat Immunol* **5,** 255–65 (2004).

225. Elliott, M. R. & Ravichandran, K. S. Clearance of apoptotic cells: implications in health and disease. *J Cell Biol* **189,** 1059–70 (2010).

226. Savill, J., Dransfield, I., Gregory, C. & Haslett, C. A blast from the past: clearance of apoptotic cells regulates immune responses. *Nat Rev Immunol* **2,** 965–75 (2002).

227. Kontos, S., Grimm, A. J. & Hubbell, J. A. Engineering antigen-specific immunological tolerance. *Curr Opin Immunol* **35,** 80–8 (2015).

228. Pupjalis, D., Goetsch, J., Kottas, D. J., Gerke, V. & Rescher, U. Annexin A1 released from apoptotic cells acts through formyl peptide receptors to dampen inflammatory monocyte activation via JAK/STAT/SOCS signalling. *EMBO Mol Med* **3,** 102–14 (2011).

229. Verbovetski, I. *et al.* Opsonization of apoptotic cells by autologous iC3b facilitates clearance by immature dendritic cells, down-regulates DR and CD86, and up-regulates CC chemokine receptor 7. *J Exp Med* **196,** 1553–61 (2002).

230. Jahndel, V. *Regulation of Dendritic Cell Activation by Apoptotic Cell-derived Annexin A1* PhD thesis (2013).

231. Yoshimura, A., Naka, T. & Kubo, M. SOCS proteins, cytokine signalling and immune regulation. *Nat Rev Immunol* **7,** 454–65 (2007).

232. Mansell, A. *et al.* Suppressor of cytokine signaling 1 negatively regulates Toll-like receptor signaling by mediating

Mal degradation. *Nat Immunol* **7,** 148–55 (2006).

233. Croker, B. A. *et al.* SOCS3 negatively regulates IL-6 signaling in vivo. *Nat Immunol* **4,** 540–5 (2003).

234. Kidani, Y. & Bensinger, S. J. Liver X receptor and peroxisome proliferator-activated receptor as integrators of lipid homeostasis and immunity. *Immunol Rev* **249,** 72–83 (2012).

235. Szondy, Z., Sarang, Z., Kiss, B., Garabuczi, E. & Koroskenyi, K. Anti-inflammatory Mechanisms Triggered by Apoptotic Cells during Their Clearance. *Front Immunol* **8,** 909 (2017).

236. Ipseiz, N. *et al.* The nuclear receptor Nr4a1 mediates anti-inflammatory effects of apoptotic cells. *J Immunol* **192,** 4852–8 (2014).

237. Fric, J., Zelante, T., Wong, A. Y., Mertes, A., Yu, H. B. & Ricciardi-Castagnoli, P. NFAT control of innate immunity. *Blood* **120,** 1380–9 (2012).

238. Bendickova, K., Tidu, F. & Fric, J. Calcineurin-NFAT signalling in myeloid leucocytes: new prospects and pitfalls in immunosuppressive therapy. *EMBO Mol Med* **9,** 990–999 (2017).

239. Herbst, S. *et al.* Phagocytosis-dependent activation of a TLR9-BTK-calcineurin-NFAT pathway co-ordinates innate immunity to Aspergillus fumigatus. *EMBO Mol Med* **7,** 240–58 (2015).

240. Elloumi, H. Z. *et al.* A cell permeable peptide inhibitor of NFAT inhibits macrophage cytokine expression and ameliorates experimental colitis. *PLoS One* **7,** e34172 (2012).

241. Conboy, I. M., Manoli, D., Mhaiskar, V. & Jones, P. P. Calcineurin and vacuolar-type H+-ATPase modulate macrophage effector functions. *Proc Natl Acad Sci U S A* **96,** 6324–9 (1999).

242. Kang, Y. J. *et al.* Calcineurin negatively regulates TLR-mediated activation pathways. *J Immunol* **179,** 4598–607 (2007).

243. Brettingham-Moore, K. H., Rao, S., Juelich, T., Shannon, M. F. & Holloway, A. F. GM-CSF promoter chromatin remodelling and gene transcription display distinct signal and transcription factor requirements. *Nucleic Acids Res* **33,** 225–34 (2005).

244. Escolano, A. *et al.* Specific calcineurin targeting in macrophages confers resistance to inflammation via MKP-1 and p38. *Embo j* **33,** 1117–33 (2014).

245. Jennings, C., Kusler, B. & Jones, P. P. Calcineurin inactivation leads to decreased responsiveness to LPS in macrophages and dendritic cells and protects against LPS-induced toxicity in vivo. *Innate Immun* **15,** 109–20 (2009).

246. Albert, M. L., Jegathesan, M. & Darnell, R. B. Dendritic cell maturation is required for the cross-tolerization of CD8+ T cells. *Nat Immunol* **2,** 1010–7 (2001).

247. Sauer, H., Wartenberg, M. & Hescheler, J. Reactive oxygen species as intracellular messengers during cell growth and differentiation. *Cell Physiol Biochem* **11,** 173–86 (2001).

248. Vander Lugt, B. *et al.* Transcriptional determinants of tolerogenic and immunogenic states during dendritic cell maturation. *J Cell Biol* **216,** 779–792 (2017).

249. Menges, M. *et al.* Repetitive injections of dendritic cells matured with tumor necrosis factor alpha induce antigen-specific protection of mice from autoimmunity. *J Exp Med* **195,** 15–21 (2002).

250. Morgan, D. J., Kreuwel, H. T. & Sherman, L. A. Antigen concentration and precursor frequency determine the rate of CD8+ T cell tolerance to peripherally expressed antigens. *J Immunol* **163,** 723–7 (1999).

251. Savina, A. *et al.* NOX2 controls phagosomal pH to regulate antigen processing during crosspresentation by dendritic cells. *Cell* **126,** 205–18 (2006).

252. Winterbourn, C. C. The biological chemistry of hydrogen peroxide. *Methods Enzymol* **528,** 3–25 (2013).

253. Poole, L. B., Karplus, P. A. & Claiborne, A. Protein sulfenic acids in redox signaling. *Annu Rev Pharmacol Toxicol* **44,** 325–47 (2004).

254. Garcia-Santamarina, S., Boronat, S. & Hidalgo, E. Reversible cysteine oxidation in hydrogen peroxide sensing and signal transduction. *Biochemistry* **53,** 2560–80 (2014).

255. Hyslop, P. A. *et al.* Mechanisms of oxidant-mediated cell injury. The glycolytic and mitochondrial pathways of ADP phosphorylation are major intracellular targets inactivated by hydrogen peroxide. *J Biol Chem* **263,** 1665–75 (1988).

256. Zmijewski, J. W., Zhao, X., Xu, Z. & Abraham, E. Exposure to hydrogen peroxide diminishes NF-kappaB activation, IkappaB-alpha degradation, and proteasome activity in neutrophils. *Am J Physiol Cell Physiol* **293,** C255–66 (2007).

257. Brown, D. I. & Griendling, K. K. Nox proteins in signal transduction. *Free Radic Biol Med* **47,** 1239–53 (2009).

258. Olofsson, P., Holmberg, J., Tordsson, J., Lu, S., Akerstrom, B. & Holmdahl, R. Positional identification of Ncf1 as a gene that regulates arthritis severity in rats. *Nat Genet* **33,** 25–32 (2003).

259. Hultqvist, M., Olofsson, P., Holmberg, J., Backstrom, B. T., Tordsson, J. & Holmdahl, R. Enhanced autoimmunity, arthritis, and encephalomyelitis in mice with a reduced oxidative burst due to a mutation in the Ncf1 gene. *Proc Natl Acad Sci U S A* **101,** 12646–51 (2004).

260. George-Chandy, A. *et al.* Th17 development and autoimmune arthritis in the absence of reactive oxygen species. *Eur J Immunol* **38,** 1118–26 (2008).

261. Mossberg, N., Movitz, C., Hellstrand, K., Bergstrom, T., Nilsson, S. & Andersen, O. Oxygen radical production in leukocytes and disease severity in multiple sclerosis. *J Neuroimmunol* **213,** 131–4 (2009).

262. Corzo, C. A. *et al.* Mechanism regulating reactive oxygen species in tumor-induced myeloid-derived suppressor cells. *J Immunol* **182,** 5693–701 (2009).

263. Kusmartsev, S. & Gabrilovich, D. I. Inhibition of myeloid cell differentiation in cancer: the role of reactive oxygen species. *J Leukoc Biol* **74,** 186–96 (2003).

264. Sharp, F. A. *et al.* Uptake of particulate vaccine adjuvants by dendritic cells activates the NALP3 inflammasome. *Proc Natl Acad Sci U S A* **106,** 870–5 (2009).

265. Ferrand, J. & Ferrero, R. L. Recognition of Extracellular Bacteria by NLRs and Its Role in the Development of Adaptive Immunity. *Front Immunol* **4,** 344 (2013).

266. Latz, E., Xiao, T. S. & Stutz, A. Activation and regulation of the inflammasomes. *Nat Rev Immunol* **13,** 397–411 (2013).

267. Fric, J., Zelante, T. & Ricciardi-Castagnoli, P. Phagocytosis of Particulate Antigens - All Roads Lead to Calcineurin/NFAT Signaling Pathway. *Front Immunol* **4,** 513 (2014).

268. Iborra, S. & Sancho, D. Signalling versatility following self and non-self sensing by myeloid C-type lectin receptors. *Immunobiology* **220,** 175–84 (2015).

269. Yamasaki, S., Ishikawa, E., Kohno, M. & Saito, T. The quantity and duration of FcRgamma signals determine mast cell degranulation and survival. *Blood* **103,** 3093–101 (2004).

270. Hamerman, J. A., Ni, M., Killebrew, J. R., Chu, C. L. & Lowell, C. A. The expanding roles of ITAM adapters FcRgamma and DAP12 in myeloid cells. *Immunol Rev* **232,** 42–58 (2009).

271. Moss, S. E. & Morgan, R. O. The annexins. *Genome Biol* **5,** 219 (2004).

272. Blank, U., Launay, P., Benhamou, M. & Monteiro, R. C. Inhibitory ITAMs as novel regulators of immunity. *Immunol Rev* **232,** 59–71 (2009).

273. Byrne, A. & Reen, D. J. Lipopolysaccharide induces rapid production of IL-10 by monocytes in the presence of apoptotic neutrophils. *J Immunol* **168,** 1968–77 (2002).

274. Reth, M. Hydrogen peroxide as second messenger in lymphocyte activation. *Nat Immunol* **3,** 1129–34 (2002).

275. Devadas, S., Zaritskaya, L., Rhee, S. G., Oberley, L. & Williams, M. S. Discrete generation of superoxide and hydrogen peroxide by T cell receptor stimulation: selective regulation of mitogen-activated protein kinase activation and fas ligand expression. *J Exp Med* **195,** 59–70 (2002).

276. Kearney, E. R., Pape, K. A., Loh, D. Y. & Jenkins, M. K. Visualization of peptide-specific T cell immunity and peripheral tolerance induction in vivo. *Immunity* **1,** 327–39 (1994).

277. Crispin, J. C. & Tsokos, G. C. Transcriptional regulation of IL-2 in health and autoimmunity. *Autoimmun Rev* **8,** 190–5 (2009).

278. Pavan Kumar, P. *et al.* Phosphorylation of SATB1, a global gene regulator, acts as a molecular switch regulating its transcriptional activity in vivo. *Mol Cell* **22,** 231–43 (2006).

279. Bandyopadhyay, S., Dure, M., Paroder, M., Soto-Nieves, N., Puga, I. & Macian, F. Interleukin 2 gene transcription is regulated by Ikaros-induced changes in histone acetylation in anergic T cells. *Blood* **109,** 2878–86 (2007).

280. Curtale, G. *et al.* An emerging player in the adaptive immune response: microRNA-146a is a modulator of IL-2 expression and activation-induced cell death in T lymphocytes. *Blood* **115,** 265–73 (2010).

281. Lu, L. F. *et al.* Function of miR-146a in controlling Treg cell-mediated regulation of Th1 responses. *Cell* **142,** 914–29 (2010).

282. Hou, J. *et al.* MicroRNA-146a feedback inhibits RIG-I-dependent Type I IFN production in macrophages by targeting TRAF6, IRAK1, and IRAK2. *J Immunol* **183,** 2150–8 (2009).

283. Lanoue, A., Bona, C., von Boehmer, H. & Sarukhan, A. Conditions that induce tolerance in mature CD4+ T cells. *J Exp Med* **185,** 405–14 (1997).

284. Dudziak, D. *et al.* Differential antigen processing by dendritic cell subsets in vivo. *Science* **315,** 107–11 (2007).

285. Fazekas de St Groth, B., Smith, A. L. & Higgins, C. A. T cell activation: in vivo veritas. *Immunol Cell Biol* **82,** 260–8 (2004).

286. Helft, J. *et al.* GM-CSF Mouse Bone Marrow Cultures Comprise a Heterogeneous Population of CD11c(+)MHCII(+) Macrophages and Dendritic Cells. *Immunity* **42,** 1197–211 (2015).

287. Inaba, K. *et al.* Generation of large numbers of dendritic cells from mouse bone marrow cultures supplemented with granulocyte/macrophage colony-stimulating factor. *J Exp Med* **176,** 1693–702 (1992).

288. Nikolic, T. & Roep, B. O. Regulatory multitasking of tolerogenic dendritic cells - lessons taken from vitamin d3-treated tolerogenic dendritic cells. *Front Immunol* **4,** 113 (2013).

Appendix

I Supplementary results

Bead optimisation

The bead preparation had to be optimised and controlled before the functional experiments described in the results section could be performed. The final bead preparation protocol is visualised in figure S1. Beads are first coated with Ova to ensure equal Ova-

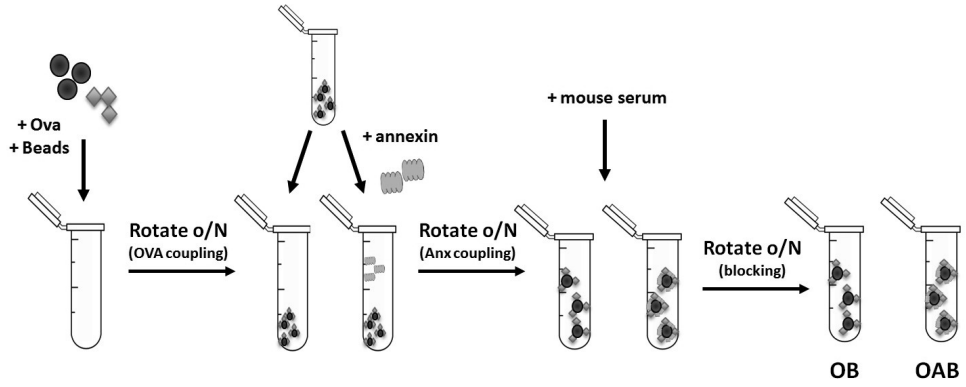

Figure S1: Bead preparation protocol. Beads were added to a Ova-solution in DPBS and rotated overnight (o/N), allowing passive adsorbtion of Ova to the bead surface. Following overnight incubation, beads were washed to remove unbound protein. Ova-coated beads were split and one part was coated additionally with Anx by o/N rotation. Beads were again washed and then blocked with DPBS containing 1 % mouse serum.

loading on different types of beads and in the end blocked with mouse serum (ms). It is noteworthy that the beads were initially produced without blocking and results generated with both blocked and unblocked beads are incorporated in the presented results. For example, figure 5 shows data from the initial unblocked bead preparations.

The first attempts to produce beads harbouring Ova and Anx utilised αFlag-antibodies to control Anx orientation on the beads. However, the presence of the antibody on the bead surface markedly reduced the IL-6 secretion of BMDC which did however not impede the subsequent T cell proliferation (fig. S2A, S2B). Beyond the altered IL-6 suppression, the presence of αFlag abrogated the Anx-mediated inhibition of T cell responses as observed when comparing beads with direct Anx-coupling (OB, OAB) and beads with αFlag as vehicle for Anx-coupling (OFB, OFAB) (fig. S2C-S2F). As a consequence of these results showing unspecific modulation on BMDC by α-Flag, Anx was directly coated to the beads. Furthermore, the functional coating of Anx was efficient without the antibody as vehicle.

The blocking step was established after functional experiments were successfully performed. However, alteration became necessary following an inexplicable loss of OAB activity. In this context, different buffers (PBS, DPBS, DPBS-Ca^{2+}) were tested in com-

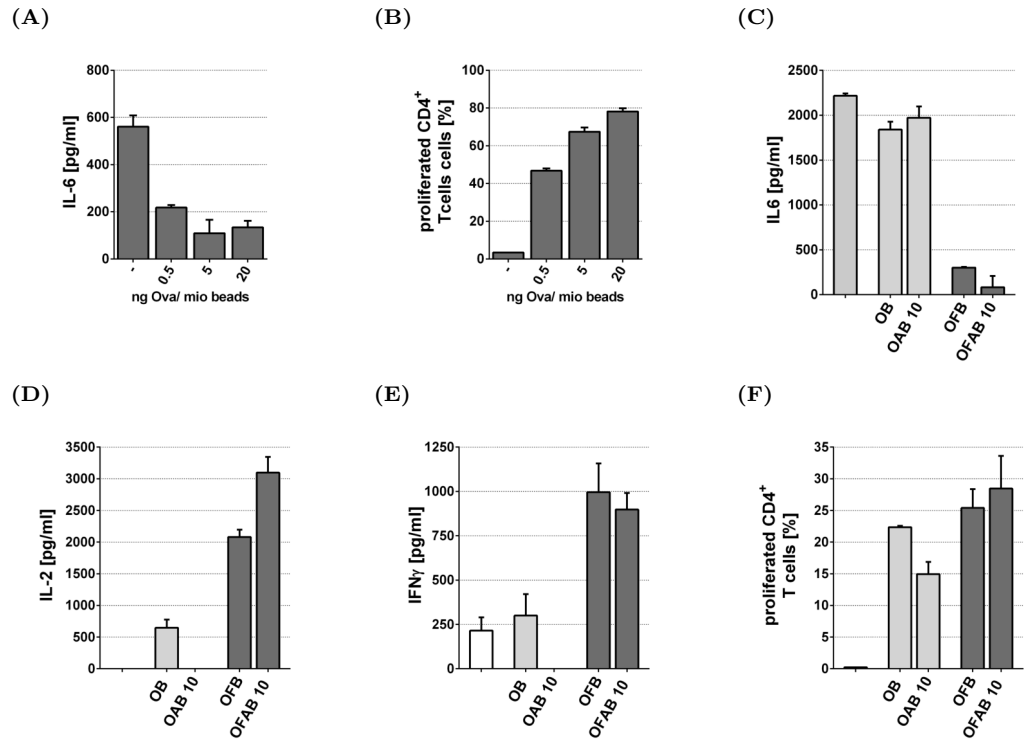

Figure S2: αFlag is no suitable vehicle for Anx-coating to beads. BMDC were pre-incubated with beads and stimulated with CpG. CFSE-labelled OT-II T cells were co-cultured with the treated BMDC. Proliferation was evaluated after 5 days of co-culture (B+F). Supernatants for cytokine analysis were collected before T cells were added (A+C) and on day 2 (D) and day 5 of co-culture (E).

bination with different blocking agents (FCS, BSA, ms) (fig. S3). Western blot analysis demonstrated stable and high affinity attachment of Anx to the beads in all tested conditions (data not shown) whereas the western blot analysis of Ova attachment were inconclusive. Ova was coupled to the beads as illustrated in figure S3A by comparing the protein in solution before the beads were added (SN input) and the protein that remained in solution after coating (SN unbound). Although the analysis of the supernatant implies that up to 7 ng Ova were bound to 10^6 beads, examination of the beads by western blot did not represent increasing concentrations of Ova. Desorption of Ova from the beads could explain this phenomenon. To test this hypothesis, the protein content in the bead solution after pelleting the beads was analysed. No Ova was detectable in supernatants taken from beads stored for several weeks (data not shown). Furthermore, neither sonification nor incubation in media at 37 °C resulted in detectable amounts of Ova in bead supernatants (fig. S3B, S3C) disproving the hypothesis of Ova desorbtion.
Interestingly, the beads recovered from the medium seemed to have a higher Ova content than beads from the bead stock which was stored at 4 °C in the meantime. Beads blocked with FCS were an exception, since comparable amounts of Ova were detected before and after medium incubation(fig. S3C). This indicates that blocking with medium or FCS may modulates Ova attachment and that western blot results were not representative for

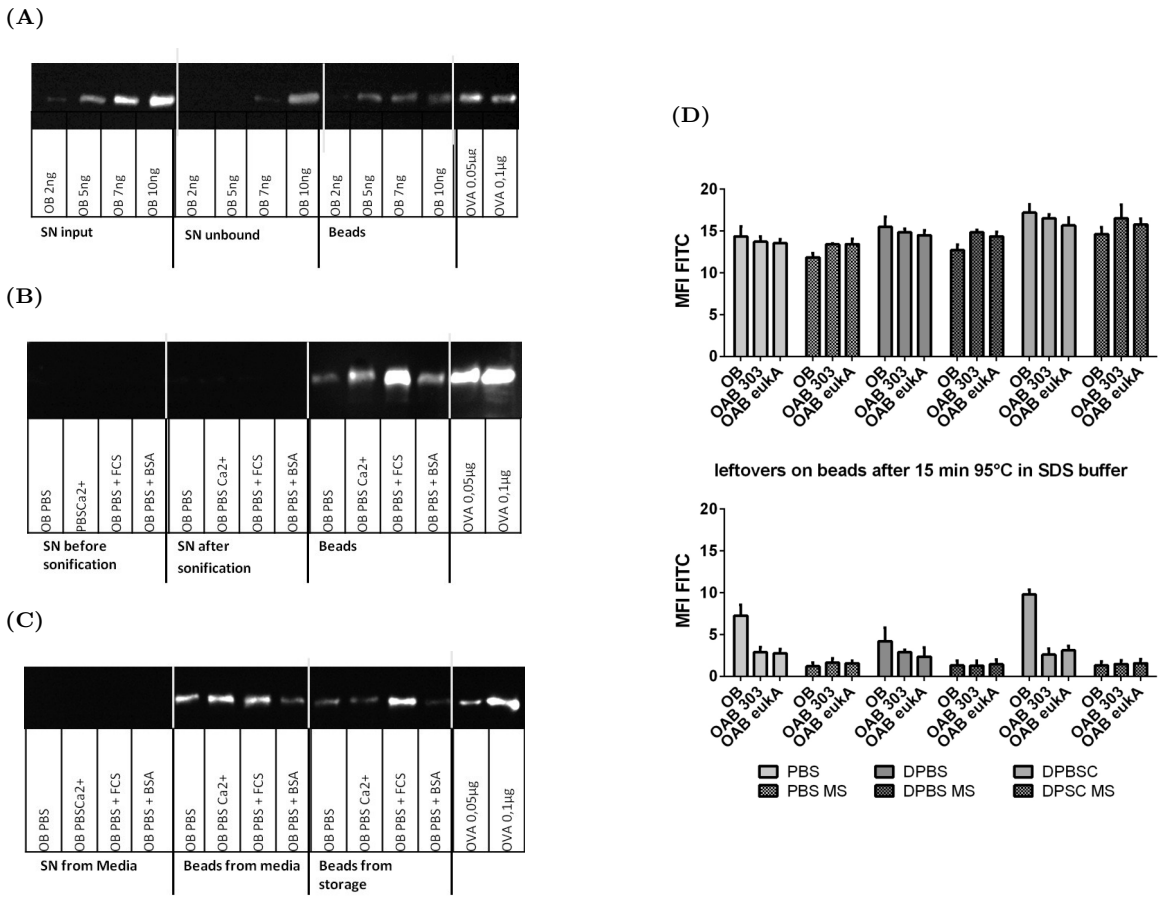

Figure S3: Attachment of Ova to beads is very stable (A-C) Bead supernatants (SN) or beads were incubated in SDS buffer at 95 °C for 15 min, loaded to SDS-PAGE to detect Ova *via* western blot. (A) illustrates the coupling of different amounts of Ova to beads. SN input are samples of the protein solution before the beads were added. SN unbound shows protein that remained in solution after incubation with the beads. (B) SN from beads generated in different buffers were analysed before and after brief sonificatio. (C) Beads generated in different buffers were incubated in medium at 37 °C. Beads and medium were then separated by centrifugation and protein content was compared with bead stocks stored at 4 °C. (D) Ova-FITC content on the bead surface was measured by FC before and after beads were incubated in SDS buffer at 95 °C for 15 min.

Ova coating of unblocked beads. A FITC-labelled variant of Ova was then utilised to examine the Ova content on the beads directly via FC. First, it was investigated whether the sample preparation for western blot analysis was efficient. Hence, beads were analysed by FC before (fig. S3D, upper panel) and after (fig. S3D, lower panel) they were cooked in SDS-buffer at 95 °C for 15 min. The harsh treatment was not sufficient to elute Ova completely from the beads. Moreover, considerably more residual Ova was detected on beads that were not blocked with serum or supplemented with Anx. Thus, it can be hypothesised that in Ova binds tightly to the beads and in this context may even change its conformation or unfold when there is no other protein that restricts the binding space on the bead surface. This type of binding to the beads might also influence the availability of the antigen in the cells. Blocking with mouse serum was introduced into the standard bead production to avoid such effects.

Coating was regularly controlled by FC exploiting the direct label of Ova and staining Anx with an APC-labelled antibody. Comparison of different bead charges as exemplified in figure S4 demonstrated that the refined bead production protocol results in reproducible bead coating in different bead charges.

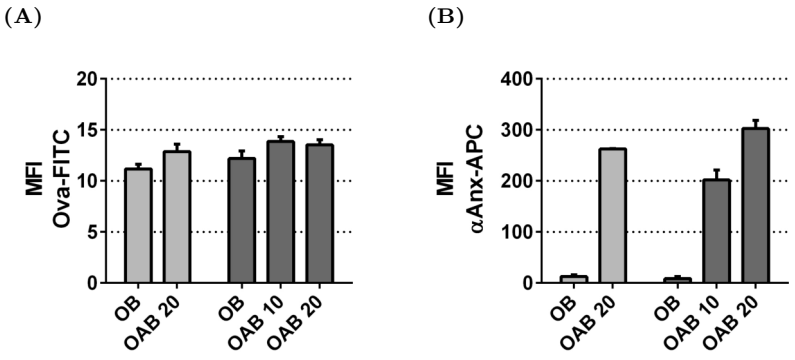

Figure S4: Different bead charges are comparably coated. Bead coating was analysed by FC. Proteins were detected directly (Ova-FITC) or by staining with a fluorescent antibody (αAnx-APC). Different bar colours indicate different bead charges.

Bead effects on BMDC cytokines

The functional analysis of the beads was preceded by titration experiments to assess the optimal bead concentration. The results from the titrations on T cell level are shown in fig-

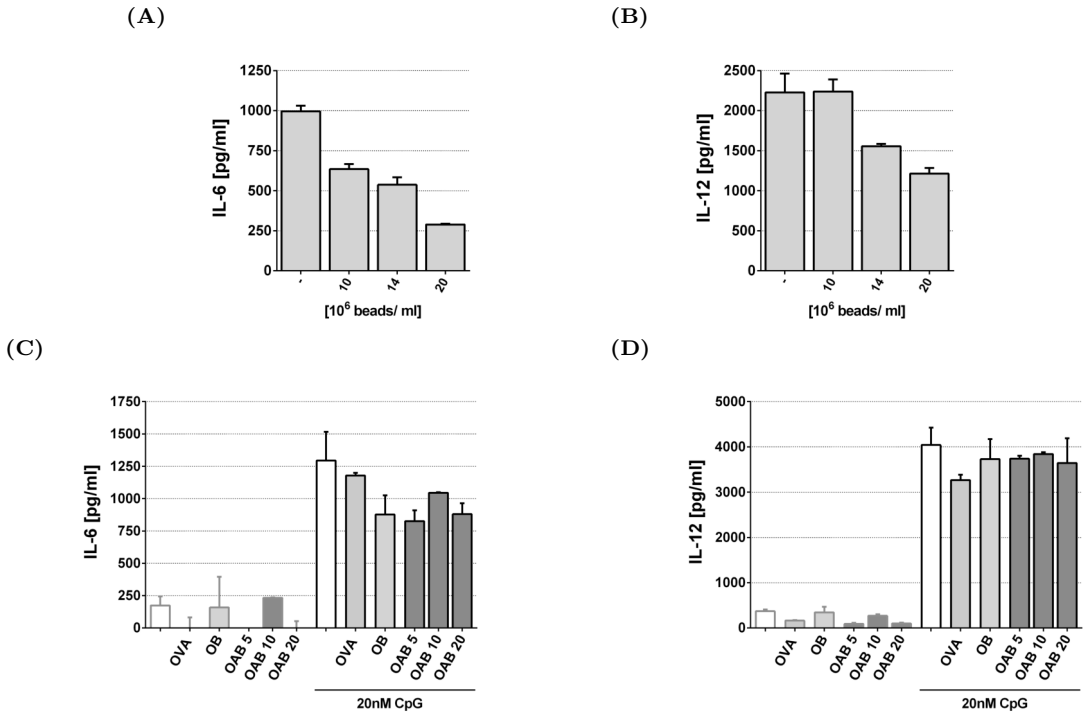

Figure S5: BMDC cytokine production following incubation with Anx-beads. (A+B) BMDC were pre-incubated with indicated concentrations of Ova-beads (OB) and stimulated with CpG. Cytokine secretion was analysed 2 days after stimulation. (C+D) BMDC were pre-incubated with soluble Ova [10 μg/ml] or beads [14 10^6/ml] and optionally stimulated with CpG as indicated. Cytokine secretion was analysed 2 days after stimulation.

ure 5B-5D while figure S5A-S5B exemplifies the effects of the control-beads on BMDC cytokine production. IL-6 and IL-12 secretion is decreased in bead-concentration-dependent manner.
Figure S5C-S5D illustrates BMDC cytokine secretion from an T cell suppression assay. This raw data further demonstrates that neither control nor Anx-beads have pro-inflammatory effects on BMDC at the cytokine level.

Effects of soluble Anx on anergy-related genes

Soluble Anx mediated attenuation of T cell proliferation, IL-2 and IFN-γ secretion, indicating an anergic phenotype. Similar to the results obtained with the Anx-beads, T cell interaction with BMDC treated with soluble Anx impaired IL-2 transcription (fig. S6A) whereas other anergy-related genes were not affected (fig. S6B-S6D).

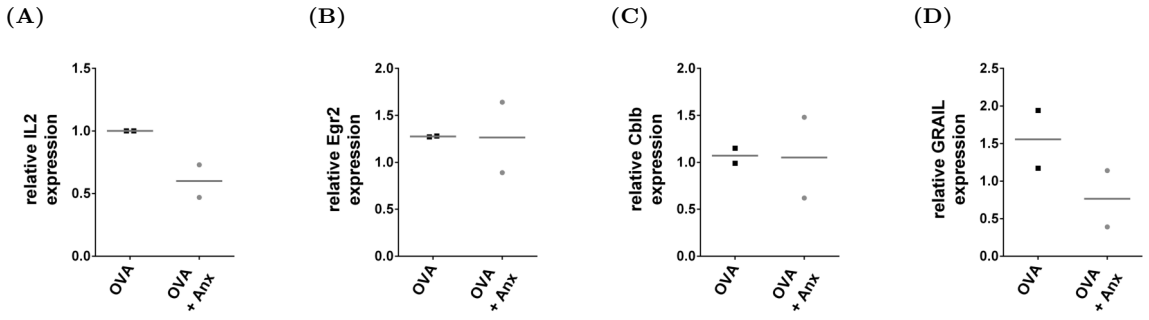

Figure S6: IL-2 is the only anergy-related genes are affected by soluble Anx BMDC were pre-incubated for 7 h with Anx [1000 nM] before Ova [10 μg/ml] and, 1 h later, CpG were added. CFSE-labelled OT-II T cells were co-cultured with treated BMDC for 4 h before they were harvested and analysed via qRT-PCR using HPRT as reference gene. (A) IL-2 expression is shown relative to the expression in the Ova-treated condition. (B-D) Expression of the indicated genes is illustrated relative to the expression of T cells co-cultured with non-pre-treated but CpG-stimulated BMDC. Dots indicate independent experiments.

II List of Abbreviations

aJ	Apoptotic JE6.1
Anx	Annexin/annexin core domain
AP-1	Activator protein 1
APC	Antigen presenting cell
APC (conjugate)	Allophycocyanin
BMDC	Bone marrow derived dendritic cells
BSA	Bovine Serum Albumin
C57BL/6	C57 Black 6 mouse
CD	Cluster of differentiation
conc	Concentration
CTL	Cytotoxic T lymphocytes
CTLA-4	Cytotoxic T-lymphocyte-associated Protein 4
DC	Dendritic cell
DCFDA	2',7'-dichlorofluorescein-diacetate
dNTP	Desoxynucleosidtriphosphate
EAE	Experimental Autoimmune Encephalomyelitis
ECDI	1-ethyl-3-(3-dimethylaminopropyl)-carbodiimide
ECL	Enhanced chemiluminescence
Egr2	Early growth response protein 2
ELISA	Enzyme Linked Immunosorbent Assay
ELISpot	Enzyme Linked Immunospot Assay
EMA	European Medicines Agency
ER	Endoplasmatic reticulum
FACS	Fluorescent Associated Cell Sorting
FC	Flow Cytometry
FCS	Fetal Calf Serum
FDA	Food and drug administration
FITC	Fluorescein-isothiocyanate
FoxP3	Forkhead box P3
FPR	Formyl Peptide Receptor
GRAIL	Gene related to anergy in lymphocytes
HA	Influenza Hemagglutinin
HRP	Horse Radish Peroxidase
ICOS	Inducible T cell co-stimulator
ICOSL	ICOS-ligand
IDO	Indoleamine-pyrrole 2,3-dioxygenase
IFN	Interferon

IgG	Immunoglobulin G
IL	Interleukin
ILT	Immunoglobulin-like transcript
ITAM	Immunoreceptor tyrosine-based activation motif
ISQ	Ovalbumin-derived MHC II peptide
i.v.	Intravenous
Lag-3	Lymphocyte activation gene 3
LPS	Lipopolysaccharide
OAB	Ova-Anx-beads
OANP	Ova-Anx-nanoparticle
OB	Ova-beads
ONP	Ova-nanoparticle
OPD	o-phenylenediaminedihydrochloride
Ova	Ovalbumin
PBMC	Peripheral blood mononuclear cells
PEG	Polyethylene Glycol
PI3K	Phosphatidylinositide 3-kinases
PKC	Protein kinase C
PLC	Phospholipase C,
PLGA	Poly(lactic-co-glycolic acid)
Mϕ	Macrophage
MHC	Major histocompability complex
MS	Multiple Sclerosis
ms	Mouse serum
mTEC	Medullary thymic epithelial cells
NFAT	Nuclear factor of activated T-cells
NF-κB	Nuclear factor kappa-light-chain-enhancer of activated B cells
NOX2	NADPH oxidase 2
NP	Nanoparticle
PAGE	Polyacrylamide Gel Electrophoresis
PAMP	Pathogen-associated molecular pattern
PBS	Phosphate Buffered Saline
PBS-T	Phosphate Buffered Saline - Tween 20
PCR	Polymerase Chain Reaction
PD-1	Programmed cell death protein 1
PD-L1/2	Programmed cell death 1 ligand 1/2
PE	Phycoerythrin
PEI	Polyethylenimin
PenStrep	Penicillin Streptomycin

PKC	Protein kinase C
PLGA	Poly(D,L-lactide-co-glycolide)
PMA	Phorbol myristate acetate
PmxB	PolymyxinB
PS	Phosphatidyl serine
PRR	Pattern recognition receptor
RES	Reticulo-endothelial System
pMHC	peptide-MHC complex
ROS	Reactive Oxygen Species
PRR	Pattern recognition receptor
RPMI	Roswell Park Memorial Institute
RT	Room Temperature
SIINF	Ovalbumin-derived MHC I peptide
SIY	Control Peptide
SN	Supernatant
SOCS	Suppressor Of Cytokine Signalling
T1D	Type 1 Diabetes
TCR	T cell receptor
TBS	Tris Buffered Saline
TBS-T	Tris Buffered Saline - Tween 20
TGF-β	Transforming growth factor β
T_H cells	T helper cells
TLR	Toll-like receptor
Tim-3	T cell immunoglobulin 3
TNF	Tumor necrosis factor
tolDC	Tolerogenic DC
Tr1 cell	Type 1 regulatory cell
Treg	Regulatory T cell
Trolox	6-Hydroxy-2,5,7,8-tetramethylchroman-2-carbonsäure
wt	Wild type

III List of Figures